GAMMA RAY ACTIVITY LEVELS AND RADIOLOGICAL HAZARD INDICES OF RADIONUCLIDES IN MINE TAILINGS FROM SELECTED MINES IN SOUTHWESTERN UGANDA

BY

TURYAHABWA EVARIST RUTAHWEIRE SILVER

A DISSERTATION SUBMITTED TO THE GRADUATE SCHOOL IN PARTIAL FULFILLMENT OF THE REQUIREMENTS FOR THE AWARD OF THE DEGREE OF MASTER OF SCIENCE IN PHYSICS OF KYAMBOGO UNIVERSITY

JANUARY 2016

DECLARATION

I, Turyahabwa Evarist Rutahweire Silver do hereby declare that this Dissertation contains my original research and has not been submitted in whole or part to any University or Academic Institution for an Academic Award.

Signed:.....

Date: 15th/01/2016

APPROVAL

This is to certify that this Dissertation was carried out under our close supervision and has been passed by the Board of Examiners and the Senate for the Award of the Degree of Master of Science in Physics of Kyambogo University.

Signed: .....

Supervisor One: Oriada Richard

Department of Physics

Kyambogo University

Date: January 15th 2016

Signed: .....

Supervisor Two: Enjiku Ben D.D.

Department of Physics

Kyambogo University

Date: 15/01/2016

DEDICATION

This Dissertation is dedicated to my Wife Winnie Kyomugisha Turyahabwa and my Children (Akatukunda Joshua and Ainomugisha Joan Kapasika).

ACKNOWLEDGEMENT

Great thanks go to the Almighty God to whom I owe my academic success and entire life. If it were not for God, the source of all wisdom and knowledge, and Blessed Mary Mother of our saviour and our divine intercessor, I would not have been able to successfully complete this dissertation.

My most sincere gratitude and heartfelt thanks go to my supervisors Oriada Richard and Enjiku Ben D.D for their encouragement, advice and guidance from start to end.

Dr. Jurua Edward and all the Staff members of the Department of Physics, Kyambogo University deserve a special mention for their input in the development of the topic for this dissertation.

To my classmates of 2012/2013 academic year, Bwayo Edward, Ariho Melkiades, Mugaiga Aron, Anguani Mike, Kamya Willy, Lugolole Robert and Jenan Loum, I extend my heartfelt thanks for their invaluable assistance and encouragement throughout the period of the course.

I am grateful to the Management of Radioisotope Laboratory, Makerere University for allowing me to use the facilities in the laboratory and above all, teaching me how to operate the NaI(Tl) gamma ray spectrometer. Special thanks go to the Technician, Kwizera Benon for he was always available and ready to assist me whenever I would find problems with the instruments.

I extend my appreciation to my family friends, Eng. Muhaya Jude, Dorah Muhaya, Arinaitwe Vianney, Ahimbisibwe Papius, Habib Lukwago and Aisha Lukwago for their physical and financial contribution in collection of the mine tailing samples at the sites and their transportation to the laboratory.

Lastly, I am greatly indebted to my Parents Emmanuel Rutahweire and Stella Rutahweire, my Wife Winnie Kyomugisha Turyahabwa and children Akatukunda Joshua and Ainomugisha Joan Kapasika. Thank you for supporting me morally, emotionally, financially and physically and for tolerating my long absence from home during the study period.

TABLE OF CONTENTS

LIST OF FIGURES

PAGE

LIST OF TABLES

PAGE

ABSTRACT

This study was designed to determine and compare the specific activity levels and the radiological hazard indices of gamma ray emitting radionuclides in mine tailings from three selected mines in Southwestern Uganda. This was achieved by analyzing 72 soil and rock mine tailing samples using the GDM 20 NaI(Tl) detector. The specific activities of the principal primordial radionuclides of ^{238}U, ^{232}Th and ^{40}K in the samples were measured. The values obtained were used to determine the absorbed dose rates, the annual effective dose rates, the radium equivalent activity, external and internal hazard index and the excess lifetime cancer risk. The mean specific activities of ^{238}U, ^{232}Th and ^{40}K in mine tailings at 90% confidence level ranged from 23±14 $Bqkg^{-1}$ to 59±16 $Bqkg^{-1}$ for ^{238}U, 49±39 $Bqkg^{-1}$ to 244±19 $Bqkg^{-1}$ for ^{232}Th, and 226±232 $Bqkg^{-1}$ to 893±167 $Bqkg^{-1}$ for ^{40}K. The mean outdoor and indoor absorbed dose rates in air for Mashonga, Kikagati and Butare were (181±36 $nGyh^{-1}$ and 338±67 $nGyh^{-1}$), (167±23 $nGyh^{-1}$ and 310±47 $nGyh^{-1}$) and (192±16 $nGyh^{-1}$ and 355±32 $nGyh^{-1}$) respectively for waste soil samples and (67±50 $nGyh^{-1}$and 127±102 $nGyh^{-1}$), (85±37 $nGyh^{-1}$ and 159±80 $nGyh^{-1}$) and (115±33 $nGyh^{-1}$ and 215±66 $nGyh^{-1}$) respectively for waste rock samples. The ratio of the mean indoor to outdoor absorbed dose rates in all the samples was 1.9 but this was 36% higher than the world average. The total annual effective dose rates, radium equivalent activities, external and internal hazard indices for waste soil samples were above the maximum permissible limits recommended for members of the public. Potential radiological hazards on miners and the people living in the neighborhood of the sites due to external irradiation are significant. There is need to improve waste management practices in the mining sites in order to prevent health hazards associated with the radionuclides in the mine tailings.

CHAPTER ONE: INTRODUCTION

1.1 Background of the Study

Human beings are always exposed to ionizing radiations of natural origin since they live in an environment that has the sources of these radiations (BEIR VII). Ionizing radiation in our environment comes as cosmic radiation from outer space and from the terrestrial sources such as the soil and rocks that contain naturally occurring radioactive materials.

Cosmic rays are streams of charged and uncharged nuclear particles consisting of protons and heavy nuclei. The interaction of cosmic radiation with nuclei present in the atmosphere produces elementary particles and also a series of radionuclides such as carbon (^{14}C), sodium (^{22}Na), tritium (^{3}H) and beryllium (^{7}Be). The intensity of cosmic radiation is dependent on both altitude and latitude and is greatest in the upper stratosphere. The energetic cosmic ray neutrons and protons descend into the lower atmosphere, producing cosmogenic radionuclides during their interaction. As a result, people living at higher altitudes receive higher doses of cosmic radiation than those living at the sea level. The worldwide average annual effective dose received by people living at the sea level from directly ionizing cosmic radiation is 0.27 Sv y^{-1} (UNSCEAR, 2008).

Naturally occurring radionuclides of terrestrial origin, also termed primordial radionuclides, are present in various degrees in all environmental media, including the human body. Only those radionuclides with half lives comparable to the age of the earth, and their decay products exist in sufficient quantity contribute significantly to population exposure (UNSCEAR, 2000). Because of their very long half lives, of the order of hundreds of millions of years, gamma ray emitting radionuclides of potassium (^{40}K), and the radionuclides in the decay series of uranium (^{238}U) and thorium (^{232}Th) are the main contributors to terrestrial radiation (IAEA Training course series 40, 2010; UNSCEAR, 2000). The magnitude of the radionuclides of ^{238}U, ^{232}Th and ^{40}K differ in the soil and rock structures and depends on the local geology and geographical conditions of the area (UNSCEAR, 2008; IAEA-TECDOC-1363, 2003). According to UNSCEAR, (2000), the worldwide weighted average absorbed dose rate from terrestrial sources is 59 nGy h^{-1}. The cosmic radiation and radiation from the decay of cosmogenic and primordial

radionuclides constitute the natural background radiation which gives rise to a dose rate of 2.4 mSv y^{-1} (UNSCEAR, 2008; IAEA-TECDOC-1363, 2003).

Natural uranium has three different radioisotopes of ^{238}U of percentage abundance of 99.276% and half life of 4.47×10^{9} years, ^{235}U of percentage abundance of 0.718% and half life 7.1×10^{8} years, and ^{234}U of percentage abundance of 0.0055% and half life 2.46×10^{5} years (US EPA, 2012). Although ^{234}U radioisotope is negligible in terms of its abundance, it is found to be dominant in ground water. Uranium (^{238}U) has an average crustal abundance of 2 – 3 ppm and decays by emitting alpha particles (IAEA-TECDOC-1363, 2003). Uranium is used in various applications such as in nuclear energy production, in production of protective shields of army tanks and also used in making armour piercing shells. Enriched uranium is used in powering nuclear propelled Navy ships and submarines, and in nuclear weapons and nuclear reactors (US EPA, 2012).

Thorium (^{232}Th), also called thoria, is a slightly radioactive element. Thorium is found in small amounts in most rocks and soils, where it is about four times more abundant than uranium. Thorium exists in nature in a single isotopic form as ^{232}Th with an average crustal abundance of 8 – 12 ppm. It has a long half-life of 1.41×10^{10} years and decays by emitting alpha particles. Some of its daughter radionuclides emit gamma radiation. Until the inherent dangers associated with its radiation were realized, thorium and its compounds found some important uses. The best known use of thorium is the manufacturing of gas mantles, and toothpastes. Thorium is still used as an alloying element with magnesium, to coat tungsten wire used in electronic equipment, to control the grain size of plutonium used for electric lamps and in the manufacture of refractory materials for the metallurgical industries. Thorium oxide is used in making high-temperature ore laboratory crucibles. It is added to glass to create glasses with a high refractive index and low dispersion used in manufacturing of lenses for cameras and scientific instruments. Like uranium, thorium could be a source of nuclear energy.

Potassium-40 is the only radioactive isotope of potassium. It has a half-life of 1.28×10^{9} years, an atomic abundance of 0.012% and an average crustal abundance of 2 – 2.5% (IAEA-TECDOC-1363, 2003). It decays by emitting beta particles to calcium-40 and electron capture to argon-40. Argon-40 subsequently undergoes gamma decay to the ground state. Potassium (^{40}K) is present in most terrestrial and biological substances such

as plants and animals which take in potassium compounds. Due to its presence in most foods, ^{40}K accounts for the greatest proportion of the naturally occurring radiation from human beings due to ingestion of plant materials by human beings (UNSCEAR, 2008; BEIR VII; UNSCEAR, 2000). Potassium is abundant in potash-rich rock forming minerals such as potassium feldspar and mica. Potassium is high in slightly weathered soils and low in highly weathered soils due to leaching (Guagliardi, et. al., 2013).

Many of the terrestrial radionuclides are exposed by mining activities. Mining involves extraction of valuable minerals or other geologically valuable materials from the earth body, lode, vein, seam, or reef, which forms the mineralized package of economic interest to the miner. Mining activities can produce a lot of wastes called mine tailings. These are the materials left over after the process of separating the mineral rich fraction from the uneconomic fraction (gangue) of the earth material. The extraction of minerals from the mineral bearing rock at the site may involve placer mining or hard rock mining depending on the nature of the mineral. Placer mining uses water and gravity to extract the valuable mineral from the ore. Hard rock mining uses pulverization of the rock where the ore is ground into fine particles and then chemicals used to extract the mineral from the ore (http://en.wikipedia.org/wingiki/Min, Accessed on 7th August 2014). The composition of tailings is directly dependent on the composition of the ore and efficiency of the process of mineral extraction used at the site. Tailings may contain trace quantities of metals found in the host ore and other metals including ^{238}U, ^{232}Th and ^{40}K. They could as well contain substantial amounts of added chemicals used in the extraction process (IAEA Safety report series 49, 2006).

Human activities such as mining, processing and use of minerals, scrap and recycled metals may lead to increased levels of naturally radioactive materials in the environment (UNSCEAR, 2000). Enhanced levels of natural background radiation have been reported in surface and underground mines around the world (UNSCEAR, 2000). In South Africa, the average annual doses received by underground gold miners were estimated at 6.3 mSv in 1997, 4.9 mSv in 1998, 5.4 mSv in 1999 and 7.0 mSv in 2000 (Wymer, 2002). The gold deposits from deep underground mines in South Africa have been found to have high concentrations of low grade uranium i.e. 0.02 to 0.05% U_3O_8 (Fleur, 2011). Between 1953 and 1995, 6 billion tones of mine tailings containing 500, 000 tonnes of uranium and 200 kg of radium-226 have been deposited in Witwatersrand basin (UNSCEAR,

2008; FSE, 2006). Annual effective doses to the population from ingestion of water, inhalation of radon and of dust from the mine tailings have been estimated to be 0.04 mSv, 0.04 mSv and 0.02 mSv respectively (UNSCEAR, 2008). This shows that the ionizing radiation from radionuclides in the mine tailings may increase the background radiation if poorly disposed of. Uranium and thorium are known to be found in heavy accessory minerals such as ilmenite, magnetite, garnet, zircon, and monazite sands. The tailings that contain radioactive elements remain active for a very long period of time and can increase the risk level of the radiation. Thus mine tailings may become a major source of external and internal radiation hazard and toxicity to the workers who handle the tailings in the mines and as well as the members of the public living around the mining area (Mangset, 2009; UNSCEAR, 2008). One of the world's worst mining disasters from radiation exposure occurred in central Canada in the old Elliot Lake uranium mines (now closed). It is estimated that about 400 healthy uranium miners suffered long and painful lung cancer deaths from excessive radon exposure in the old Elliot Lake uranium mines of central Canada (Fergal, 2009). Radiation exposure from radon in the old Elliot Lake uranium mines has been documented as the cause of at least 221 of these deaths (Fergal, 2009).

Southwestern Uganda is endowed with valuable minerals such as gold, copper, tin, iron ore, kaolin, gypsum, and limestone. Gold, in Southwestern Uganda, is mined mainly by artisanal miners, from mines in Buhweju goldfield and Kigezi goldfield. In Buhweju goldfield, the gold ore contains cassiterite and monazite and is recovered from phyllites, shales, schists and quartzites of potassium-aluminium (K-A) rocks (Nagudi, 2011). In Kigezi gold field, gold is found to be contained in cassiterite, tungsten, bismutite, zircon, monazite, chalcopyrite and rutile. The gold is contained in potassium-aluminium (K-A) system rocks or in granite and quartz veins as well as in ironstone lenses (Nagudi, 2011). Tin is recovered from quartz-mica-cassiterite veins in shales and sandstones of potassium-aluminium in granite rocks (Nagudi, 2011). Tin is mined in Rwaminyinya within Kisoro District and in Kikagati and Ndaniyankoko in Isingiro District. Iron occurs in the form of hematite and magnetite. Hematite iron ore is mined in Southwestern Uganda in the Districts of Kabale, Kisoro and Mbarara while magnetite iron ore is mined from Eastern Uganda. Tembo steel company uses these iron ores as an additive in its steel

scrap smelting industry. Hima and Tororo cement industries are the other industries that use iron ore as an additive in the manufacture of cement.

The granite and sedimentary rocks in Southwestern Uganda contain ^{238}U and ^{232}Th radionuclides (Baguma, 2009). The sand and gravels at Mashonga contain ^{238}U, ^{232}Th and ^{40}K radionuclides in addition to the heavy accessory minerals such as monazite and zircon (Baguma, 2009). Nagudi, (2011) reported that uranium, in the forms of euxenite, microlite and kasolite exists in pegmatite rocks and was also detected in spring waters in the Western rift valley. At Nanseke in Toro, uranium was found in more than trace amounts, about 11% U_3O_8 (Nagudi, 2011). Thorium exists in monazite formed by weathering of granite rocks. The thorium containing mineral is found in Kalapata and Kalere river valley in the quartz-rutile-ilmenite nodules in the biotite gneiss. The mineral varies in colour from typical honey yellow to almost black and contains up to 11% ThO_2. The weathered granite and pegmatite rocks in Buhweju and other places in Uganda contain up to 0.5% ThO_2 (Nagudi, 2011). An aerial geological survey conducted in 2006 covered 80% of the Country (Uganda) and confirmed the existence of the thorium mineral in the Karagwe-Ankolean and Buganda-Toro systems in pegmatite and granite rocks (Department of Geological survey and Mines, 2012).

Radionuclides in the soil and rocks emit several kinds of ionizing radiation including alpha particles, beta particles and gamma rays. Alpha and beta particles have a low penetration range and so they are absorbed in the soil and rocks but gamma rays have a higher penetration range, can go through the soil and rocks and into the air where they can be detected (IAEA-TECDOC-1363, 2003). The long term exposure to radioisotopes such as uranium, radium and thorium and other heavy metals such as lead, through inhalation, ingestion or direct exposure of dust particles and radon and its short lived decay products may have severe health effects such as lung cancer, leukemia, bone cancer and liver damage (UNSCEAR, 2008). Other diseases caused by ionizing radiation exposure include radiation burns, eye cataracts, sterility, kidney and pancreas diseases (Avwiri, 2012; IAEA-DS379, 2009; WHO, 2009; BEIR VII).

1.2 Statement of the Problem

Rocks in Southwestern Uganda are of granite, pegmatite and sedimentary origin which are known to contain ^{238}U, ^{232}Th and ^{40}K radionuclides and their gamma activity levels

are unknown. Mining activities involving extraction of mineral from rocks in Southwestern Uganda have been going on for many years with no proper disposal of mine tailings containing natural radionuclides. If they are transferred to agricultural soils, they are absorbed by plants. Crops grown in the soil containing radioactive materials and water running through areas having rock types likely to contain radioactive materials could contaminate the food and drinking water. Consuming food and drinking water contaminated with radioactive materials increases the amount of the radionuclides a person is exposed to and this could increase the health risks associated with exposure to the ionizing radiation. There is no published data on the gamma radiation activity levels of the radionuclides in the mine tailings in Uganda.

1.3 Aim of the Study

This study was therefore aimed at determining the gamma ray activity levels and radiological hazard indices of radionuclides in mine tailings from selected mines in Southwestern Uganda.

1.4 Objectives of the Study

To determine the

(a) specific activity levels of ^{238}U, ^{232}Th and ^{40}K radionuclides in mine tailings.

(b) gamma dose rates of ^{238}U, ^{232}Th and ^{40}K radionuclides in mine tailings.

(c) radiological hazard indices of ^{238}U, ^{232}Th and ^{40}K radionuclides in mine tailings.

1.5 Scope of the Study

The study was carried out using waste soil and rock (mine tailing) samples obtained from three mines located in Southwestern Uganda in the districts of Bushenyi, Isingiro and Kabale. The samples of mine tailings for the study were obtained from Mashonga Gold Mine located in Bushenyi District, Kikagati Tin Mine located in Isingiro District, and Butare Iron Ore Mine located in Kabale District as indicated in Figure 1.1. The samples were collected from the above stated mines and their analyses were carried out at Makerere University Physics Laboratory. The three mines were selected for the study based on the type of minerals being mined at each of the mines. The three minerals considered were gold, tin and iron ore. The assumption made in considering these three

minerals was that these minerals are likely to have traces of ^{238}U, ^{232}Th and ^{40}K radionuclides in their ores which may be left in the mine tailings. The study was carried out over a period of six months from January 2014 to June 2014.

The study had the following limitation.

Mining companies operating in Southwestern Uganda could not allow the researcher to access their mines and collect samples there. As a result, the samples used in this study were obtained from mine tailings of unlicensed mines only. This suggests the possibility of higher gamma dose rates from mine tailings from the companies' mining activities.

Figure 1.1: Map of South Western Uganda showing Study Sites

1.6 Significance of the Study

This study determined the gamma activity levels of radionuclides in mine tailings in Southwestern Uganda. The study also determined the gamma dose rates, radium

equivalent activity, external hazard index, internal hazard index and excess lifetime cancer risk for the purpose of estimating the radiation exposure risk from mine tailings.

The results from this study can be used by the Atomic Energy Council of Uganda (AEC) as baseline data for monitoring the radiation environment to detect changes in the natural background radiation in Southwestern Uganda.

The results of this study can be used as reference data for radioelement mapping in mines using gamma ray spectrometer.

The results can also be used for further research interests in environmental radiation for example to determine the gamma activity levels in building materials from mine tailings in Southwestern Uganda.

CHAPTER TWO: REVIEW OF RELATED LITERATURE AND THEORY

2.1Introduction

This chapter discusses the major sources of natural radioactivity, and the nature of radiations from radioactive materials. It also covers the discussion on the natural decay series, exposure and absorption of radiations from radionuclides and their effects on the human body. The detection and measurement of radiations from radionuclides are also discussed.

2.2 Radioactivity

All matter is made up of atoms. Atoms may be stable or unstable. Atoms with excess energy and nucleons are unstable or radioactive. Unstable or radioactive atoms decay by emitting nuclear particles such as alpha (α), beta (β) particles and gamma (γ) radiation and become more stable. Radioactivity can be artificial or natural.

Artificial radioactivity is the spontaneous decay of artificial radioisotopes made in a reactor or accelerator. Iodine-131, Cobalt-57, Cisium-137, Cobalt-60, Americium-241, Sodium-22 and Manganese-54 are some of the manmade radioisotopes. Artificial radioisotopes are used in medical procedures such as diagnosis and treatment of disease. They find applications in agriculture in production of new varieties of disease resistant grains and cereals, study of uptake of phosphate fertilizers in plants and also used in sterilizing food items. Some artificial radioisotopes are also used in pacemakers, smoke detectors, and industrial radiography, tracers, self-illuminating exit signs, nuclear energy generation and nuclear weapons production (US EPA, 2007; UNSCEAR, 2000).

Natural radioactivity is the spontaneous disintegration of naturally occurring radioactive materials mainly found in the earth's crust. The major sources of natural radioactivity are cosmic radiation and terrestrial radiation.

Cosmic radiation is composed of subatomic particles from outer space, mostly energetic protons, electrons, gamma rays, and x-rays (Keith et al., 1999). Cosmic rays which have not yet interacted with matter in the earth's atmosphere, lithosphere, or hydrosphere, are termed primary cosmic rays. Primary cosmic rays are composed of protons (about 85%) and alpha particles (about 14%), with much smaller fluxes (<1%) of heavier nuclei.

Secondary cosmic rays on the other hand are produced by interactions of the primary rays with the atmosphere and consist largely of subatomic particles such as pions, muons, and electrons. At the sea level, nearly all the observed cosmic radiation consists of secondary cosmic rays, with some 68% of the flux accounted for by muons and 30% by electrons. Less than 1% of the flux at sea level consists of protons. Primary cosmic rays are positively charged and usually possess tremendous kinetic energy of the order of 2 to 30 GeV. The high energies of primary cosmic rays enable them to literally blast apart atoms in the earth's atmosphere upon collision. Cosmic ray intensity increases sharply with altitude, latitude and solar flare activity (BEIR VII) until a maximum is reached at an altitude of about 20 km. From 20 km to the limit of the atmosphere (up to 50 km), the intensity decreases due to increase in production of secondary cosmic rays as the density of the atmosphere increases. Cosmic rays in their interaction with the earth's atmosphere produce a variety of radionuclides such as sodium-22 (half-life 2.605 years) and carbon-14 (half-life 5715 years). The contribution of these radionuclides to the radiation absorbed doses is not significant (IAEA-TECDOC-1363, 2003). At the sea level, the average absorbed dose rate arising from exposure to directly ionizing cosmic radiation is 31 nGy h^{-1} equivalent to an annual effective dose rate of 0.270 mSv y^{-1} (UNSCEAR, 2008, 2000). At 41,000 feet (12.497 km) above the sea level, over the poles, the equivalent dose varies from 12 μSv to 100 μSv (BEIR VII).

The second major source of natural radioactivity is terrestrial radiation. It arises from terrestrial or primordial radionuclides in the earth's crust. Primordial radionuclides have half lives of the order of 100 million years comparable to the age of the earth. They are mainly uranium-238, thorium-232 and radionuclides in their decay series and potassium-40 (IAEA-TECDOC-1363, 2003). Uranium and thorium each initiate a chain of radioactive progeny, which are nearly always found in the presence of the parent radionuclides. Although many of the daughter radionuclides are short-lived, they are distributed in the environment because they are continually being formed from their long-lived parent radionuclides. Primordial radionuclides are present in the soil, rocks, air, water, food, building materials and even the human body itself (UNSCEAR, 2008).

Radioactive substances in the human body irradiate different body tissues and are responsible for the internal radiation and contamination. These substances have a terrestrial and extraterrestrial origin since they are ingested with food and water, or

inhaled with air. They include mainly carbon-14, potassium-40, uranium, thorium and radium (UNSCEAR, 2000) and their concentrations in the human body tissues are 22 ng, 17 mg, 90 μg, 30 μg and 31 pg respectively (www.physics.isu.edu, Accessed on: 27th December 2014).

2.3 Radioactive Decay

Radioactive decay expresses the rate of decrease in the number of unstable atoms with time. All radioactive decays follow an exponential law and are statistical. Considering a radioactive sample containing N unstable atoms, the decrease in the number, dN, decaying in a time interval dt is directly proportional to N. This is shown in the relation

$$-\frac{dN}{dt} \propto N \tag{2.1}$$

where $\propto$ is symbol of proportionality. The relation shown above can be written as a differential equation of the form

$$-\frac{dN}{dt} = \lambda N \tag{2.2}$$

where λ is a constant of proportionality called decay constant of the radionuclide. The solution of equation 2.2 called the Exponential Law is shown in the equation

$$N_t = N_0 e^{-\lambda t} \tag{2.3}$$

where N_t is the number of unstable atoms present after a time interval t and N_0 is the number of original unstable atoms at $t = 0$. The decay constant expresses the probability per unit time that a radionuclide will decay and it is constant.

Radioactive decay is a random statistical process (IAEA-TECDOC-1363, 2003). This is because each radioactive decay occurs completely independent of every other decay event and the time between the decays is not constant. For a large number of randomly decaying atomic nuclei, the frequency of the radioactive decay follows Poisson's distribution (Turner, 2007). If μ is the average decay rate, the probability, $P(N)$, that the number of atomic nuclei, N, will decay within a time unit is given by the equation given below.

$$P(N) = \frac{\mu^{-N} e^{-\mu}}{N!} \tag{2.4}$$

Poisson's distribution holds that the variance σ^2 of the distribution is equal to its average value i.e. $\sigma^2 = \mu$, where σ is the standard deviation of the distribution. The range of $\pm 1\sigma$ about the mean covers 68.3% of the distribution, $\pm 2\sigma$ covers 95.5% of the distribution, and $\pm 3\sigma$ covers 99.7% of the distribution. The emission of particles and gamma rays in radioactive decay is proportional to the number of disintegrating atoms, and the standard deviation may be used to estimate the range of deviations and errors of the radiometric measurements. If N counts are recorded in time t, then the standard deviation of the recorded counts is given in equation given below (Turner, 2007; IAEA-TECDOC-1363, 2003).

$$\sigma(N) = \sqrt{\overline{N}} \tag{2.5}$$

where $\overline{N}$ is the mathematical expectation of the number of counts (the mean count of repeated measurements).

2.4 Types of Radioactive Decay

An unstable atom can spontaneously emit excess energy or breakup to emit excess energy in order to become stable. When it does so, it is said to undergo radioactive decay. Alpha (α) decay, beta (β) decay, gamma (γ) decay and spontaneous fission are the major radioactive schemes.

In the α-decay of an unstable atom, an α-particle which is a nucleus of a helium atom that has lost two electrons is emitted from nuclei of heavy elements i.e. $Z \geq 83$ (Turner, 2007; IAEA-TECDOC-1363, 2003). Alpha particles have a discrete energy that is specific for a particular radionuclide (IAEA-TECDOC-1363, 2003). Alpha particles lose most of their energy due to intense ionization, have a very short range in air (about 10^{-2} m) and can be stopped by 10^{-5} m of rock. Alpha particles can also be stopped by a thin sheet of paper. External exposure (external to the body) is of far less concern than internal exposure, because alpha particles lack the energy to penetrate the outer dead layer of the skin. Internally, alpha particles can be very harmful. If alpha emitters are inhaled, ingested (swallowed), or absorbed into the blood stream, sensitive living tissue can be exposed to alpha radiation that can be fatal (US EPA, 2012).

In β-decay of an unstable atom, β-particles which are fluxes of high energy electrons are emitted. Beta particles have a continuous energy spectrum up to a maximum energy,

which depends on the particular radionuclide emitting them. The initial velocity of beta particles may approach the velocity of light. The penetration range for beta particles depends on the initial energy of the particles. Beta radiation passing through matter loses its energy by ionization and generates electromagnetic radiation called bremsstrahlung (IAEA-TECDOC-1363, 2003). Beta particles are more penetrating than alpha particles but are less damaging than alpha particles over equally traveled distances. They travel considerable distances in air but can be reduced or stopped by a layer of clothing or by few millimeters of aluminum. Some beta particles are capable of destroying the skin and causing radiation damage, such as skin burns. However, just like alpha-emitters, beta-emitters are more hazardous when they are inhaled or ingested (US EPA, 2012; Turner, 2007).

Gamma rays are electromagnetic radiations. They are emitted from the nuclei of some unstable atoms following alpha or beta decay. Because of their high energy, gamma photons travel at the speed of light and can cover hundreds to thousands of meters in air before they are considerably attenuated. Gamma rays are more penetrating than alpha or beta particles, can penetrate through the rocks and soil into the air and can be stopped by thick lead metal (IAEA-TECDOC-1363, 2003). The primary source of gamma ray exposure is naturally occurring radionuclides, particularly potassium-40, which is found in the soil and water. However, the increasing use of nuclear medicine (e.g., bone, thyroid, and lung scans) contributes an increasing proportion of the total gamma radiation dose for exposed people. Also, some manmade radionuclides that have been released to the environment, by fallout from nuclear reactors and atomic bomb tests, also emit gamma rays (UNSCEAR, 2000).

In spontaneous fission, the nucleus spontaneously breaks up without any apparent external cause. Spontaneous fission process is the only spontaneous source of energetic heavy charged particles with masses greater than that of the alpha particle. All heavy nuclei are, in principle, unstable against spontaneous fission into two lighter fragments. For all but the extremely heavy nuclei, however, the process is inhibited by the large potential barrier that must be overcome in the distortion of the nucleus from its original near spherical shape. Spontaneous fission is therefore not a significant process except for some isotopes of very large mass number (Turner, 2007; Knoll, 1999).

2.5 Natural Decay Series

There are three naturally occurring radioactive series; namely Uranium series, Actinium series and Thorium series (IAEA-TECDOC-1363, 2003; Shleien, and Terpilak, 1987; Lederer, and Shirley, 1978). The uranium decay series (Table 2.1) starts from ^{238}U which decays by alpha emission to produce thorium (^{234}Th) which is itself unstable and further decays by beta emission to produce protactinium (^{234}Pa) and this process goes on until stable lead (^{206}Pb) is produced.

The actinium decay series (Table 2.2) starts from ^{235}U and decays by alpha emission to produce thorium (^{231}Th) which is also unstable and further decays by beta emission to produce protactinium (^{231}Pa) and the process goes on until stable lead (^{207}Pb) is produced.

The thorium decay series (Table 2.3) begins from ^{232}Th and decays by alpha emission to radium (^{228}Ra), which decays by beta emission to actinium (^{228}Ac) and this process goes on until stable lead (^{208}Pb) is produced.

Each of the three natural radioactivity series contains a radioactive daughter nuclide which is gaseous i.e. ^{222}Rn (radon-^{238}U series), ^{219}Rn (actinon-^{235}U series) and ^{220}Rn (thoron-^{232}Th series). Radium (^{226}Ra) decays by alpha emission to radon, ^{222}Rn, which is a radioactive inert gas. Radon decays by alpha emission to give a progeny of radioactive daughters. The existence of this gas (mainly radon and thoron) in the chains is one of the main reasons for the public health concerns about the naturally occurring environmental radioactivity. The gas diffuses from the soil and rocks into the air and can concentrate in poorly ventilated homes, public buildings and underground mines (WHO, 2009; Turner, 2007; UNSCEAR, 2000). The concentration of radon gas depends on the concentration of uranium and thorium radionuclides in the soil, rocks and building materials. The radioactive radon daughters which are solids under ordinary conditions attach themselves to atmospheric dust. Radon and its progeny radionuclides (^{218}Po, ^{214}Pb, ^{214}Bi, ^{214}Po, ^{210}Pb, ^{210}Bi, ^{210}Po and ^{206}Pb) in dust present a health hazard since both radon and dust may be inhaled into the lungs. The alpha particles emitted from the decay of radon and its progeny damage the lung tissue thus causing lung cancer (WHO, 2009; BEIR VII; UNSCEAR, 2000).

The decay scheme of ^{226}Ra shown in Figure 2.1 below (Turner, 2007), show how radon gas is produced by alpha emission from ^{226}Ra. The two modes of alpha decay of ^{226}Ra along with the alpha-particle energies and frequencies are shown by the two slanting arrows. Either changes the nucleus from that of ^{226}Ra to that of ^{222}Rn. When the lower energy particle is emitted, the radon nucleus is left in an excited state (5.5 %) with energy 186 keV above the ground state. The subsequent gamma ray of energy 186 keV, is emitted almost immediately to take ^{222}Rn gas to its ground state as shown by the vertical wavy line in the Fig 2.1 below.

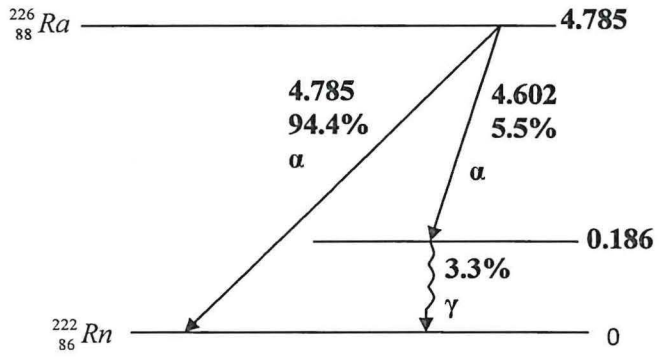

Figure 2.1: Decay Scheme of Ra-226

The frequency of 3.3% associated with this photon emission implies that an internal-conversion electron is emitted in the other 2.2% of the total number of disintegrations. When an internal conversion electron is emitted, it leaves a vacancy in the K or L shell of ^{222}Rn. Thus characteristic x-rays are also emitted (Turner, 2007).

There are also non-series naturally occurring radioisotopes that are alpha, beta and gamma radiation emitters. They include, potassium (^{40}K, 89%β and 11% γ), rubidium (^{87}Rb, 100%β), lanthanum (^{138}La, 100%β, 30%and 70%γ), samarium (^{147}Sm, 100%α), lutetium (^{176}Lu, 100%β, 15%, 85% and 95%γ) and rhenium (^{187}Re, 100%β) (Lederer and Shirley, 1978). Potassium-40 is found in the soil and rocks with an isotopic abundance of 0.0118% in the earth's crust (IAEA-TECDOC-1363, 2003; Lederer and Shirley, 1978).

Table 2.1: Uranium Decay Series

Nuclide	Half-life	Major radiation energies (MeV) and intensities*		
		α	β	γ
^{238}U	4.468×10^9 y	4.15 (23%) 4.19 (77%)	–	–
^{234}Th	24.1 d	–	~0.103 (19%) 0.191 (81%)	0.063 (3.5%) 0.093 (4%)
^{234}Pa	1.18 m	–	2.29 (98%) 1.001 (0.60%)	0.765 (0.30%)
99.86% ↓ 0.14%				
^{234}Pa	6.7 h	–	0.53 (66%) 1.13 (13%)	0.10 (50%) 0.70 (24%) 0.90 (70%)
^{234}U	2.48×10^5 y	4.72 (28%) 4.77 (72%)	–	0.053 (0.2%)
^{230}Th	7.52×10^4 y	4.62 (24%) 4.68 (76%)	–	0.068 (0.6%) 0.142 (0.07%)
^{226}Ra	1602 y	4.60 (5.5%) 4.78 (94.5%)	–	0.186 (4%)
^{222}Rn	3.825 d	5.49 (~100%)	–	0.510 (0.07%)
^{218}Po	3.05 m	6.11 (100%)	0.33 (100%)	–
99.98% ↓ 0.02%				
^{214}Pb	26.8 m	–	1.03 (6%)	0.295 (19%) 0.352 (36%)
^{218}At	2s	6.65 (6%) 6.70 (94%)	0.67 (94%)	–
^{214}Bi	19.7m	5.61 (100%)	3.26 (100%)	0.609 (47%) 1.120 (17%) 1.764 (17%)
99.96% ↓ 0.04%				
^{214}Po	164 μs	7.83 (100%)	–	0.799 (0.014%)
^{210}Tl	1.32 m	–	2.3 (100%)	0.296 (80%) 0.795 (100%) 1.31(21%)
^{210}Pb	~22 y	3.7 (1.8×10^{-8} %) 0.064 (15%)	0.017 (85%)	0.047 (4%)
^{210}Bi	5.02 d	4.93 (60%) 4.89 (34%) 4.59 (5%)	1.155 (100%)	–
~100% ↓ ~.00001%				
^{210}Po	138.3d	5.30 (100%)	–	0.803 (0.0011%)
^{206}Tl	4.19m	–	1.520 (100%)	–
^{206}Pb	Stable	–	–	–

Table 2.2: Actinium Decay Series

Nuclide	Half-life	Major radiation energies (MeV) and intensities*		
		α	β	γ
^{235}U	7.13×10^8 y	4.36 (18%) 4.39 (57%) 4.1-4.6 (8%)	–	0.143 (11%) 0.185 (54%) 0.204 (5%)
^{231}Th	25.64 h	–	0.300 (~100%)	0.026 (2%) 0.084 (10%)
^{231}Pa	3.43×10^4 y	5.01 (<20%) 4.99 (25.4%) 4.94 (22.8%)	–	0.027 (6%) 0.29 (6%)
^{227}Ac	22 y	4.95 (48.7%) 4.94 (36.1%) 4.87 (6.9%)	0.046 (100%)	0.070 (0.08%)
98.8% / 1.2%				
^{227}Th	18.17 d	5.76 (21%) 5.98 (24%) 6.04 (23%)	–	0.050 (8%) 0.237 (15%) 0.31 (8%)
^{223}Fr	21 m	5.34 (.005%)	1.15 (100%)	0.050 (40%) 0.080 (13%) 0.234 (4%)
^{223}Ra	11.68 d	5.61 (26%) 5.71 (53.7%) 5.75 (9.1%)	–	0.149 (10%) 0.270 (10%) 0.33 (6%)
^{219}Rn	3.92s	6.42 (8%) 6.55 (11%) 6.82 (81%)	–	0.272 (9%) 0.401 (5%)
^{215}Po	1.83 ms	7.38 (100%)		–
^{211}Pb	36.1 m	–	0.95 (1.4%) 0.53 (5.5%) 1.36 (92.4%)	0.405 (3.4%) 0.427 (1.8%) 0.832 (3.4%)
^{211}Bi	2.16 m	6.28 (17%) 6.62 (83%)	0.60 (0.28%)	0.351 (14%)
0.32% / 98.68%				
^{211}Po	0.52 s	7.43 (99%)	–	0.570 (0.5%) 0.90 (0.5%)
^{207}Tl	4.79 m	–	1.44 (100%)	0.897 (0.16%)
^{207}Pb	Stable	–	–	–

Table 2.3: Thorium Decay Series

Nuclide	Half-life	Major radiation energies (MeV) and intensities*		
		α	β	γ
^{232}Th	$1.39x10^{10}$ y	3.95 (24%) 4.01 (76%)	–	–
↓				
^{228}Ra	5.75 y	–	0.055 (100%)	–
↓				
^{228}Ac	6.13h	–	2.11(100%)	0.34 (15%) 0.908 (25%) 0.96 (20%)
↓				
^{228}Th	1.913 y	5.34 (28%) 5.42 (71%)	–	0.084 (1.6%) 0.214 (0.3%)
↓				
^{224}Ra	3.64d	5.45 (5.5%) 5.68 (94.5%)	–	0.241(3.7%)
↓				
^{220}Rn	55.6 s	6.30 (~100%)	–	0.55 (0.07%)
↓				
^{216}Po	0.145 s	6.78 (100%)	–	–
↓				
^{212}Pb	10.64 h	–	0.580	0.239 (47%) 0.300 (3.2%)
↓				
^{212}Bi	60.5 m	6.05 (70%) 6.09 (30%)	2.25 (100%)	0.040 (2%) 0.727 (7%) 1.620 (1.8%)
↓ 64.0%	↓ 36.0%			
^{212}Po	304 ns	8.78 (100%)	–	–
	^{208}Tl 3.1 m	–	1.80 (100%)	0.511 (23%) 0.583 (86%) 0.860 (12%) 2.614 (100%)
↓				
^{208}Pb	Stable	–	–	–

2.6 Ionizing Radiation Exposure Pathways

Human beings are exposed to ionizing radiation via three basic pathways; inhalation, ingestion and direct exposure.

Exposure by the inhalation pathway occurs when people breathe radioactive materials into their lungs. The main concerns are radioactively contaminated dust, smoke, or gaseous radionuclides such as radon (UNSCEAR, 2008). Radioactive particles can lodge in the lungs and may remain there for a long time. As long as the radioactive particles remain in the lungs and continue to decay there, the exposure continues. Inhalation is of most concern for radionuclides that are alpha or beta particle emitters. Alpha and beta

particles can transfer large amounts of energy to surrounding tissue, damaging DNA or other cellular material. This damage can eventually lead to cancer or other diseases and mutations (US EPA, 2012). According to the World Health Organisation (WHO, 2009), inhalation of radon and its progeny are the major causes of lung cancer in the US (United States of America) and the UK (United Kingdom). It is believed that every year more than 15 000 deaths from lung cancer occur due to radon exposure in the United Sates and more than 2 500 deaths in the United Kingdom (WHO, 2009). Exposure to radon and its progeny is the main cause of lung cancer in non-smokers and is more likely to cause lung cancer in smokers. Radon is estimated to cause between 3 – 14% of all lung cancers, depending on the average radon level in the country (WHO, 2009).

Exposure by the ingestion pathway occurs when someone swallows radioactive materials in radioactively contaminated water from polluted underground water sources, and food contaminated with radioactive materials from the soil and air. Nuclear reactor accidents like Windscale in 1957, Three Mile Island in 1979 and Chernobyl nuclear power plant in 1986 have caused widespread exposure and contamination of the members of the public and the surrounding environment with iodine-131, caesium-134 and caesium-137 radionuclides (UNSCEAR, 2000). Chernobyl nuclear power plant disaster alone resulted in widespread radioactive contamination of millions of people and the environment by iodine-131and caesium-137 in three most affected countries of Belarus, the Russian Federation and Ukrain (BEIR VII). Alpha and beta emitting radionuclides are of most concern for ingested radioactive materials because they release large amounts of energy directly to tissue, causing DNA and other cell damage and may expose the entire digestive system, the kidneys and other organs, as well as the bones. Radionuclides in the body tend to concentrate in specific organs because of their chemical nature (UNSCEAR, 2000). For instance, radioactive iodine tends to concentrate in the thyroid gland because the body needs iodine to function normally and cannot differentiate radioactive and non radioactive iodine. Thus radioiodine can cause the cancer of the thyroid gland. Radium (^{226}Ra) tends to concentrate in calcium rich areas such as the teeth and the bones. Thus radium may cause bone cancer due to its accumulation in the bones (US EPA, 2012).

External exposure is mainly due to gamma rays emitted by radionuclides from natural sources or fallout from atomic bomb tests and nuclear accidents (UNSCEAR, 2008; BEIR VII). Since gamma rays are more penetrating than alpha or beta particles, they can

penetrate the skin and generate a dose in various tissues. The skin offers some protection against low penetrating ionizing radiations such as alpha and beta particles but not gamma rays.

The effects of ionizing radiation exposure depend on a number of factors such as the radiation dose, its source (internal or external), its distribution in the body and the duration over which it is received and sensitivity of the exposed individual which can be influenced by both sex and age (HPA, 2011).

2.7 Effects of Ionizing Radiation on the Human Body

Ionizing radiation has sufficient energy to strip off electrons from atoms or even breakup the chemical bonds (BEIR VII). Ionizing radiation exposure may cause damage to body tissues or organs. This damage may impair the functioning of tissues or organs and can produce acute health effects such as skin redness and blackening of the skin, hair loss, radiation burns, or radiation poisoning. The health effects from exposure of the human body range from minor to severe depending on the dose of the radiation received. These health effects are divided into stochastic and non-stochastic (Micheal, 2014).

Stochastic effects are associated with low-level, long-term (chronic) exposure to ionizing radiation (Micheal, 2014). Stochastic effects may ensue if an irradiated cell is modified rather than killed. Modified cells may, after a prolonged delay, develop into a cancer. The body's repair and defense mechanisms make this a very improbable outcome at small doses without a threshold dose below which cancer cannot result. The probability of occurrence of cancer is higher for higher doses, but the severity of any cancer that may result from irradiation is independent of the dose. If the cell damaged by radiation exposure is a germ cell, whose function is to transmit genetic information to progeny, it is conceivable that hereditary effects of various types may develop in the descendants of the exposed individual (IAEA-DS379, 2009). The likelihood of stochastic effects is directly proportional to the dose received, without a dose threshold. The cancer risk is higher for children and adolescents, as they are significantly more sensitive to ionizing radiation exposure than adults (UNSCEAR, 2000). Other stochastic effects that occur include changes or mutations in DNA. Sometimes the body processes fail to repair these mutations or even creates further mutations during the repair processes. The mutations can be teratogenic or genetic. Teratogenic mutations are caused by exposure of the fetus

to ionizing radiation in the uterus and affect only the exposed mother. For the exposure of the mother above various threshold dose values during certain periods of pregnancy, severe mental retardation and congenital malformations of the fetus may occur (IAEA-DS379, 2009). Genetic mutations are passed on to off-springs (Micheal, 2014; BEIR VII; US EPA, 2012; IAEA Training course series 40, 2010).

Deterministic or non-stochastic effects are the result of various processes, mainly cell death and delayed cell division, caused by exposure to high levels of ionizing radiation. If extensive enough, these can impair the function of the exposed tissue. The severity of a particular deterministic effect in an exposed individual increases with the dose above the threshold for the occurrence of the effect. Non-cancerous health effects of exposure to ionizing radiation such as radiation burns and radiation sickness are non-stochastic. The short-term and high-level exposure to ionizing radiation is referred to as acute exposure. Unlike cancer, health effects from acute exposure to ionizing radiation usually appear within minutes, days or months after exposure. Acute health effects such as radiation burns and sickness (radiation poisoning) may cause premature aging or even death. For fatal dose of 3 - 5 Sv, death may occur within minutes or hours. The symptoms of radiation sickness include: nausea, weakness, hair loss, skin burns or diminished organ function (Micheal, 2014; US EPA, 2012; IAEA training course series 40, 2010; IAEA-DS379, 2009; ICRP 60).

2.8 Detection and Measurement of Ionizing Radiation

Ionizing radiation can be measured by utilizing its physical and chemical effects on matter. The field and laboratory methods of detecting ionizing radiation are based mainly on the ionizing properties of the radiation. Radiation detection and measurements are taken in two modes: pulse counting and spectrometry. In pulse counting, the number of pulses is recorded and not their heights. In spectrometry, both the number of pulses and their heights are measured; the pulses are then sorted to the channels of a multichannel analyzer according to their heights. Pulse counting can only be used for samples containing one single radionuclide or when gross pulse rates are measured. Whenever information on the energy of the pulses is needed, for example in the identification of radionuclides from a mixture, spectrometry is used. The main radiation detection and

measuring devices are gas-filled, semiconductor and scintillation (liquid or solid) detectors (Dirk, 2011; Parks, 2009; Turner, 2007).

Gas-filled detectors are used for x-rays or low energy gamma rays. They include ionization chambers, proportional counters and Geiger-Müller counters. The gas ionization detector is typically an argon gas-filled metal tube with an end window or windowless, where a metal wire in the middle of the tube acts as the anode, while the tube wall is the cathode. A voltage potential is applied between the electrodes to create an electric field in the fill gas. When the ionizing particle enters the chamber through the window, the neutral gas atoms in the chamber are ionized. The electric field created by the high voltage applied in the chamber causes the electrons and positive ions to drift towards the anode and the cathode respectively. This generates an ionization current pulse which can be measured by an electrometer (Turner, 2007). The principle of operation of the gas ionization detector is illustrated in Figure 2.2 and Figure 2.3 below.

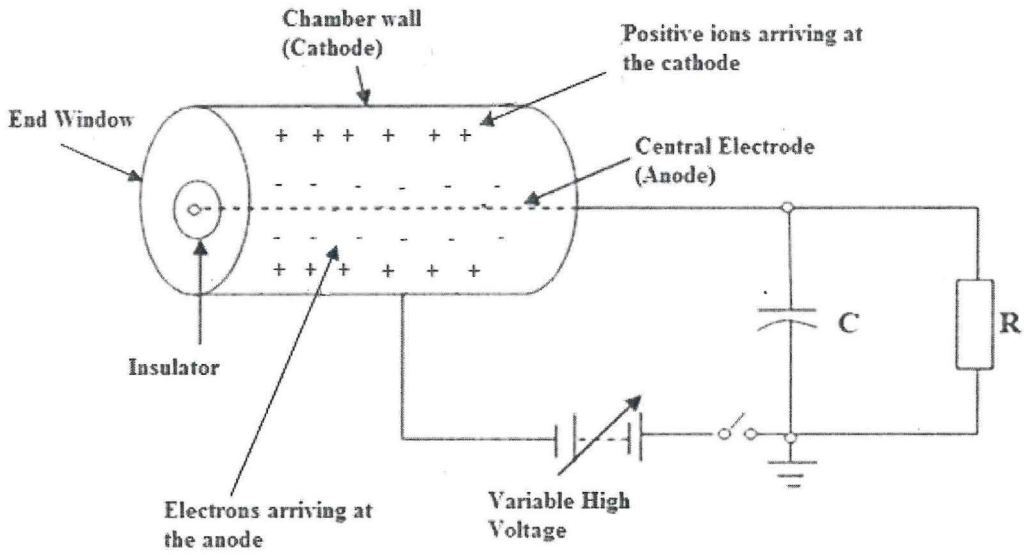

Figure 2.2: Schematic illustration of Gas Ionization Chambers

Since the number of ion pairs produced in the chamber is directly proportional to the initial energy of the ionizing particle, then the magnitude of the current pulse can be used to determine the energy spectrum of the incident ionizing particle (Joseph, 2013; Dirk, 2011; Turner, 2007). Figure 2.3 (Parks, 2009; Turner, 2007) below illustrates the

detection properties of different gas filled detectors on operational range of the anode voltage.

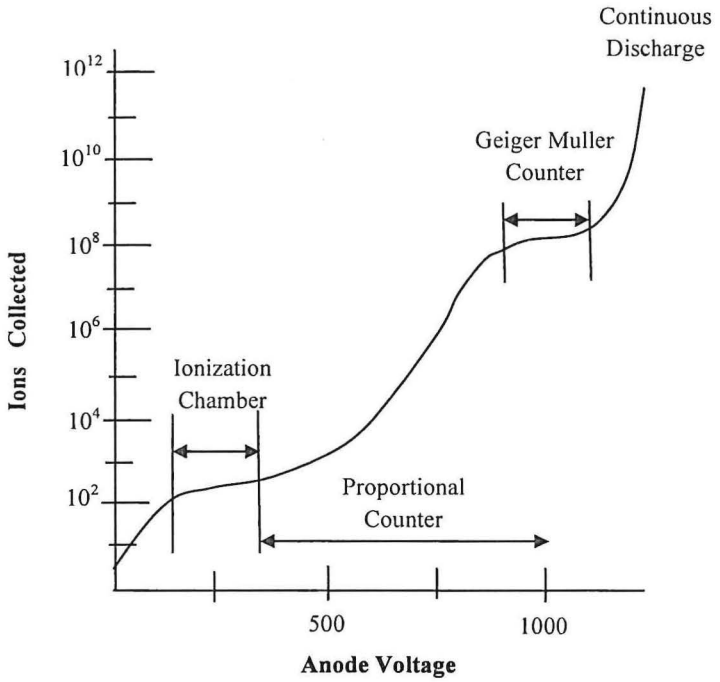

Figure 2.3: Operational range of Gas filled Detectors

If the anode voltage is low, the electrons may recombine with the ions and not all of them are collected at the anode. Recombination could also occur for a high density of ions. As the anode voltage is increased nearly all electrons are collected, and the detector becomes known as an ionization chamber. At a higher anode voltage the generated electrons are accelerated towards the anode at energies high enough to ionize other atoms, thus creating a cascade process and a larger number of electrons. The number of electrons collected is directly proportional to the initial ionization. This type of detector is known as a proportional counter. At still higher voltages on the anode, the electron multiplication is even greater, and the number of electrons collected is independent of the initial ionization. This region of operation yields the Geiger-Müller counter. The large output pulse in this type of detector is the same for all the photons. If the anode voltage is increased further, a continuous discharge occurs and this region is unsuitable for the counting process. The Geiger-Müller counter produces a large voltage pulse that is easily counted without further amplification. No energy measurements are possible since the

output pulse height is independent of initial ionization (Turner, 2007). The operating voltage is in the plateau region, which can be relatively flat over a wide range of bias voltage. The discharge produced by ionization must be quenched in order for the detector to be returned to a neutral ionization state and be ready for the next pulse. This is achieved by using a fill gas that contains a small amount of a halogen in addition to a noble gas. The voltage drop across a large resistor between the anode and bias supply will also serve to quench the discharge since the operating voltage will be reduced below the plateau. The Geiger-Müller counter is insensitive or dead after each pulse until the quenching is complete. Geiger-Müller counters are available in a wide variety of sizes, generally with a thin mica window (Joseph, 2013; Dirk, 2011; Turner, 2007). The detection efficiency of Geiger Muller counters is less than 2% and the dead time is of the order of 10^{-4} s, which limits the counter to low count rate applications (Knoll, 2000).

Semiconductor detectors such as silicon and germanium are widely used in gamma and alpha spectrometry. Silicon semiconductor detectors are mainly used in alpha spectrometry while germanium detectors are used in gamma spectrometry. In a semiconductor detector, two semiconducting parts are attached together. One part is an n-type semiconductor with mobile electrons, while the other part is a p-type semiconductor with positive holes. When an electric field is applied across the p-n in a reverse bias mode, a region depleted of holes and electrons is formed at the interface of the n and p type semiconductors. When a gamma ray or alpha particle hits this depleted region, electron-hole pairs are formed in the region making conduction possible. The electric field then produces an electric pulse which can be recorded in the external circuit. Germanium semiconductor detectors use electronic charge carriers (electron-ion and electron-hole pairs) created by the absorption of gamma ray photons in the germanium detector. These charge carriers form directly on the detector electrodes, causing a flow of electric current through the semiconductor and produce an output voltage pulse of amplitude proportional to the energy of the incident gamma ray photon. The detector consists of a germanium crystal mounted in a vacuum cryostat cooled to -196 °C. Cooling is achieved by insertion of the cryostat into a dewar vessel filled with liquid nitrogen, or by electrically powered cryogenic refrigerators. Germanium detectors are generally of small volume, are used in in-situ gamma ray spectrometry and have superior energy resolution (0.5% at 122 keV) as compared to scintillation detectors.

A scintillation detector consists of a scintillator such as sodium iodide and a photomultiplier. A scintillator is a substance which emits light when struck by an ionizing particle (Joseph, 2013; Dirk, 2011; Parks, 2009; Turner, 2007). An incident gamma ray photon interacts with the material of the scintillation crystal to produce scintillations. The scintillation photons induce the ejection of electrons from the photocathode of the Photomultiplier Tube (PMT). The ejected electrons are multiplied in the PMT with ten or more dynodes, each multiplying the number of electrons by a certain factor. This is accomplished by an electric field of about one thousand volts applied at the end of the tube, achieving an electron multiplication factor in the range of 10^7 - 10^{10} (Turner, 2007). At the end of the tube, the electrons generate an electric current signal whose magnitude is directly proportional to the scintillation light photon output, which is also directly proportional to the energy of the incident ionizing particle (Parks, 2009; Turner, 2007).

Since materials emit and absorb photons of the same wavelength, impurities are usually added to the scintillators to act as wavelength shifters, such that the wavelength of the emitted light photon does not fall into a self-absorption region (Turner, 2007). This is why thallium is added to sodium iodide crystals so that the designation is always NaI(Tl).

Scintillation detectors are widely used in gamma ray spectrometry. Thallium-activated sodium iodide [NaI(Tl)] crystals are mainly used as detectors in field gamma ray surveys (IAEA-TECDOC-1363, 2003). Sodium iodide detector crystals are transparent, with a high density (3.66 g/cm), and can be manufactured in large volumes. They have a detection efficiency of up to 13% (Turner, 2007). The dead time is of the order of 10^{-7} s and the energy resolution for Cs-137 at 662 k eV ranges from 7 – 10%, depending on the volume of the detector. The NaI(Tl) detectors are hygroscopic, they can age and are fragile, and the photomultiplier tube function is dependent on temperature (Joseph, 2013). Their large crystal volumes are an advantage in applications such as airborne gamma ray surveying where measurement times are short. Thallium-activated Caesium-iodide CsI(Tl) crystals are neither hygroscopic nor fragile i.e. do not break easily. They have a density of 4.51 g cm^{-3}, and a dead time of the order 10^{-9} s. But they are too expensive for widespread use (IAEA-TECDOC-1363, 2003).

2.9 Gamma Ray Spectroscopy

Gamma ray spectroscopy is one of the most developed and important techniques used in experimental nuclear physics because gamma ray detection and its energy measurement form an essential part of experimental nuclear physics research. Gamma ray spectroscopy is the quantitative study of the energy spectra of gamma ray sources. It is an analytical method that allows the identification and quantification of gamma ray emitting isotopes in a variety of matrices. In one single measurement and with little sample preparation, gamma ray spectrometry allows detection of several gamma ray emitting radionuclides in the sample. The measurement gives a spectrum of gamma lines which can be used to measure the intensity and energy of the emitted gamma rays (IAEA-TECDOC-1363, 2003).

There are different factors that determine the choice of a suitable gamma ray spectroscopy system for ionizing radiation detection and measurement. These are: the resolution which determines the complexity of the spectrum that can conveniently be analyzed; the detection efficiency which dictates the source strength necessary for the measurement of a spectrum; the simplicity of the arrangement and the ease of data accumulation; and secondary factors such as, the response linearity, the stability, the photoelectric interactions to Compton interactions ratio and the timing accuracy as well as detector availability.

Two of the major gamma spectroscopy devices used in gamma spectroscopy are: High purity Germanium (HpGe) spectrometer and Sodium Iodide (NaI) spectrometer (IAEA-TECDOC-1363, 2003). The sodium iodide (NaI) scintillator detector provides high efficiency gamma ray detection at moderate energy resolution. The high-purity germanium (HpGe) semiconductor detector gives high resolution energy spectra at low efficiency. One disadvantage of NaI detectors is that NaI absorbs water from the atmosphere which destroys the crystal and for this reason the crystal must be kept sealed. Another disadvantage of any scintillation counter is that the scintillation photons are detected using a photomultiplier tube (PMT).

In gamma ray spectroscopy using NaI(Tl) detector, the gamma rays interact with the detector atoms by three principal mechanisms: the photoelectric absorption, the Compton

scattering and the pair production (Parks, 2009; Turner, 2007). The interaction mechanisms are illustrated in the Figure 2.4 below.

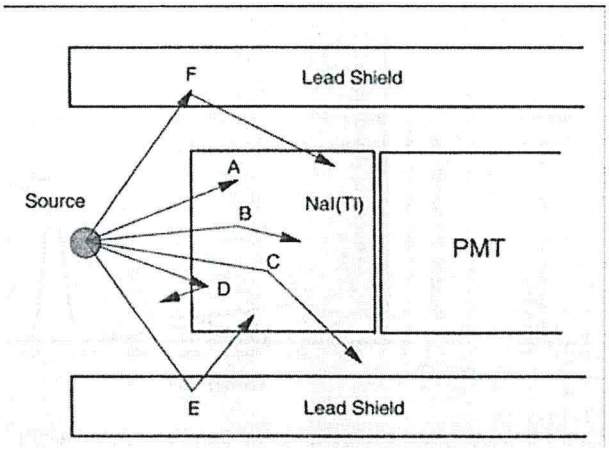

A. Photoelectric absorption
B. Compton Scattering and Photoelectric
C. Compton Scattering
D. Photoelectric with characteristic X-ray escape
E. Compton Scattered photon from lead shield
F. Characteristic X-ray from lead shield

Figure 2.4: Interaction of gamma rays with the detector material

Photoelectric absorption is the main mode of interaction of low energy gamma rays with the detector. In the photoelectric absorption process, a gamma photon, incident on an absorber atom, is completely absorbed. In its place, an energetic photoelectron is ejected by the atom from one of its bound shells. For gamma photons of sufficient energy, the most probable origin of the photoelectron is the most tightly bound or K shell of the atom. The photoelectron appears with kinetic energy given by the equation

$$E_{e^-} = E - E_b \tag{2.6}$$

where E_{e^-} is the kinetic energy of the ejected photoelectron, E is the energy of the incident gamma ray and E_b is the binding energy of the photoelectron in its original shell. Since the energy of the incident gamma ray (typically about 0.5 MeV) is much greater than the binding energy of the electron of the ion (typically 10 - 100 eV), the energy of the freed electron may be considered to be equal to that of the incoming gamma ray. Thus the photoelectric effect results in a peak, called the photopeak, in the photomultiplier spectrum at energy equal to that of the incident gamma ray. Photoelectric effect increases with atomic numbers of the absorber atoms. This interaction leaves the absorber atoms in an ionized state with a vacancy in one of the bound electron shells. A free electron may then be captured from the medium or an electron from the higher (outer) shell orbitals of the absorber atom may make a transition to fill the vacancy left. In this cause,

characteristic x-rays are produced. These x-rays may be re-absorbed in the detector through photoelectric absorption involving electrons from less tightly bound shells and Auger electrons may also be produced (Turner, 2007; Parks, 2009; Knoll, 1999).

In Compton scattering interaction, the incoming gamma ray photon is deflected through an angle θ with respect to its original direction. The photon transfers a portion of its energy to the electron (assumed to be initially at rest with respect to the incident photon), which is then known as a recoil electron. Because all angles of scattering are possible, the energy transferred to the recoil electron varies from zero and has a maximum value when the scattering angle is 180^0 (Turner, 2007; Knoll, 1999). The electron recoils with speed v at some angle, ϕ with the initial direction of the photon. This is illustrated in Figure 2.5 below.

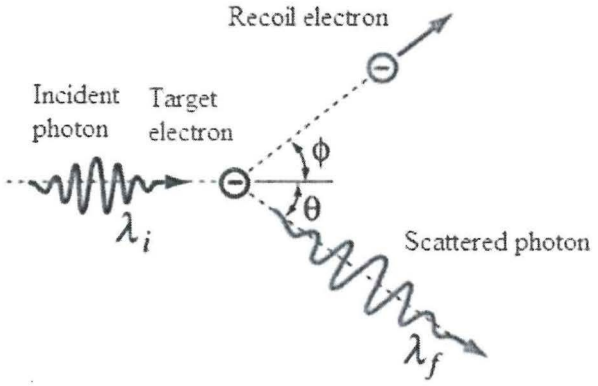

Figure 2.5: Schematic illustration of Compton scattering of photons

The probability of Compton scattering per atom of the absorber depends on the number of electrons in the atom and so it linearly increases with atomic number (Turner, 2007). The gamma ray's initial wavelength is $\lambda = \frac{hc}{E} = \frac{1240}{E}$ nm, where E in joules, is the energy of the incident gamma ray. The change in the wave-length due to reduction in energy of the gamma ray increases with the scattering angle, Θ according to the Compton formula given as

$$\Delta\lambda = \frac{h}{mc}(1-\cos\theta) = 0.00243(1-\cos\theta) \qquad (2.7)$$

where h = 6.63×10^{-34} Js, is Planck's constant, m = 9.11×10^{-31} kg, is the mass of the electron and c = 3.0×10^{8} ms^{-1}, is the speed of light (Parks, 2009). The energy of the

scattered electron varies from zero to a maximum value, the Compton edge, due to a wavelength shift of 0.00486 nm. The energy distribution of Compton scattered electrons is essentially a constant. The Compton spectrum produced by a photomultiplier tube is a flat plateau from zero energy up to the Compton edge where it drops off sharply at a rate limited by the energy resolution of the tube. The scattered photon may interact again with the atoms of the detector material. The probability of a second interaction taking place depends on four factors: the size of the detector material, the position of the first interaction in the detector material, the energy possessed by the scattered photon, and the nature of the detector material (Dirk, 2011; Parks, 2009). The Figure 2.6 below illustrates the characteristic spectrum of ^{137}Cs generated by NaI(Tl) scintillation detector.

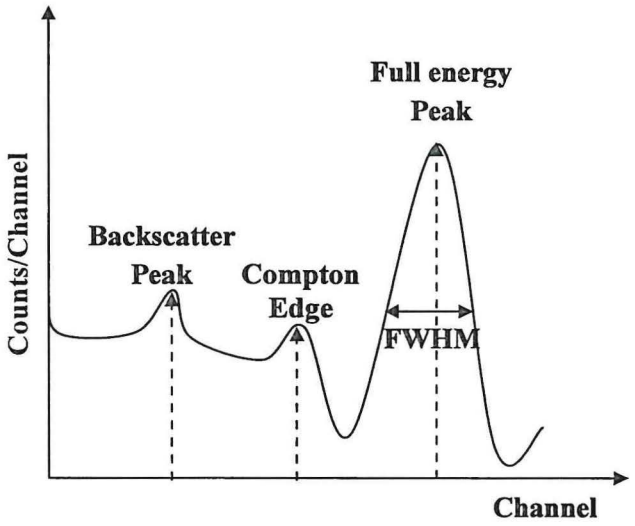

Figure 2.6: NaI(Tl) spectrum of Cs-137

The spectrum of Cs-137 has a back scatter peak at 181 keV, a Compton edge at 441 keV and a full energy peak at 622 keV (Dirk, 2011; Parks, 2009; Turner, 2007).

Pair production is another mechanism of interaction of gamma rays with the detector which pre-dominates at energies greater than twice the electron rest mass i.e. 1.02 MeV. If the incoming gamma ray energy is above 1.02 MeV, the gamma ray may spontaneously create an electron-positron pair and be totally absorbed. All the excess energy possessed by the photon above the 1.02 MeV required to create the pair appears as the kinetic energy of the positron and the electron pair. Because the electron-positron pair annihilate after slowing down in the absorbing medium, two annihilation photons each of energy

0.51MeV are normally produced as secondary products of the interaction. The annihilation photons are emitted in opposite directions in order to conserve the momentum of the original photon. The probability of pair production interaction per atom varies approximately as the square of the absorber atomic number (Knoll, 1999). The total kinetic energy of the emitted electron-positron pair is given by the equation

$$E_{e^-} + E_{e^+} = E - 2m_o c^2 \tag{2.8}$$

where E_{e^-} and E_{e^+} are kinetic energies of the electron and the positron respectively and E is the energy of the incident gamma ray photon. Pair production produces a full energy peak at energy E, one-escape peak at $E - mc^2$ and two escape peaks at $E - 2mc^2$, depending on whether both annihilation photons are absorbed in the scintillation detector. The relative importance of the three processes discussed above for different absorber materials and gamma ray energies is illustrated in Figure 2.7 (Parks, 2009) shown below.

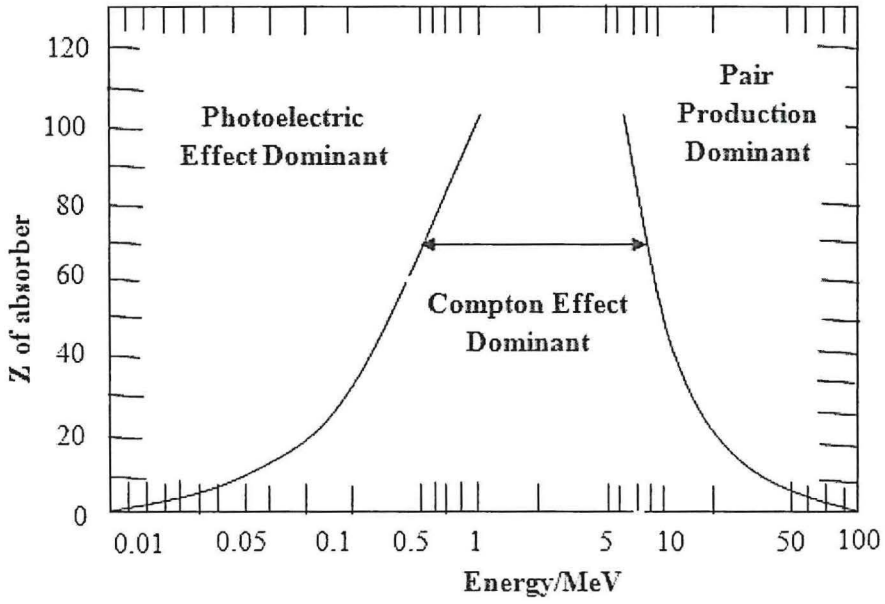

Figure 2.7: Dependence of the gamma ray interaction mechanisms on Z

The curve in the sketch above and on the left represents the energy at which photoelectric absorption and Compton scattering are equally probable as a function of the absorber atomic number, Z. The curve on the right represents the energy at which Compton scattering and pair production are equally probable. Three areas are thus defined on the

plot within which photoelectric absorption, Compton scattering and pair production each pre-dominate. The curves show the values of the atomic number, Z and energy for which the two neighbouring effects are just equal (Parks, 2009).

For a narrow beam of gamma ray photons, the gamma ray attenuation by the detector follows an exponential function expressed in the equation given below (Turner, 2007).

$$I = I_0 e^{-\mu x} \tag{2.9}$$

where I_0 is the initial intensity of the photons incident on the detector, I is the intensity of photons transmitted through the detector to a depth, x and μ is the linear attenuation coefficient (Turner, 2007). Gamma rays can cover hundreds to thousands of meters in air, up to 0.5 m in rocks and a few cm in lead (IAEA-TECDOC-1363, 2003).

2.10 Structure of a Sodium Iodide Detector

The sodium iodide detector doped with thallium is the most commonly used solid scintillation detector for gamma rays. This is because it can be produced in large crystal, yielding good efficiency. It also produces intense bursts of light compared to other spectroscopic scintillators. It can be produced in single crystal of up to 0.75 m in diameter and thickness of 0.25 m, with the properties described below. The thallium added to the crystal so that the detector becomes designated as NaI(Tl), provides an additional set of energy bands in the solid that contribute to the conversion of the energy of electrons into light photons (Turner, 2007; Knoll, 1999).

NaI crystal has a very high efficiency as a gamma ray detector due to its relatively high density of 3.67×10^3 kg m^{-3} and high atomic number combined with its large volume. The emission spectrum of NaI has peaks at 410 nm, and it's light conversion efficiency of 11.3%, is the highest of all the inorganic scintillators (Knoll, 1999). It is brittle, hygroscopic and sensitive to temperature gradient and thermal shocks. Potassium as an impurity in NaI crystals creates an internal gamma radiation background in the NaI detector because of radioactive Potassium, K-40. The NaI crystal is sealed in a cylindrical aluminum container with a face of beryllium or Mylar to prevent it from absorbing atmospheric moisture and to permit low energy radiation entry.

When gamma rays are absorbed in the NaI crystal, the atoms of the crystal are excited. As the atoms of the crystal return to their ground state, they emit photons (scintillations) of

light. The scintillations incident on the photocathode produce electrons by photoelectric emission (IAEA-TECDOC-1363, 2003).

The Photomultiplier Tube (PMT) is an integral part of a scintillation counter. It is made up of an evacuated glass tube in which photons are admitted through a window to the photocathode material. The anode and dynodes are biased by a chain of resistors typically located in a plug on tube base assembly. Photomultipliers acquire light through a glass or quartz window that covers a photosensitive surface, called a photocathode, which then releases electrons that are multiplied by electrodes known as metal channel dynodes. At the end of the dynode chain is an anode or collection electrode. The current flowing from the anode to ground is directly proportional to the photoelectron flux generated by the photocathode. The Figure 2.8 below illustrates the principle of operation of a Photomultiplier Tube (PMT).

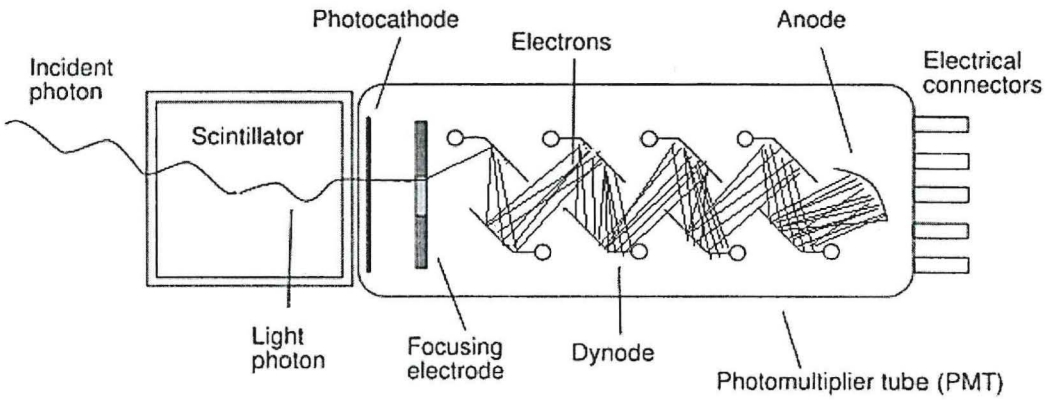

Figure 2.8: Schematic of a Photomultiplier Tube

The spectral response, quantum efficiency, sensitivity, and dark current of a photomultiplier tube are determined by the composition of the photocathode. The best photo-cathodes capable of responding to visible light are less than 30% efficient, meaning that 70% of the photons impacting on the photocathode do not produce a photoelectron and are therefore not detected. Spectral sensitivity of the photomultiplier depends on the chemical composition of the photocathode with the best devices having gallium arsenide elements, which are sensitive from 300 – 800 nm. The photocathode thickness is an important factor that must be considered to ensure the proper response from the absorbed photons. If the photocathode is too thick, more photons will be absorbed but fewer

electrons will be emitted from the back surface, but if it is too thin, too many photons will pass through without being absorbed. Photoelectrons are ejected from the front face of the photocathode and angled toward the first dynode. Electrons emitted by the photocathode are accelerated toward the dynode chain of up to 14 dynodes. Focusing electrodes are usually present to ensure that photoelectrons emitted near the edges of the photocathode will be likely to land on the first dynode. Upon impacting the first dynode, a photoelectron will cause the release of additional electrons that are accelerated toward the next dynode, and so on. The surface composition and geometry of the dynodes determines their ability to serve as electron multipliers. Because gain varies with the voltage across the dynodes and the total number of dynodes, electron gains of 10 million are possible if 12 – 14 dynode stages are employed. Photomultipliers produce a signal even in the absence of light due to a so called dark current arising from thermal emissions of electrons from the photocathode, leakage current between dynodes, as well as stray high-energy radiation. Electronic noise also contributes to the dark current and is often included in the dark-current value (Parks, 2009; Turner, 2007; Knoll, 2000).

The Figure 2.9 below illustrates the electronic block diagram of a NaI(Tl) gamma ray spectrometer. The assembly includes a NaI(Tl) detector, photomultiplier tube, high voltage (AC/DC) power supply, pulse amplifier and multichannel analyzer.

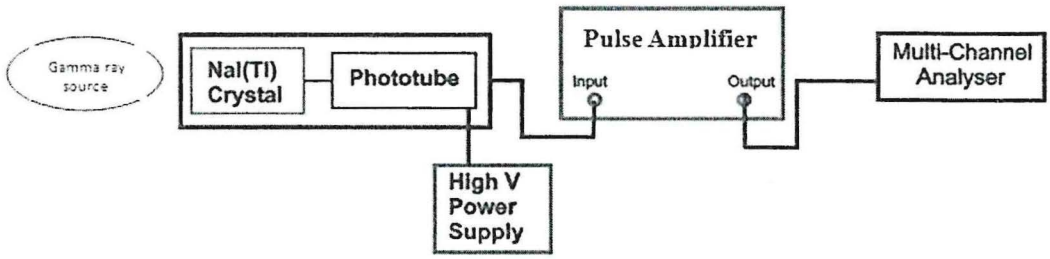

Figure 2.9: Electronic Block Diagram of NaI(Tl) detector system

The primary purpose of the pulse amplifier is to provide coupling between the detector and the rest of the counting system. It also minimizes any electronic noise pulses, which may be transmitted along with the pulse and improves the energy resolution of the system. The pulse output of the amplifier section is fed into the Single Channel Analyzer (SCA) or Multichannel Analyzer (MCA).

A multichannel analyzer whose central component is the Analog to Digital Converter (ADC) converts the analog voltage pulses from the pulse amplifier into digital signals which can be used by the computer. The multichannel analyzer software (installed in the computer) sorts each pulse as it arrives from the pulse amplifier according to its pulse amplitude and generates a fine-grained histogram of the number of voltage pulses from the detector versus pulse amplitude and, therefore, energy deposited in the scintillator. The pulse amplifier output is proportional to the energy of the incoming signal with a maximum of 10 V (Knoll, 1999).

The spectra produced by NaI(Tl) detectors have a Gaussian shape due to the limited energy resolution (IAEA-TECDOC-1363, 2003). The energy resolution of a detector is a measure of its ability to distinguish between two gamma rays of only slightly different energies. Resolution values are given with reference to specified gamma ray energies expressed in absolute (i.e., eV or MeV) values or relative terms. To express the resolution, R in relative terms, the Full Width of a photo peak at Half the Maximum amplitude (FWHM) in eV or MeV is divided by the energy of the gamma ray and multiplied by 100% (IAEA-TECDOC-1363, 2003). This is shown in the equation

$$R = \frac{FWHM}{E} \times 100\% \tag{2.10}$$

Figure 2.10 below shows how energy resolution of a gamma ray spectrometer may be determined.

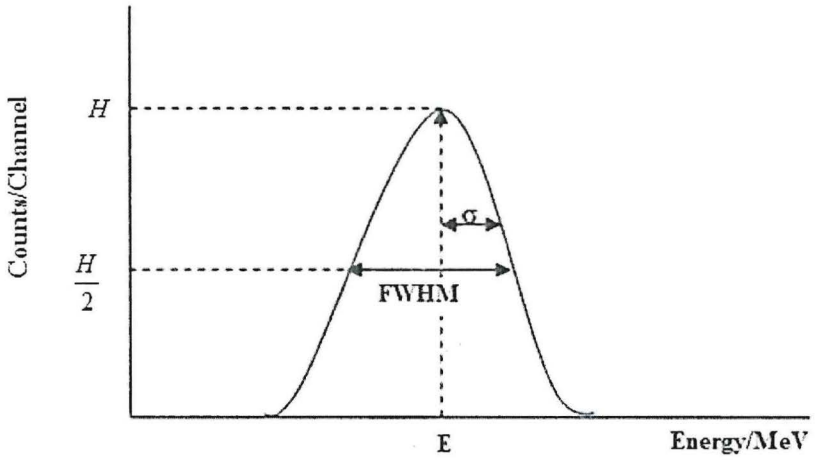

Figure 2.10: Energy Resolution by a Gamma ray spectrometer

In Figure 2.10 above, H represents the maximum pulse amplitude and σ is the standard deviation of the Gaussian function. For photopeaks with the Gaussian shape, the Full Width at Half Maximum amplitude (FWHM) is a function of the standard deviation, σ and this is shown in the equation (Turner, 2007)

$$\text{FWHM} = 2.35\sigma \tag{2.11}$$

The standard deviation is proportional to the square root of N as shown in the equation

$$\sigma = k\sqrt{N} \tag{2.12}$$

where N is the number of charge carriers generated as a result of a gamma ray interaction with the detector atoms and k is a constant of proportionality.

Thus equation 2.11 can be expressed in terms of N as shown in the equation

$$\text{FWHM} = \frac{2.35}{\sqrt{N}} \tag{2.13}$$

Equation 2.13 shows that the energy resolution of the detector improves as N is increased. Thus to achieve an energy resolution of less than 1%, the number of counts, N required must be greater than 55 000 (Knoll, 2000).

Not all gamma rays emitted by the source and pass through the detector will produce a count in the detector system (Knoll, 2000). The efficiency of a detector measures the probability that an incident photon will be absorbed in the detector and be detected. Efficiency of the detector is the ratio of number of detected photons to the total number of incident photons. The detection efficiency depends on the energy of the incident gamma ray, the detector crystal, the materials surrounding the crystal, the source/sample - detector geometry and attenuation in the source material.

Efficiency, like resolution, can be expressed in absolute terms or relative terms. Absolute efficiency is a measure of the probability that a gamma ray of a specified energy passing through a detector will interact and be detected. It relates to the number of gamma ray photons emitted by the source to the number of counts detected anywhere in the spectrum by the detector. This takes into account the full energy peak and all incomplete absorptions represented by the Compton continuum. Relative efficiency is a general performance measure relating the efficiency of detection of the 1332 keV ^{60}Co gamma ray for a point source placed centrally 25cm above the detector to that of the standard 7.6 cm x 7.6 cm sodium iodide scintillation detector (Joseph, 2013; David, 2006).

Detector efficiency can be determined experimentally by measuring calibration standard radionuclides with known activities. These may be cobalt-60, sodium-22, caesium-137 or europium-152. An efficiency calibration curve may be obtained by plotting the detector efficiency at various gamma ray energies emitted by standard radionuclides against the energy. The curve may be used to determine unknown gamma radiation energies in a given sample (Joseph, 2013; IAEA-TECDOC-1363, 2003).

2.11 Ionizing Radiation Quantities and Units

There are many quantities used in the measurement of ionizing radiation. Only quantities relevant to this study such as exposure, activity, specific activity, absorbed dose rate, dose equivalent rate, radium equivalent activity, external hazard index and internal hazard index have been discussed.

Exposure is defined for gamma rays and x-rays in terms of the amount of ionization they produce in air. The unit of exposure is called the roentgen (R). It was originally defined as that amount of gamma radiation or x-radiation that produces in air 1 electrostatic unit (esu) of charge of either sign per 0.001293 g of air. This mass of air occupies a volume of 1 cm^3 at standard temperature and pressure. The charge involved in the definition of the roentgen includes both the ions produced directly by the incident photons as well as ions produced by all secondary electrons. Since 1962, exposure has been defined by the International Commission on Radiation Units and Measurements (ICRU) as the quotient $\frac{\Delta Q}{\Delta m}$ where ΔQ is the sum of all charges of one sign produced in air when all the electrons liberated by photons in a mass Δm of air are completely stopped in air. The unit roentgen is now defined as 1 R = 2.58×10^{-4} C kg^{-1} (Turner, 2007; IAEA-TECDOC-1363, 2003). The concept of exposure applies only to electromagnetic radiation; the charge and mass used in its definition, as well as in the definition of the roentgen, refer only to air (Turner, 2007).

Activity is the measure of the amount of ionizing radiation being emitted or given off by a given radioactive source. The historical unit of measurement of activity is the curie (Ci) and the SI unit of measurement is the becquerel (Bq). One becquerel is equal to one radioactive decay per second. One curie (Ci) is equal to 3.7×10^{10} Bq (IAEA-DS379, 2009).

When the radioactive material decays, the amount of its radioactivity per unit mass is the specific activity. The unit of the specific activity is the becquerel per kilogram. The specific activity is used to describe the radionuclide content of soil, rocks, building materials etc (IAEA-TECDOC-1363, 2003). The Specific Activity (S.A) of a radionuclide in a sample is determined by use of the equation

$$\text{S.A} = \frac{\left(\frac{N_s}{t_s} - \frac{N_b}{t_b}\right)}{\eta \times k \times m} \text{ Bqkg}^{-1} \tag{2.14}$$

where N_s is the total number of counts of radionuclides in the sample, t_s is the duration of the sample counting in seconds, N_b is the total number of background counts obtained by collecting the background spectrum without the sample, t_b is the time in seconds of collecting the background spectrum, η is the detection efficiency of the spectrometer, k is the branching ratio (gamma radiation yield) of the radionuclide and m is the sample mass in kilograms. The branching ratio of a radionuclide is the probability that the decay of the radionuclide results in emission of the gamma ray. In the radionuclide table provided in IAEA-PUB-1287, (2007), the branching ratios of radionuclides are expressed in percentage.

When ionizing radiation strikes a material, it will deposit energy in that material through its interactions with the body. The fundamental dosimetric quantity in radiation protection is the absorbed dose, D. This is the energy absorbed by a material per unit mass and its unit is the joule per kilogram, which is given the special name gray (Gy). The ionizing radiation absorbing materials such as air, water, organ or tissue must be specified since energy deposition depends on the type of material exposed (IAEA training course series 40, 2010; Turner, 2007). Absorbed dose rate (ADR) or just dose rate (DR), D' is the ratio of an incremental dose, dD, in a time interval dt, expressed as

$$D' = \frac{dD}{dt} = \sum_R A_R \times D_{CC,R} \text{ nGyh}^{-1} \tag{2.15}$$

where $D_{CC,R}$ is the dose rate conversion factor (nGyh^{-1} per Bqkg^{-1}) and A_R is the specific activity of the radionuclide in the sample. The dose rate conversion factors recommended in UNSCEAR (2000) report for the gamma dose rate in soil samples are 0.462 nGyh^{-1} per Bqkg^{-1}, 0.604 nGyh^{-1} per Bqkg^{-1} and 0.0417 nGyh^{-1} per Bqkg^{-1} for ^{238}U (^{226}Ra), ^{232}Th

and ^{40}K respectively. Using the recommended conversion factors, the absorbed gamma dose rate, D'_a (nGyh^{-1}) in air may be calculated using the equation

$$D'_a = 0.462\,A_{Ra} + 0.604\,A_{Th} + 0.0417\,A_K \tag{2.16}$$

where A_{Ra}, A_{Th} and A_K are the average specific activities of ^{238}U (^{226}Ra), ^{232}Th and ^{40}K in the sample.

The external indoor Radiation Absorbed Dose Rate (D_{in}) is calculated for materials containing ^{238}U(^{226}Ra), ^{232}Th and ^{40}K by using the equation (EC 112, 1999) below.

$$D_{in} = 0.92\,A_U + 1.1A_{Th} + 0.08\,A_K \text{ nGy h}^{-1} \quad \text{.....(2.17)}$$

where 0.92 nGy h^{-1} per Bq kg^{-1}, 1.1 nGy h^{-1} per Bq kg^{-1} and 0.08 nGy h^{-1} per Bq kg^{-1} are the indoor absorbed dose rate conversion coefficients for ^{238}U(^{226}Ra), ^{232}Th, and ^{40}K (EC 112, 1999) and A_U, A_{Th}, and A_K are their respective specific activities.

The biological effects of an absorbed dose in a tissue are dependent on the type and the energy of the ionizing radiation incident on the material. The probability of stochastic effects is found to depend not only on the absorbed dose, but also on the type and energy of the radiation. The absorbed dose is weighted by a factor related to the type of radiation. The weighting factor is called the radiation weighting factor, W_R, and the weighted dose is called the equivalent dose (IAEA-DS379, 2009; Turner, 2007; ARPNSA Publication No 1, 2002). The equivalent dose is equal to the absorbed dose rate multiplied by a radiation weighting factor that takes into account the way in which a particular type of radiation distributes energy in the tissue. The weighting factor caters for the relative biological effectiveness of different radiations in a tissue or organ. The equivalent dose, H_T, is determined using the equation shown below;

$$H_T = \sum_R W_R D_{T,R} \tag{2.18}$$

where $D_{T,R}$ is the absorbed dose averaged over the tissue or organ, T, due to radiation, R. The unit of equivalent dose is joule per kilogram and has a special name sievert (Sv) (Turner, 2007; IAEA-DS379, 2009; ICRP 60). The values of radiation weighting factors for specified types and energy of radiations have been selected by the International Commission on Radiological Protection to be representative of values of the relative biological effectiveness of that radiation in inducing stochastic effects at low doses and are given in Table 2.4 below (Roger, 2011; IAEA-PUB-1287, 2007; ICRP 60).

Table 2.4: Weighting Factors for different kinds of Ionizing Radiation

Type of radiation	Radiation weighting factor W_R
Photons (x-rays and gamma rays)	1
Electrons and muons	1
Protons and charged pions	2
Alpha particle, fission fragments and heavy ions	20

The relationship between the probability of stochastic effects and equivalent dose is found also to depend on the irradiated organ or tissue. A further dosimetric quantity, effective dose, is therefore defined and takes into account the radiological sensitivities of different tissues. If the whole body were uniformly irradiated, the fractional contribution of each organ or tissue, T, to the total detriment resulting from the exposure to the radiation is represented by a tissue weighting factor, W_T. The effective dose, E, is the sum of the weighted equivalent doses in all tissues and organs and is given by the equation:

$$E = \sum_T W_T \times H_T \tag{2.19}$$

The organ or tissue weighting factor, W_T, is a dimensionless quantity just like the radiation weighting factor, W_R. The effective dose and the equivalent dose have the same unit which is the sievert (Sv). The effective dose is expressed in millisievert (mSv) because the quantity is very small (IAEA-DS379, 2009). For environmental gamma radiation, the effective dose is calculated using the equation given below.

$$E = D'_a \times t \times 10^{-6} \times 0.7 \tag{2.20}$$

where E is the effective dose (mSv), D'_a is the dose rate ($nGyh^{-1}$), t is the exposure time (hours) and 0.7 $SvGy^{-1}$ is the conversion factor for the human organs recommended in UNSCEAR, (2000) report.

To estimate the external outdoor annual effective dose rates, the conversion coefficient from absorbed dose rate in air to effective dose (0.7 $SvGy^{-1}$) for adult humans and outdoor occupancy factor of 0.2 proposed by UNSCEAR 2000 are used. In Uganda, about 82% of the labour force is majorly rural (UBOS, 2013). The average time spent on economic and care labour activity per week by rural dwellers is 55 hours (about 7.86 hours per day) and the national average is 57 hours (UBOS, 2013). The national average time spent working is about 8.14 hours per day. The average time spent outdoors by the

rural community is 7.86 hours per day which is about 33%. Therefore the average outdoor and indoor occupancy factors for the rural community are 0.33 and 0.67 respectively. The world average outdoor and indoor occupancy factors are 0.2 and 0.8 respectively (UNSCEAR, 2000). Thus the external outdoor Annual Effective Dose Rate (E_{out}) for South Western Uganda may be calculated using the equation given below (UNSCEAR, 2000).

$$E_{out} = [D_{out} \times T \times 0.7 \times 0.33 \times 10^{-6}] \text{ mSvy}^{-1} \quad (2.21)$$

where D_{out} (nGyh^{-1}) is the outdoor external absorbed dose rate in air and T is the number of hours in a year equal to 8760 h, E_{out} (mSvy^{-1}) is the external outdoor annual effective dose rate.

Since people spend most of their time indoors, the effect of exposure to gamma radiation from radionuclides in building materials may be significant. In order to assess the effect of indoor gamma radiation, the external indoor annual effective dose rate is calculated using the equation (UNSCEAR, 2000) below.

$$E_{in} = [D_{in} \times T \times 0.7 \times 0.67 \times 10^{-6}] \text{ mSvy}^{-1} \quad (2.22)$$

where D_{in} (nGyh^{-1}) is the external indoor absorbed dose rate in air and T is the number of hours in a year equal to 8760 h and E_{in} (mSvy^{-1}) is the external indoor annual effective dose rate.

The natural radioactivity in building materials is determined using the specific activities of ^{226}Ra (^{238}U), ^{232}Th and ^{40}K contents (UNSCEAR, 2000; EC 112, 1999). The radiation hazards from exposure of the human body to materials containing ^{226}Ra (^{238}U), ^{232}Th and ^{40}K may be expressed in terms of radium equivalent activity, external hazard index and internal hazard index (Beretka and Mathew, 1985).

Radium equivalent activity (Ra_{eq}) is a radioactivity measure introduced to represent the specific activities of ^{226}Ra, ^{232}Th and ^{40}K by a single quantity in Bq kg^{-1}, which takes into account the radiation hazards associated with them. It accounts for the gamma radiation output from different mixtures of radionuclides in a material. It is assumed that 370 Bq kg^{-1} of ^{226}Ra, 259 Bqkg^{-1} of ^{232}Th and 4810 Bq kg^{-1} of ^{40}K produce the same gamma radiation dose in a material (Xinwei, 2006). The radium equivalent activity may be determined using the equation below (Beretka and Mathew, 1985):

$$Ra_{eq} = A_{Ra} + 1.43 A_{Th} + 0.077 A_K \text{ Bqkg}^{-1} \quad (2.23)$$

where A_{Ra}, A_{Th} and A_K are the average specific activities of ^{226}Ra (^{238}U), ^{232}Th and ^{40}K respectively in the material. The value of radium equivalent activity of 370 Bqkg^{-1} corresponds to a dose equivalent of 1 mSv y^{-1} for a member of the public. It is therefore recommended that the value of radium equivalent activity in building material be lower than 370 Bqkg^{-1} in order to keep the exposure level of the public to less than 1 mSvy^{-1} (UNSCEAR, 2000).

External hazard index, H_{ex} is used as a measure of the radiation exposure due to natural radioactivity in environmental materials. The value of this index must be less than one (unity) in order to keep the dose equivalent of less than 1mSv per year for the public (UNSCEAR, 2000). The External hazard index, H_{ex} may be found using the equation

$$H_{ex} = \frac{A_{Ra}}{370} + \frac{A_{Th}}{259} + \frac{A_K}{4810} \tag{2.24}$$

where A_{Ra}, A_{Th} and A_K are the average specific activities of ^{226}Ra (^{238}U), ^{232}Th and ^{40}K respectively.

Also, radon and its short-lived decay products emanating from building materials and underground mines are hazardous to the respiratory organs. Internal hazard index, H_{in} is used to measure the radiation exposure due to radon and its progeny radionuclides in building materials. As radon gas decays, the alpha particles it emits may inflame the internal body organs and the non-gaseous decay products may get trapped in the respiratory tract. These may cause serious radiation health hazards such as inflammation of the digestive system and lung cancer. The Internal hazard index may be determined using the equation

$$H_{in} = \frac{A_{Ra}}{185} + \frac{A_{Th}}{259} + \frac{A_K}{4810} \tag{2.25}$$

where A_{Ra}, A_{Th} and A_K are the average specific activities of ^{226}Ra (^{238}U), ^{232}Th and ^{40}K respectively in the material. The value of this index must be less than one (unity) for the radiation hazard to be considered negligible i.e. in order to keep the dose equivalent of less than 1mSv per year for the public (UNSCEAR, 2000).

The Excess Lifetime Cancer Risk (ELCR) is a parameter used in this study to measure the probability of cancer induction in the mine workers and the members of the public who get exposed to the radionuclides in mine tailings. The excess lifetime cancer risk depends on the magnitude of the annual effective dose, the average lifetime of the exposed

population and the fatal cancer risk factor proposed in ICRP, (1991) Publication 60. According to UNSCEAR, (2000) report, the world average lifetime is taken to be 70 years, which is not applicable to Uganda, where the average life expectancy is 50.4 years (UBOS, 2012). The Risk Factor for cancer induction due to exposure to low doses of ionizing radiation is 0.05 Sv^{-1} according to ICRP Publication 60. Thus using the average life expectancy of Uganda of 50.4 years and the fatal cancer risk factor of 0.05 Sv^{-1}, the Excess Lifetime Cancer Risk for the mine workers and the members of the public in South Western Uganda was calculated using the equation given below.

$$ELCR = AEDE\ (mSv\ y^{-1}) \times 50.4\ y \times 0.05\ (Sv^{-1}) \quad (2.26)$$

where AEDE (mSv y^{-1}) is the total annual effective dose rate (sum of the outdoor and indoor annual effective dose rates) received by the adult population from exposure to the radionuclides in the tailings of Mashonga, Kikagati and Butare mines.

2.12 Related Studies on Natural Radioactivity in the Soil and Rock Mine Tailings

The study of gamma radiation as a form of ionizing radiation due to decay of naturally occurring radionuclides in materials has attracted a lot of attention because of their harm to humans. This study has included some related previous studies on the gamma activity levels of radionuclides in mines. Some of the studies have been discussed below.

A study by Isinkaye, (2013) of the activity levels of natural radionuclides in tailing enriched soil and sediment samples collected from two mining sites (abandoned gold mining site located at Itagunmodi village in Ilesa and tin, tantalite and kaolin mining sites in Ijero-Ekiti) both in Southwest Nigeria revealed that the mean specific activities of ^{226}Ra, ^{232}Th and ^{40}K were 20.04±10.95 $Bqkg^{-1}$, 106.40±48.67 $Bqkg^{-1}$ and 901.67±305.37 $Bqkg^{-1}$ respectively for soil samples and 30.84±11.34 $Bqkg^{-1}$, 94.32±25.36 $Bqkg^{-1}$ and 888.77±248.64 $Bqkg^{-1}$ respectively for sediment samples from Ijero mine. For samples from Ilesa mine, the mean specific activity concentration of ^{226}Ra, ^{232}Th and ^{40}K were 37.52±20.31 $Bqkg^{-1}$, 41.88±17.80 $Bqkg^{-1}$ and 441.71±126.04 $Bqkg^{-1}$ respectively for soil samples and 43.76±18.87 $Bqkg^{-1}$, 56.74±25.91 $Bqkg^{-1}$ and 592.94±353.18 $Bqkg^{-1}$ respectively for sediment samples. The mean specific activities of the radionuclides in soil and sediment obtained in this study area are higher than their world-wide average crustal values of 33 $Bqkg^{-1}$, 45 $Bqkg^{-1}$, and 420 $Bqkg^{-1}$ reported in UNSCEAR, (2000) report for ^{226}Ra, ^{232}Th and ^{40}K respectively. In order to evaluate the radiological hazards

of the natural radioactivity, the radium equivalent activity, external hazard index, absorbed gamma dose rates and the annual effective dose rates were determined in this study. The mean radium equivalent activity for soil and sediment samples were 240.28±75.22 $Bqkg^{-1}$ and 234.15±38.42 $Bqkg^{-1}$ respectively for Ijero mine and 131.41±28.08 $Bqkg^{-1}$ and 170.55±55.54 $Bqkg^{-1}$ respectively for Ilesa mine. The mean external hazard index for Ijero mine was 0.65±0.20 and 0.63±0.10 for soil and sediment samples respectively while that for Ilesa mine was 0.36±0.08 and 0.46±0.15 for soil and sediment samples respectively. The mean absorbed dose rates and the annual effective dose rates for Ijero were (110.78±32.92, 108.55±17.38) nGy h^{-1}, and (0.136±0.040, 0.133±0.021) mSv y^{-1} respectively for soil and sediment samples. For soil and sediment samples from Ilesa, the mean absorbed dose rates were (61.18±12.58, 79.39±26.14) $nGyh^{-1}$ and the mean annual effective dose rates were (0.075±0.015, 0.097±0.032) $mSvy^{-1}$ respectively. The mean values of these hazard indices are higher than the world average values i.e. 58 $nGyh^{-1}$ and 0.07 $mSvy^{-1}$ (UNSCEAR, 2008) respectively. This study did not determine the internal hazard index and excess lifetime cancer risk from exposure of the human body to radionclides in the tailings of the studied sites.

A study by Faanu, Darko, and Ephraim, (2011) on soil, rock, waste and tailing samples from Tarkwa gold mine in Ghana revealed that the mean specific activity levels of ^{238}U (^{226}Ra), ^{232}Th and ^{40}K were 13.61 ± 5.39 $Bqkg^{-1}$, 24.22 ± 17.15 $Bqkg^{-1}$ and 162.08 ± 63.69 $Bqkg^{-1}$, respectively which are below the world averages of 33 $Bqkg^{-1}$, 45 $Bqkg^{-1}$ and 420 $Bqkg^{-1}$ (UNSCEAR, 2000). The mean absorbed dose rate, mean outdoor annual effective dose rate and mean radium equivalent activity were 27.55 ± 15.10 $nGyh^{-1}$, 0.17 ± 0.09 $mSvy^{-1}$ and 61.00 ± 33.33 $Bqkg^{-1}$ respectively. The mean absorbed dose rate is about 0.47 times the world average of 59 $nGyh^{-1}$ (UNSCEAR, 2008). The mean annual effective dose is about 2.4 times the world average outdoor dose rate of 0.07 $mSvy^{-1}$ and the mean radium equivalent activity is about 0.16 times the maximum limit of 370 $Bqkg^{-1}$ (UNSCEAR, 2000). The external and internal hazard indices were less than unity with mean values of 0.16 and 0.20, respectively. The results obtained show that soil, rock and waste materials that may be used for construction of buildings may not pose any significant radiological hazards to the inhabitants in the study area. The excess lifetime cancer risk from radionuclides exposure in the studied samples of Tarkwa gold mine was not determined.

Usikalu, Anoka, and Balogun, (2011), measured the natural radioactivity levels of ^{226}Ra and ^{232}Th in Jos tin mine tailings in Northern Nigeria. The mean specific activities of ^{226}Ra and ^{232}Th in the tailings of site one were 512.24 $Bqkg^{-1}$ and 2635.78 $Bqkg^{-1}$ which were 15.52 and 58.56 times world averages (UNSCEAR, 2000) respectively. The mean absorbed dose rates and the mean annual effective dose rates in the tailings of site one for ^{226}Ra and ^{232}Th were 1828.66 $nGyh^{-1}$ and 2.28 $mSvy^{-1}$ which were 30.99 and 32.57 times the world averages respectively (UNSCEAR, 2000). For the tailings in site two, the mean specific activity of ^{226}Ra and ^{232}Th were 51.36 $Bqkg^{-1}$ and 378.08 $Bqkg^{-1}$ respectively and were 1.56 and 8.40 times their respective world averages. The mean absorbed dose rates and the mean annual effective dose rates in the tailings of site two for ^{226}Ra (^{238}U) and ^{232}Th were 252.08 $nGyh^{-1}$ and 0.31 $mSvy^{-1}$ which were 4.27 and 4.43 times their world averages respectively. This study did not determine the excess lifetime cancer risk, the radium equivalent activity, external hazard index and internal hazard index in Jos tin mine tailings.

Zaini, Ahmad, Mashuri and Redzuan, (2008) measured the surface radiation and natural radioactivity levels in amang (tailings) in an ex-tin mining area, Kg Gajah , Kinta valley Perak, in Malaysia. The mean specific activities of $^{226}Ra(^{238}U)$, $^{228}Ra(^{232}Th)$ and ^{40}K obtained in this study were 3798±419 $Bqkg^{-1}$, 12896±1533 $Bqkg^{-1}$ and 2521±298 $Bqkg^{-1}$ which were 115.09, 286.58 and 6.00 times the world averages (UNSCEAR, 2000) respectively. In this study, gamma dose rates, excess lifetime cancer risk, radium equivalent activity, external hazard index and internal hazard index were not determined.

A study by Lemeriga, (1998) on the activity levels of ^{238}U, ^{232}Th and ^{40}K in the soils of some places in Mbale District, Mukono District and Hoima District in Uganda revealed that the average specific activity of the three radionuclides were 23.97 $Bqkg^{-1}$, 173.88 $Bqkg^{-1}$ and 241.95 $Bqkg^{-1}$ respectively. The mean specific activity of ^{232}Th was four times higher than the world average (UNSCEAR, 2000). In this study by Lemeriga, gamma dose rates, excess lifetime cancer risk, radium equivalent activity, external hazard index and internal hazard index were not determined.

CHAPTER THREE: METHODOLOGY OF THE STUDY

3.1 Introduction

In this chapter, the procedures followed in mine tailing sample selection and processing and the method used to investigate the radionuclides present in the samples of the mine tailings are presented. The procedures of determination of the Specific Activity, Gamma dose rates and Radiological hazard index levels of the ionizing radiation by radionuclides present in the samples have also been discussed.

3.2 Research Design

The research focused on the description of parameters of the radionuclides measured in mine tailings. The values of the specific activity, gamma dose rate, radium equivalent activity and radiological hazard indices were determined. The findings were used to characterize the parameters of the radionuclides in the tailings of the three mines. The readings were obtained from experimental measurements using NaI(Tl) gamma spectroscopy technique.

3.3 Sampling and Sampling Technique

The top soil surface of the tailings was first removed to expose the fresh soil underneath. Then four or five sub-samples of waste soil were cored out using a hand shovel and mixed together to obtain one representative sample and labeled. Simple random sampling technique was used to collect all the samples as recommended by International Atomic Energy Agency (IAEA-TECDOC-1415, 2004) to ensure a good statistical representation of the sampling sites. Unwanted materials such as grasses, roots, stones and sticks were removed. Also twelve waste rock samples were also collected randomly from the rock tailing heaps around the mine. Tailings near the roads or paths were excluded to minimize contamination due to radionuclides from other places such as farms and gardens that may be carried to the mine by animals or rain water. Table 3.1 indicates the number of each type of mine tailing that was sampled based on the mining activity of the selected site.

Table 3.1: Sample selection matrix per mining site

District	Mine/Site	Mineral	Waste Soil	Waste Rock	Total
Bushenyi	Mashonga	Gold	12	12	24
Isingiro	Kikagati	Tin	12	12	24
Kabale	Butare	Iron Ore	12	12	24
Total			36	36	72

3.4 Sample Preparation

The waste soil and rock samples were sun dried for a period of one week and there after oven dried at a temperature of 200 ^{0}C. This was done to ensure that moisture was completely removed from the samples to avoid clamping of the sample particles during crushing. The samples were crushed using a locally made cylindrical mortar and pestle into smaller particles in order to increase the surface area and sieved using a sieve (mesh size 3 mm) to obtain uniform particle sizes. The sieved samples were weighed using an analog triple beam balance and sealed in standard plastic Marinelli beakers of volume 500 ml. An error limit of ±0.0001 kg was allowed in the measurement of mass.

3.5 Measurement of Gamma Radiation Levels in Mine Tailings

The specific activities of gamma ray emitting radionuclides in mine tailings were measured using NaI(Tl) scintillation detector, GDM 20 series. The system made use of an IBM compartible personal computer. The detector operated using a cylindrical NaI(Tl) crystal of height 7.62 cm and diameter of 7.62 cm. The detector was first calibrated before any nuclear radiation measurements were done.

The GDM 20 NaI(Tl) detector system and its photomultiplier tube are mounted on a box (with a built-in high voltage module). The detector is surrounded by a silvered lead cylinder containing lead shot for shielding the detector from the detector from background radiation. The hermetic seal protects the hygroscopic NaI from moisture absorption and external radiological influence. To reduce the gamma ray background, a cylindrical lead (10 cm thick) with a fixed bottom and a movable copper envelopes the detector. The lead shield contains an inner concentric cylinder of copper (0.3 mm thick) in order to absorb characteristic X-rays generated in the lead shield. The detector is

connected to the computer with a multichannel analyser (MCA) card (Accuspec) and AutoDAS version 3.16. The detector system used in this study is presented in the Figure 3.1 below. It has an A/D converter of 1024 channels and an amplifier time constant of 2 μs (www.gammadata.net. Accessed on 14th January 2016).

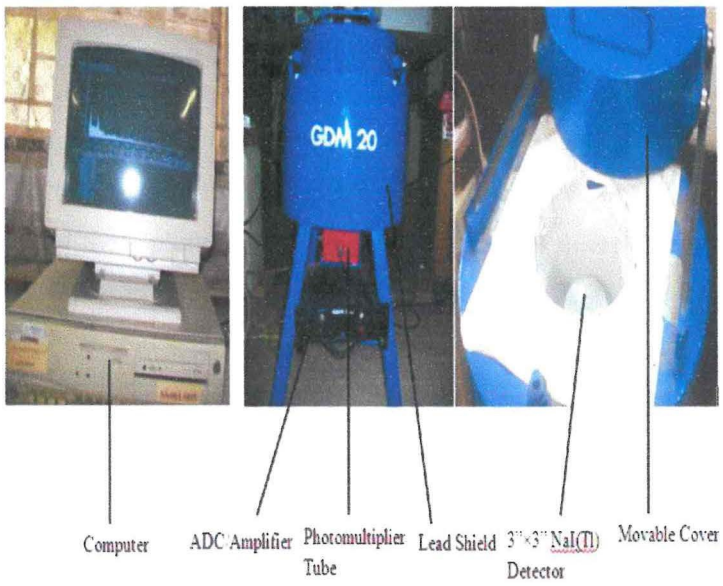

Figure 3.1: GDM 20 NaI(Tl) gamma ray spectrometer

When gamma rays interact with the NaI(Tl) crystal, it creates a weak light. The light is collected and converted into electrical pulses in the photomultiplier tube (PMT). The pulses are amplified and converted into digital information by the A/D converter. The information is then processed by the computer which presents it on the monitor as a frequency diagram of the distribution of the energy of the gamma quanta.

Before the NaI(Tl) detector was used for counting, it was first energy and efficiency calibrated. The energy calibration was done using Eu-152 solution over the energy range of 0.344 MeV to 1.41 MeV. The Eu-152 radioisotope was selected because it emits gamma rays of known energies and sufficient intensity. The 0.344 MeV gamma ray energy is at the beginning and 1.41 MeV energy is at the end of the range. These two gamma energy peaks were analysed using AutoDAS 3.16 to calibrate the energy axis of the detector.

The efficiency calibration of the detector was done at different gamma ray energies. The Eu-152 solution emits gamma quanta per second of energy 0.244 MeV. The activity was measure for a live time, t, and the area, A, of the corresponding photo peak was then calculated using the equation

$$\eta = \frac{Y}{At} \tag{3.1}$$

To obtain an efficiency curve, equation 3.1 was used to obtain efficiency of the detector at other gamma ray energy peaks from Eu-152. The energies used were 0.122 MeV, 0.245 MeV, 0.344 MeV, 0.780 MeV, 0.964 MeV, and 1.41 MeV (IAEA-PUB-1287, 2007). The efficiency was then plotted against the gamma ray energy to obtain an efficiency calibration curve. A efficiency curve of degree two given by the equation

$$\eta = 6.3128\,E^2 - 15.857\,E + 11.834 \tag{3.2}$$

where η is the efficiency for gamma rays with energy E, was fitted using the computer software (Ms Office Excel 2007 software). This is shown in the Figure 3.3 below.

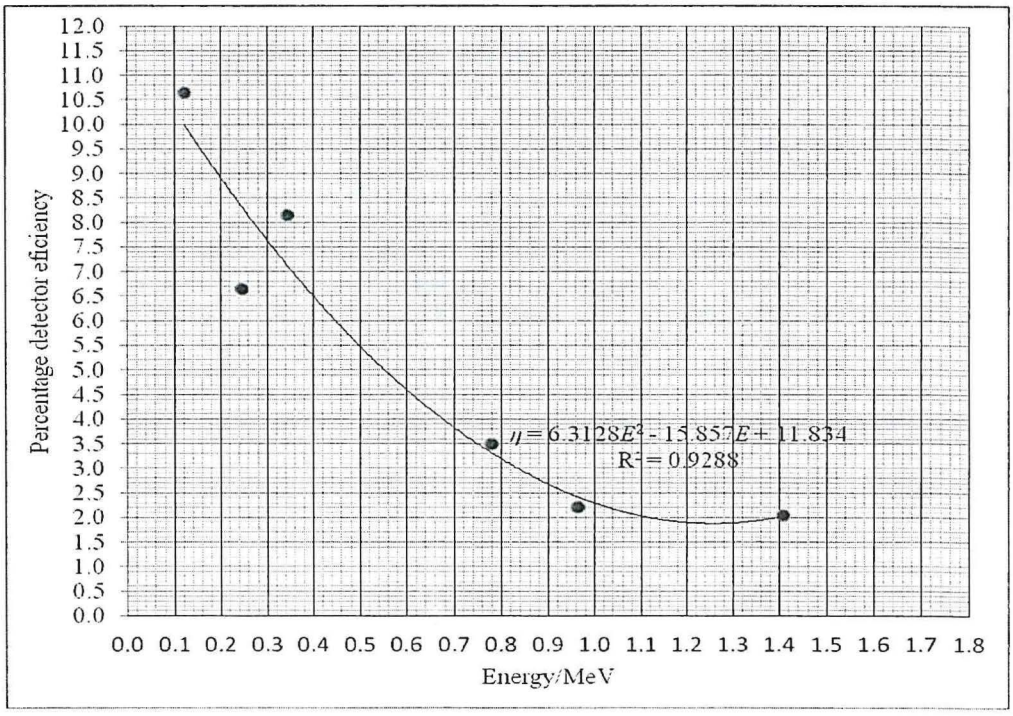

Figure 3.2: Efficiency Calibration of NaI(Tl) Detector

The efficiency curve (equation 3.2) was used to calculate the efficiency of the detector for gamma rays emitted by ^{238}U, ^{232}Th decay products and ^{40}K radionuclide in the samples.

After efficiency calibration of the GDM 20 NaI(Tl) detector, the correction detection efficiency, c for each radionuclide detected in each sample was determined using the equation

$$c = k\eta \tag{3.3}$$

where k is the branching ratio of the radionuclide and η is the detector efficiency. The branching ratios (gamma ray emission probabilities) were obtained in the Standard Radionuclide data tables from IAEA-PUB-1287, (2007). The correction efficiencies for the GDM 20 sodium iodide gamma spectrometer are as presented in Table 3.2 below (Technical Data for GDM 20, Makerere University Radioisotope Laboratory).

Table 3.2: Correction efficiencies for the Detected Radionuclides

Energy /keV	Radionuclide	Series	Correction Efficiency (c)
238.6	^{212}Pb	^{232}Th	0.06080
295.2	^{214}Pb	^{238}U	0.02370
351.9	^{214}Pb	^{238}U	0.03000
583.2	^{208}Tl	^{232}Th	0.01010
1460.8	^{40}K	None	0.00234

The values of the correction efficiency shown in the Table 3.2 above were used in calculating the specific activity of the corresponding radionuclides for each sample.

In study, all the 72 coded mine tailing samples were analysed using the NaI(Tl) gamma ray spectrometer. The sample in a Marinelli beaker to be analysed was placed on the detector. The analysis was run for a live time of 6000 s to obtain a spectrum of gamma rays. The spectrum obtained was stored with a specific file name such as BTS1 for waste soil samples from Mashonga gold mine in Bushenyi District. This procedure was followed for all the samples.

The background radiation due to impurity radionuclides in the detector was measure for a live time of 5000 s for an empty Marinelli beaker. The spectrum of the background was stored in the computer with a file code of BKGS2015.

The net photo peak count was computed for each sample spectrum after subtracting the background spectrum counts. The centroid, the standard deviation, the Full Width at Half Maximum (FWHM), net area (sum between markers), and the count rate were obtained.

Statistical analysis of results, MaTlab software was used to plot the bar charts and Excel Windows software was used to find the mean and standard deviation in the computed values. The Standard deviation, σ in the specific activity and other parameters of the radionuclides was obtained using the equation

$$\sigma = \sqrt{\frac{\left(X_i - \overline{X}\right)^2}{n-1}} \tag{3.4}$$

where $\overline{X}$ is the Mean value is X_i is the i^{th} observation and n is the sample size. The Standard Error (S.E) of the Mean was obtained by use of the equation;

$$\text{S.E} = \frac{\sigma}{\sqrt{n}} \tag{3.5}$$

The maximum error of the mean was determined using the equation given below.

$$\text{Maximum error of the mean} = t_\alpha \times \frac{\sigma}{\sqrt{n}} \tag{3.6}$$

where t_α is the t Statistic value at the α-level of confidence. The levels of confidence this study has used are: α = 0.10, 0.05 and 0.01 and their corresponding critical t_α values for eleven degrees of freedom are 1.796, 2.201 and 3.106 respectively. The number of degrees of freedom, ν is equal to the sample size minus one.

In order to determine the statistical significance of the results, the t test of two sample means for small samples was done. The t test statistic value for unpaired small random samples drawn from normal populations was calculated using the equation given below.

$$t = \frac{\overline{X_1} - \overline{X_2}}{\sqrt{\frac{(n_1-1)s_1^2 + (n_2-1)s_2^2}{n_1+n_2-2}\left(\frac{1}{n_1}+\frac{1}{n_2}\right)}} \tag{3.7}$$

where n_1 and n_2 are the sample sizes and $\overline{X_1}$ and $\overline{X_2}$ are their corresponding mean values. The statistical t test theoretical table values for 22 degrees of freedom, at 90%, 95% and 99% confidence levels are 1.717, 2.074 and 2.819 respectively. For two sample

means to be statistically significantly different, the calculated t value for the two means must be greater than the theoretical table t value.

CHAPTER FOUR: RESULTS OF THE STUDY

4.1 Introduction

The results of the study have been presented in this chapter. The results presented are the specific activity, radiation absorbed dose rates and radiological hazard indices. The results of the specific activity, radiation gamma dose rates and radiological hazard indices are presented for waste soil and rock tailings from Mashonga gold mine, Kikagati tin mine and Butare iron ore mine. All the results originated from analysis of the spectra of gamma rays of radionuclides in the samples as discussed in chapter three. The gamma ray spectrum for the waste soil sample (BTS1) from Mashonga gold mine in Bushenyi District is as shown in Figure 4.1 below.

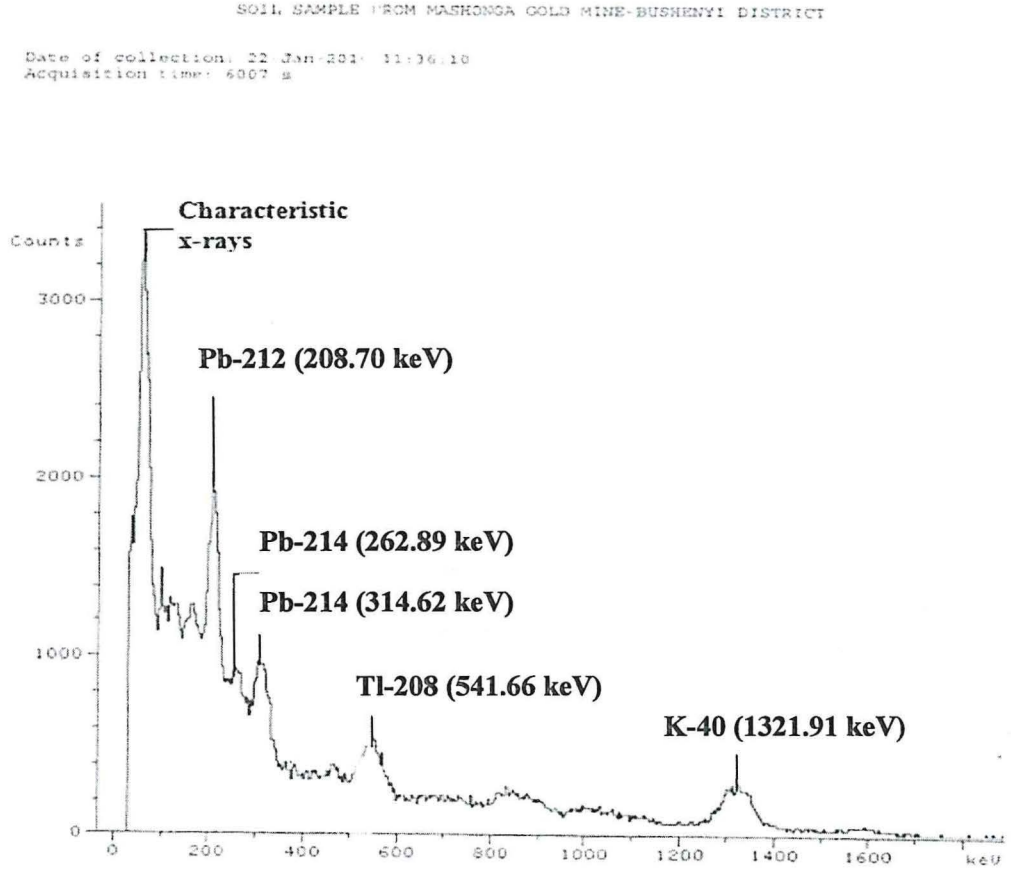

Figure 4.1: Spectrum of Radionuclides in a waste Soil tailing Sample (BTS1)

Identification of radionuclides was based on the prominent photopeaks on the spectrum generated by gamma rays from each radionuclide in the sample. The detected gamma rays at the energies of 262.89 keV and 314.62 keV corresponded to 295.22 keV and 351.93 keV from ^{214}Pb in the standard radionuclide tables which is a daughter radionuclide of ^{238}U (^{226}Ra). This confirmed presence of ^{238}U radionuclide in the samples. Gamma rays at the energies of 208.70 keV and 541.66 keV detected in the samples corresponded to 238.63 keV from ^{212}Pb and 583.19 keV from ^{208}Tl, which are all daughter radionuclides of ^{232}Th. Hence ^{232}Th radionuclide was present in the samples. The gamma ray at the energy of 1321.91 keV detected in the samples corresponded to 1460.82 keV from ^{40}K radionuclide. Hence ^{40}K radionuclide was also present in the samples. The obtained experimental gamma ray energy, theoretical energy, detected radionuclide, resolution and detector efficiencies are presented in Table 4.1 below.

Table 4.1: Radionuclides detected in mine tailing samples

Energy±Standard Deviation /keV		Radio-isotope	FWHM /keV	Resolution /%	Efficiency (c)
Experimental	**Theoretical**				
208.70 ± 9.94	238.63	^{212}Pb (^{232}Th)	20.407	09.78	0.06080
262.89 ± 8.68	295.22	^{214}Pb (^{238}U)	23.354	08.88	0.02370
314.62 ± 12.66	351.93	^{214}Pb (^{238}U)	29.748	09.46	0.03000
541.66 ± 23.51	583.19	^{208}Tl (^{232}Th)	55.237	10.20	0.01010
1321.91 ± 41.77	1460.82	^{40}K	98.150	07.42	0.00234

The values in Table 4.1 above describe the characteristics of the nuclides in a mine tailing soil sample from Mashonga gold mine. The standard deviations give the variation in the measured gamma energies and hence the range of possible gamma energies expected from the nuclides in the samples at the stated detector efficiencies. The resolution of the NaI(Tl) scintillation detector used in this study was in the range 7 – 10%.

4.2 Gamma Activity levels in Mine Tailings

The Specific Activity ($S.A$) of ^{238}U, ^{232}Th and ^{40}K in each sample was determined using the equation $S.A = \frac{N}{t \times m \times c}$ Bqkg^{-1}

where N is the net photopeak count, t is the counting time, m is the mass of the sample and c is the efficiency of the detector.

The specific activity of ^{238}U was calculated from the gamma ray spectrum of ^{214}Pb at the energy of 295.22 keV and 351.93 keV. The specific activity of ^{232}Th was determined from the gamma ray spectra of ^{212}Pb and ^{208}Tl at the energy of 238.63 keV and 583.19 keV respectively while the specific activity of ^{40}K was determined through its own gamma ray spectrum at the energy of 1460.82 keV. The mean specific activities of ^{238}U, ^{232}Th and ^{40}K obtained in this study were compared to the world population weighted average specific activities of ^{238}U, ^{232}Th and ^{40}K of 33 $Bqkg^{-1}$, 45 $Bqkg^{-1}$ and 420 $Bqkg^{-1}$ (UNSCEAR, 2000) respectively.

4.2.1 Gamma activity levels in mine tailings from Mashonga gold mine

The mean activity levels of ^{238}U, ^{232}Th and ^{40}K in waste soil samples from tailings from Mashonga gold mine are given in Table 4.2 below.

Table 4.2: Specific Activity levels in waste Soil Samples from Mashonga Gold Mine

Parameter	Specific Activity/$Bqkg^{-1}$		
	^{238}U	^{232}Th	^{40}K
Mean	58.75	193.46	892.90
Standard deviation	30.62	68.66	322.78
Standard error of the Mean	8.84	19.82	93.18
Maximum error of the Mean ($t_{\alpha=0.10}$)	15.87	35.60	167.35
Maximum error of the Mean ($t_{\alpha=0.05}$)	19.45	43.63	205.08
Maximum error of the Mean ($t_{\alpha=0.01}$)	27.45	61.57	289.41

The mean specific activities of 58.75 $Bqkg^{-1}$, 193.46 $Bqkg^{-1}$ and 892.90 $Bqkg^{-1}$ for ^{238}U, ^{232}Th and ^{40}K in the waste soil samples were 1.78, 4.30 and 2.13 times the world-wide averages respectively. The ^{232}Th to ^{238}U, ^{40}K to ^{238}U and ^{40}K to ^{232}Th ratios in the waste soil were 3.29, 15.20 and 4.62. The mean specific activity levels of ^{238}U, ^{232}Th and ^{40}K in waste rock samples from tailings obtained from Mashonga Gold Mine were found to be as given in Table 4.3 below.

Table 4.3: Specific Activity levels in waste rock samples from Mashonga Gold Mine

Parameter	Specific Activity/Bqkg^{-1}		
	^{238}U	^{232}Th	^{40}K
Mean	23.30	48.66	647.23
Standard deviation	26.15	75.38	1128.41
Standard error of the Mean	7.55	21.76	325.74
Maximum error of the Mean ($t_{\alpha=0.10}$)	13.56	39.08	585.04
Maximum error of the Mean ($t_{\alpha=0.05}$)	16.62	47.90	716.96
Maximum error of the Mean ($t_{\alpha=0.01}$)	23.45	67.59	1011.76

The mean specific activities of 23.30 Bqkg^{-1}, 48.66 Bqkg^{-1} and 647.23 Bqkg^{-1} for ^{238}U, ^{232}Th and ^{40}K in the waste rock samples were 0.71, 1.08 and 1.54 times the world-wide averages respectively. The ^{232}Th to ^{238}U, ^{40}K to ^{238}U and ^{40}K to ^{232}Th ratios in the waste rock tailings were 2.09, 27.78 and 13.30. The mean specific activity levels in the waste soil and rock samples obtained from Mashonga gold mine were compared using column charts as presented in Figure 4.2 below.

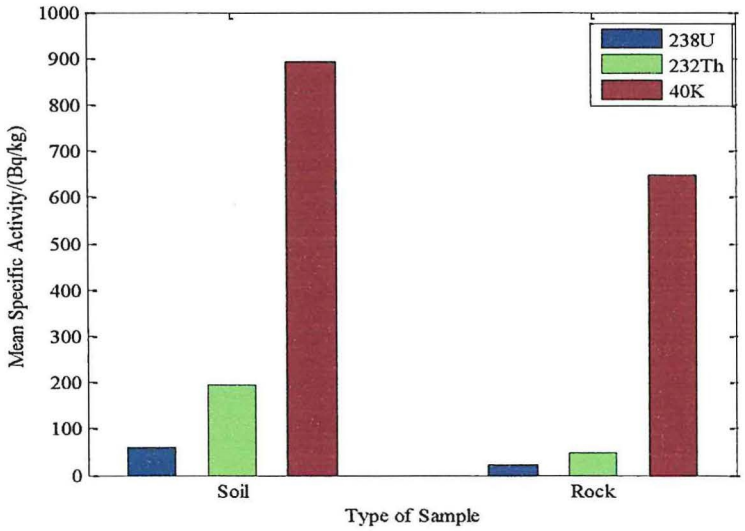

Figure 4.2: Mean Specific Activities for mine tailings from Mashonga Gold Mine

The mean specific activities of ^{238}U, ^{232}Th and ^{40}K in the waste soil tailings from Mashonga gold mine were about 2.5, 4.0 and 1.4 times that in the waste rock tailings respectively.

4.2.2 Gamma activity levels in mine tailing from Kikagati tin mine

The mean the specific activity levels of ^{238}U, ^{232}Th and ^{40}K in waste soil samples from Kikagati tin mine obtained in this study are presented in Table 4.4 below.

Table 4.4: Specific Activity levels in waste soil samples from Kikagati Tin Mine

Parameter	Specific Activity/Bqkg^{-1}		
	^{238}U	^{232}Th	^{40}K
Mean	49.72	211.69	391.53
Standard deviation	10.90	60.15	163.63
Standard error of the Mean	3.15	17.36	47.23
Maximum error of the Mean ($t_{\alpha=0.10}$)	5.65	31.19	84.83
Maximum error of the Mean ($t_{\alpha=0.05}$)	6.93	38.22	103.96
Maximum error of the Mean ($t_{\alpha=0.01}$)	9.77	53.94	146.71

The mean specific activities of 49.72 Bqkg^{-1}, 211.69 Bqkg^{-1} and 391.53 Bqkg^{-1} for ^{238}U, ^{232}Th and ^{40}K in the waste soil samples from Kikagati tin mine were 1.51, 4.70 and 0.93 times the world-wide averages respectively. The ^{232}Th to ^{238}U, ^{40}K to ^{238}U and ^{40}K to ^{232}Th ratios in the waste soil tailings were 4.26, 7.87 and 1.85. The mean specific activity levels of ^{238}U, ^{232}Th and ^{40}K in waste rock samples obtained from Kikagati tin mine were found to be as presented in Table 4.5 below.

Table 4.5: Specific Activity levels in waste rock samples from Kikagati Tin Mine

Parameter	Specific Activity/Bqkg^{-1}		
	^{238}U	^{232}Th	^{40}K
Mean	24.87	69.03	751.66
Standard deviation	17.95	68.67	771.85
Standard error of the Mean	5.18	19.82	222.82
Maximum error of the Mean ($t_{\alpha=0.10}$)	9.30	35.60	400.18
Maximum error of the Mean ($t_{\alpha=0.05}$)	11.40	43.63	490.42
Maximum error of the Mean ($t_{\alpha=0.01}$)	16.09	61.57	692.06

The mean specific activities of 24.87 Bqkg^{-1}, 69.03 Bq kg^{-1} and 751.66 Bqkg^{-1} for ^{238}U, ^{232}Th and ^{40}K in the waste rock samples from Kikagati tin mine were 0.75, 1.53 and 1.79 times the world-wide averages respectively. The ^{232}Th to ^{238}U, ^{40}K to ^{238}U and ^{40}K to

^{232}Th ratios in the waste rock tailings were 2.78, 30.22 and 10.89. The mean specific activity levels in the mine tailings from Kikagati tin mine were compared using column charts as presented in Figure 4.3 below.

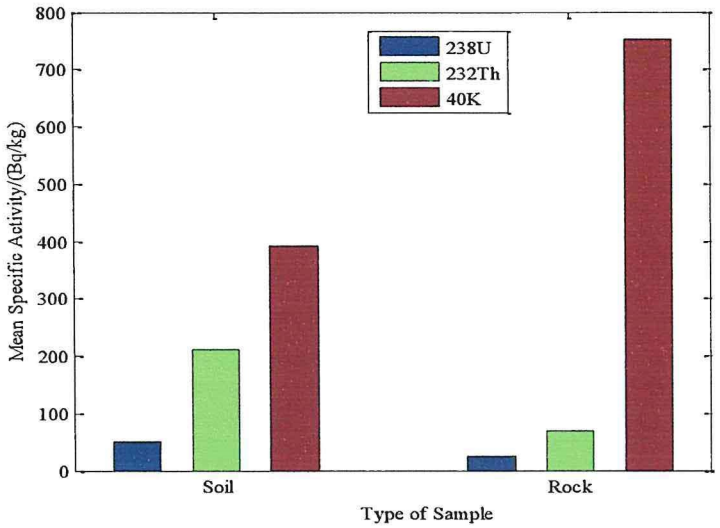

Figure 4.3: Mean Specific Activities for mine tailings from Kikagati Tin Mine

The mean specific activities of ^{238}U, ^{232}Th and ^{40}K in the waste soil samples from Kikagati tin mine were about 2.0, 3.1 and 0.5 times that in the waste rock samples.

4.2.3 Gamma activity levels in mine tailings from Butare Iron Ore Mine

The mean values specific activity levels of radionuclides in waste soil samples from Butare iron ore mine are presented in Table 4.6 below.

Table 4.6: Specific Activity levels in waste soil samples from Butare Iron Ore Mine

Parameter	Specific Activity/Bqkg^{-1}		
	^{238}U	^{232}Th	^{40}K
Mean	57.62	244.43	416.43
Standard deviation	9.76	36.61	162.34
Standard error of the Mean	2.82	10.57	46.86
Maximum error of the Mean ($t_{\alpha=0.10}$)	5.06	18.98	84.17
Maximum error of the Mean ($t_{\alpha=0.05}$)	6.20	23.26	103.15
Maximum error of the Mean ($t_{\alpha=0.01}$)	8.75	32.83	145.56

The mean specific activities of 57.62 Bqkg^{-1}, 244.43 Bqkg^{-1} and 416.43 Bqkg^{-1} for ^{238}U, ^{232}Th and ^{40}K in the waste soil samples from Butare iron ore mine were 1.75, 5.43 and 0.99 times the world-wide averages respectively. The ^{232}Th to ^{238}U, ^{40}K to ^{238}U and ^{40}K to ^{232}Th ratios in the waste soil tailings were 4.24, 7.23 and 1.70. The mean specific activity levels in waste rock samples from Butare iron ore mine are given in Table 4.7 below.

Table 4.7: Specific Activity levels in waste rock samples from Butare Iron Ore Mine

Parameter	Specific Activity/Bqkg^{-1}		
	^{238}U	^{232}Th	^{40}K
Mean	58.59	129.74	226.43
Standard deviation	19.18	67.57	447.16
Standard error of the Mean	5.54	19.50	129.08
Maximum error of the Mean ($t_{\alpha=0.10}$)	9.94	35.03	231.83
Maximum error of the Mean ($t_{\alpha=0.05}$)	12.18	42.93	284.11
Maximum error of the Mean ($t_{\alpha=0.01}$)	17.19	60.58	400.93

The mean specific activities of 58.59 Bqkg^{-1}, 129.74 Bqkg^{-1} and 226.43 Bqkg^{-1} for ^{238}U, ^{232}Th and ^{40}K in the waste rock samples from Butare iron ore mine were 1.78, 2.88 and 0.54 times the world-wide averages respectively. The ^{232}Th to ^{238}U, ^{40}K to ^{238}U and ^{40}K to ^{232}Th ratios in the waste rock tailings were 2.21, 3.86 and 1.75. The mean specific activity levels in the mine tailings from Butare iron ore mine were compared using column charts as presented in Figure 4.4 below.

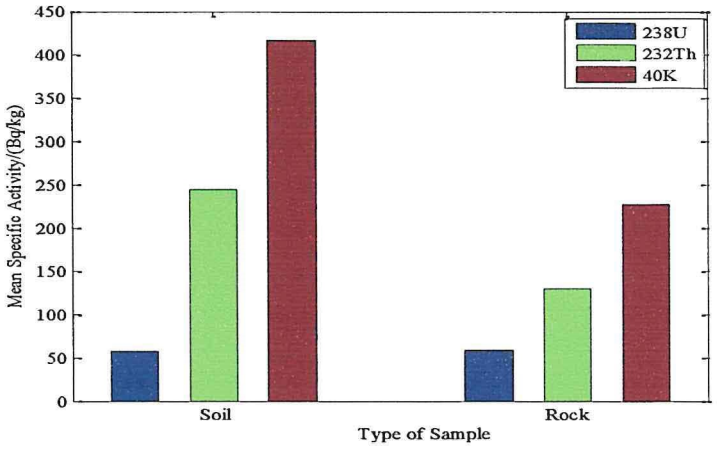

Figure 4.4: Mean Specific Activities for mine tailings from Butare Iron Ore Mine

The mean specific activities of ^{238}U, ^{232}Th and ^{40}K in the waste soil samples from Butare iron ore mine were about 0.98, 1.88 and 1.84 times that in the waste rocks.

The mean specific activity levels of ^{238}U, ^{232}Th and ^{40}K in the waste soil samples from Mashonga gold mine, Kikagati tin mine and Butare iron ore mine are as presented in the Table 4.8 below.

Table 4.8: Comparison of Mean Specific Activities in waste soil Samples

Site/Mine	Mass/kg± 0.0001	Mean Specific Activity/Bqkg^{-1}		
		^{238}U	^{232}Th	^{40}K
Mashonga	0.5623	58.75± 15.87	193.46±35.60	892.90±167.35
Kikagati	0.6163	49.72± 5.65	211.69± 31.19	391.53±84.83
Butare	0.5119	57.62±5.06	244.43± 18.98	416.43±84.17

The mean specific activity levels in the waste soil samples from Mashonga, Kikagati and Butare mines were compared using the column charts as presented in Figure 4.5 below.

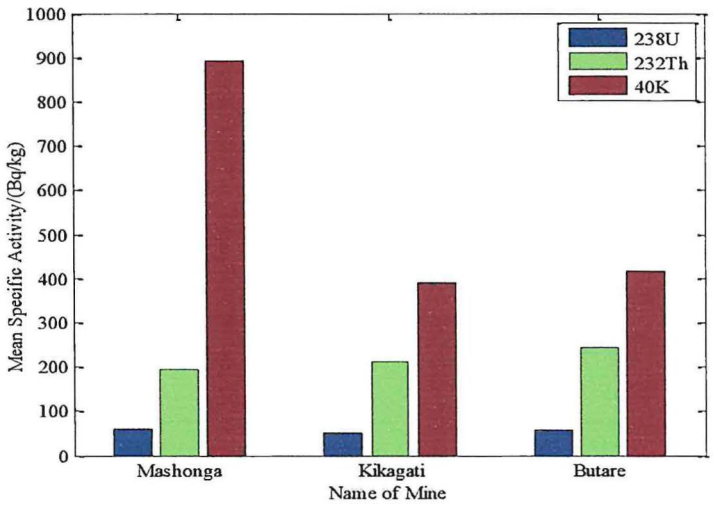

Figure 4.5: Comparison of Mean Specific Activities for waste soil samples

The mean specific activity levels in all the waste soil samples were in the order of ^{238}U $<^{232}Th$ $<^{40}K$. Mashonga mine had the highest mean specific activity of ^{40}K of 892.90±167.35 Bqkg^{-1} followed by 416.43±84.17 Bqkg^{-1} for Butare mine and

391.53±84.83 Bqkg^{-1} for Kikagati mine. The highest mean specific activity of ^{232}Th was 244.43±18.98 Bqkg^{-1} for Butare mine followed by 211.69± 31.19 Bqkg^{-1} for Kikagati mine and 193.46±35.60 Bqkg^{-1} for Mashonga mine. The mean specific activity of ^{238}U of 58.75± 15.87 Bqkg^{-1} for Mashonga mine was the highest followed by 57.62±5.06 Bqkg^{-1} for Butare mine and 49.72± 5.65 Bqkg^{-1} for Kikagati mine.

Table 4.9: Comparison of Mean Specific Activity levels in waste rock samples

Site/Mine	Mass/kg± 0.0001	Mean Specific Activity/Bqkg^{-1}		
		^{238}U	^{232}Th	^{40}K
Mashonga	0.3118	23.30±13.56	48.66±39.08	647.23±585.04
Kikagati	0.4963	24.87±9.30	69.03±35.60	751.66±400.18
Butare	0.2735	58.59±9.94	129.74±35.03	226.43±231.83

The mean specific activity levels in waste rock samples from the three mines are as presented in the column charts in Figure 4.6 below.

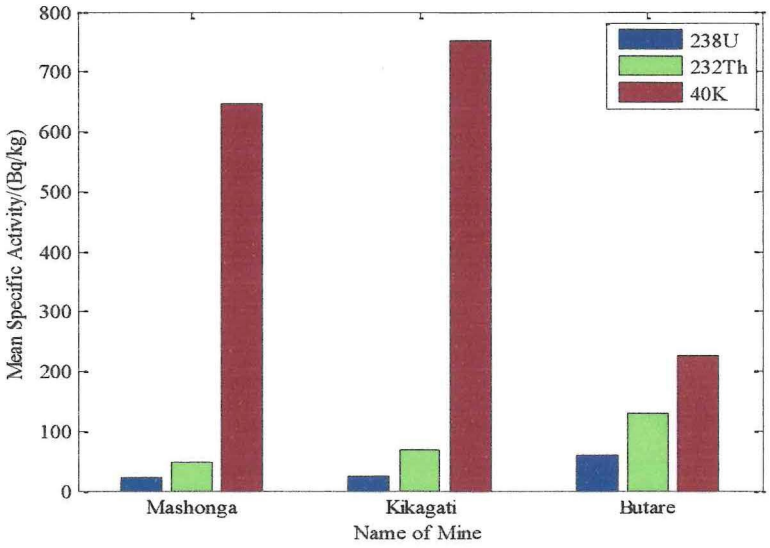

Figure 4.6: Comparison of Mean Specific Activities for waste rock samples

The mean specific activity levels in all the waste rock samples were in the order of ^{238}U <^{232}Th <^{40}K. Kikagati mine had the highest mean specific activity of ^{40}K of 751.66±400.18 Bqkg^{-1} followed by 647.23±585.04 Bqkg^{-1} for Mashonga mine and

226.43±231.83 Bqkg^{-1} for Butare mine. The highest mean specific activity of ^{232}Th was 129.74±35.03 Bqkg^{-1} for Butare mine followed by 69.03±35.60 Bqkg^{-1} for Kikagati mine and 48.66±39.08 Bqkg^{-1} for Mashonga mine. The mean specific activity of ^{238}U of 58.59±9.94 Bqkg^{-1} for Butare mine was the highest followed by 24.87±9.30 Bqkg^{-1} for Kikagati mine and 23.30±13.56 Bqkg^{-1} for Mashonga mine.

The Table 4.10 below give the t test values (at 90% confidence level) obtained in this study for the soil and rock tailing samples respectively.

Table 4.10: Statistical t test for Mean Specific Activities

Waste soil samples

	^{238}U	^{232}Th	^{40}K
Mashonga	58.75	193.46	892.9
Kikagati	49.72	211.69	391.53
Df	22	22	22
Calculated $t_{\alpha=0.10}$	0.96	-0.69	4.8
Table value $t_{\alpha=0.10}$	1.72	1.72	1.72

(a)

Waste soil samples

	^{238}U	^{232}Th	^{40}K
Kikagati	49.72	211.69	391.53
Butare	57.62	244.43	416.43
df	22	22	22
Calculated $t_{\alpha=0.10}$	-1.87	-1.61	-0.37
Table value $t_{\alpha=0.10}$	1.72	1.72	1.72

(b)

Waste soil samples

	^{238}U	^{232}Th	^{40}K
Mashonga	58.75	193.46	892.9
Butare	57.62	244.43	416.43
Df	22	22	22
Calculated $t_{\alpha=0.10}$	0.12	-2.27	4.57
Table value $t_{\alpha=0.10}$	1.72	1.72	1.72

(c)

Waste rock samples

	^{238}U	^{232}Th	^{40}K
Mashonga	23.3	48.66	647.23
Butare	58.59	129.74	226.43
df	22	22	22
Calculated $t_{\alpha=0.10}$	-3.77	-2.77	1.2
Table value $t_{\alpha=0.10}$	1.72	1.72	1.72

(d)

Waste soil samples

	^{238}U	^{232}Th	^{40}K
Mashonga	23.3	48.66	647.23
Kikagati	24.87	69.03	751.66
Df	22	22	22
Calculated $t_{\alpha=0.10}$	-0.17	-0.69	-0.26
Table value $t_{\alpha=0.10}$	1.72	1.72	1.72

(e)

Waste soil samples

	^{238}U	^{232}Th	^{40}K
Kikagati	24.87	69.03	751.66
Butare	58.59	129.74	226.43
df	22	22	22
Calculated $t_{\alpha=0.10}$	-4.45	-2.18	2.04
Table value $t_{\alpha=0.10}$	1.72	1.72	1.72

(f)

Since the calculated values of $t_{\alpha=0.10}$ in (d) for ^{40}K, in (b) for ^{238}U and in (c) for ^{232}Th and ^{40}K for waste soil samples were greater than the table values, the difference between the activity levels by various radionuclides were significantly different. For waste rock samples, the calculated values of $t_{\alpha=0.10}$ in and in (d) for ^{238}U and ^{232}Th and in (f) for ^{238}U, ^{232}Th and ^{40}K were greater than the table values. Therefore the activity levels by various radionuclides in the waste rock tailings for those mines were statistically significantly different.

4.3 Gamma Dose Rates in Mine Tailings

In this section of the chapter, the results of the mean external outdoor and indoor radiation absorbed dose rates and the mean external outdoor and indoor annual effective dose rates for soil and rock samples from tailings have been presented for the mines. The outdoor radiation absorbed dose rates (D_{out}) were calculated using the equation $D_{out} = 0.462\,A_U + 0.604\,A_{Th} + 0.0417\,A_K$ nGyh^{-1} and the indoor radiation absorbed dose rates (D_{in}) were calculated using the equation

$$D_{in} = 0.92\,A_U + 1.1A_{Th} + 0.08\,A_K \text{ nGyh}^{-1}$$

where $A_U(A_{Ra})$, A_{Th} and A_K are the mean specific activities of ^{238}U, ^{232}Th and ^{40}K radionuclides. The results of the external radiation absorbed dose rates obtained in this study for soil and rock samples from tailings were compared to the world wide average of 59 nGy h^{-1} and 84 nGy h^{-1} for outdoor and indoor respectively and the average population weighted indoor to outdoor dose rate ratio of 1.4 and range of 0.6 – 2.3 (UNSCEAR, 2000).

The outdoor annual effective dose rate (E_{out}) was determined using the equation

$$E_{out} = D_{out}\times T\times CF\times OF_{out}\times 10^{-6} \text{ mSvy}^{-1}.$$

The indoor annual effective dose rate (E_{in}) was determined using the equation

$$E_{in} = D_{in}\times T\times CF\times OF_{in}\times 10^{-6} \text{ mSvy}^{-1}$$

where D_{out} (nGy h^{-1}) and D_{in} (nGyh^{-1}) are the outdoor and indoor mean radiation absorbed dose rates in air outdoor and indoor respectively, T is time of exposure to the ionizing radiation, equal to one year (i.e. 8760 h), CF is the conversion factor equal to 0.7 SvGy^{-1} (UNSCEAR, 2000), OF_{out} = 0.33 is the outdoor occupancy factor for South Western Uganda and OF_{in} = 0.67 is the indoor occupancy factor. The mean outdoor and indoor

annual effective dose rates obtained in this study were compared to the world-wide averages outdoor of 0.07 $mSvy^{-1}$ and indoor of 0.41 $mSvy^{-1}$ (UNSCEAR, 2000).

The total (sum of outdoor and indoor) annual effective dose rates from terrestrial sources obtained in this study were compared with the world-wide range of 0.3 – 0.6 $mSvy^{-1}$ and average of 0.48 $mSvy^{-1}$ and the natural background radiation of 2.4 $mSvy^{-1}$ (UNSCEAR, 2000).

4.3.1 Gamma dose rates in mine tailings from Mashonga gold mine

The mean radiation absorbed dose rates and the annual effective dose rates in waste soil samples from Mashonga gold mine are as presented in Table 4.11 below.

Table 4.11: Gamma Dose Rates in waste soil samples from Mashonga Gold Mine

Parameter	Absorbed Dose Rate/$nGyh^{-1}$		Annual Effective Dose Rate/$mSvy^{-1}$		
	D_{out}	D_{in}	E_{out}	E_{in}	Total
Mean	181.23	338.29	0.37	1.39	1.76
Standard deviation	66.79	129.52	0.14	0.53	0.67
Standard error	19.28	37.39	0.04	0.15	0.19
Maximum error of Mean ($t_{\alpha=0.10}$)	34.63	67.15	0.07	0.28	0.35
Maximum error of Mean ($t_{\alpha=0.05}$)	42.44	82.29	0.09	0.34	0.42
Maximum error of Mean ($t_{\alpha=0.01}$)	59.89	116.13	0.12	0.48	0.60

The mean outdoor and indoor absorbed dose rates obtained in this study for the waste soil samples from Mashonga gold mine were 181.23 $nGyh^{-1}$ and 338.29 $nGyh^{-1}$ respectively. The indoor to outdoor absorbed dose rates ratio was 1.87 which was in the world range but greater than the weighted average by 33.6%. The mean outdoor and indoor absorbed dose rates were 3 and 4 times the world averages respectively. The mean outdoor annual effective dose of 0.37 $mSvy^{-1}$ and the mean indoor annual effective dose of 1.39 $mSvy^{-1}$ were about 5.29 and 3.39 times the world wide average. The total annual effective dose rate was 1.76 $mSvy^{-1}$. This was about 3.67 times the world-wide average and 73% of the natural background radiation.

The mean radiation absorbed dose rate and the annual effective dose rates in waste rock samples from Mashonga gold mine are as presented in Table 4.12 below.

Table 4.12: Gamma Dose Rates in waste rock samples from Mashonga Gold Mine

Parameter	Absorbed Dose Rate/nGyh^{-1}		Annual Effective Dose Rate/mSvy^{-1}		
	D_{out}	D_{in}	E_{out}	E_{in}	Total
Mean	67.15	126.75	0.14	0.52	0.66
Standard deviation	93.46	197.25	0.19	0.81	1.00
Standard error of the Mean	26.98	56.94	0.05	0.23	0.29
Maximum error of the Mean ($t_{\alpha=0.10}$)	48.46	102.27	0.10	0.42	0.52
Maximum error of the Mean ($t_{\alpha=0.05}$)	59.38	125.33	0.12	0.51	0.64
Maximum error of the Mean ($t_{\alpha=0.01}$)	83.80	176.86	0.17	0.73	0.90

The mean outdoor and indoor absorbed dose rate in the waste rock samples Mashonga gold mine were 67.15 nGyh^{-1} and 126.75 nGyh^{-1}. These values were about 1.14 and 1.51 times the world-wide average respectively. The indoor to outdoor absorbed dose rate ratio was 1.89. This ratio was in the range of the world but greater than the world average by 35.0%. The mean outdoor annual effective dose of 0.14 mSvy^{-1} and the mean indoor annual effective dose of 0.52 mSvy^{-1} were about 2 and 1.27 times the world average respectively. The total annual effective dose rate was 0.66 mSvy^{-1} which was about 1.38 times the world-wide average and 27.5% of the natural background radiation.

4.3.2 Gamma dose rates in mine tailings from Kikagati tin mine

The mean radiation absorbed dose rates and the annual effective dose rates in waste soil samples from Kikagati tin mine are as presented in Table 4.13 below.

Table 4.13: Gamma Dose Rates in waste soil Samples from Kikagati Tin Mine

Parameter	Absorbed Dose Rate/nGyh^{-1}		Annual Effective Dose Rate/mSvy^{-1}		
	D_{out}	D_{in}	E_{out}	E_{in}	Total
Mean	167.16	309.92	0.34	1.27	1.61
Standard deviation	42.14	89.29	0.09	0.37	0.45
Standard error of the Mean	12.17	25.77	0.02	0.11	0.13
Maximum error of the Mean ($t_{\alpha=0.10}$)	21.85	46.29	0.04	0.19	0.23
Maximum error of the Mean ($t_{\alpha=0.05}$)	26.78	56.73	0.05	0.23	0.29
Maximum error of the Mean ($t_{\alpha=0.01}$)	37.78	80.06	0.08	0.33	0.41

The mean outdoor and indoor absorbed dose rates obtained in this study for the waste soil samples from Kikagati tin mine were 167.16 $nGyh^{-1}$ and 309.92 $nGyh^{-1}$. These values were 2.83 and 3.69 times the world average. The indoor to outdoor absorbed dose rate ratio was 1.85 which was in the world range but greater than the world average by 32.1%. The mean outdoor annual effective dose rate of 0.34 $mSvy^{-1}$ and the mean indoor annual effective dose of 1.27 $mSvy^{-1}$ were about 4.86 and 3.10 times the world average respectively. The total annual effective dose rate was 1.61 $mSvy^{-1}$. This was about 3.35 times the world-wide average and 67.1% of the natural background radiation.

The mean radiation absorbed dose rates and the annual effective dose rates in the waste rock samples from Kikagati tin mine are as presented in Table 4.14 below.

Table 4.14: Gamma Dose Rates in waste rock samples from Kikagati Tin Mine

Parameter	Absorbed Dose Rate/$nGyh^{-1}$		Annual Effective Dose Rate/$mSvy^{-1}$		
	D_{out}	D_{in}	E_{out}	E_{in}	Total
Mean	84.53	158.95	0.17	0.65	0.82
Standard deviation	67.65	153.80	0.14	0.63	0.77
Standard error of the Mean	19.53	44.40	0.04	0.18	0.22
Maximum error of the Mean ($t_{\alpha=0.10}$)	35.07	79.74	0.07	0.33	0.40
Maximum error of the Mean ($t_{\alpha=0.05}$)	42.98	97.72	0.09	0.40	0.49
Maximum error of the Mean ($t_{\alpha=0.01}$)	60.66	137.90	0.12	0.57	0.69

The mean outdoor and indoor absorbed dose rates in the waste rock samples from Kikagati tin mine were 84.53 $nGyh^{-1}$ and 158.95 $nGyh^{-1}$. These values were 1.43 and 1.89 times the world average respectively. The indoor to outdoor absorbed dose rate ratio was 1.88 which was in the world range but greater than the world average by 34.3%. The mean outdoor annual effective dose rate of 0.17 $mSvy^{-1}$ and the mean indoor annual effective dose rate of 0.65 $mSvy^{-1}$ were about 2.43 and 1.59 times the world average respectively. The total annual effective dose rate was 0.82 $mSvy^{-1}$. This was about 1.71 times the world average and 34.2% of the natural background radiation.

4.3.3 Gamma dose rates in mine tailings from Butare iron ore mine

The mean radiation absorbed dose rates and the annual effective dose rates in waste soil samples from Butare iron ore mine are as presented in Table 4.15 below.

Table 4.15: Gamma Dose Rates in waste soil samples from Butare Iron Ore Mine

Parameter	Absorbed Dose Rate/nGyh^{-1}		Annual Effective Dose Rate/mSvy^{-1}		
	D_{out}	D_{in}	E_{out}	E_{in}	Total
Mean	191.62	355.20	0.39	1.46	1.85
Standard deviation	30.05	62.24	0.06	0.26	0.32
Standard error of the Mean	8.67	17.97	0.02	0.07	0.09
Maximum error of the Mean ($t_{\alpha=0.10}$)	15.58	32.27	0.03	0.13	0.16
Maximum error of the Mean ($t_{\alpha=0.05}$)	19.09	39.55	0.04	0.16	0.20
Maximum error of the Mean ($t_{\alpha=0.01}$)	26.94	55.81	0.05	0.23	0.28

The mean outdoor and indoor absorbed dose rates in the waste soil samples from Butare iron ore mine were 191.62 nGyh^{-1} and 355.20 nGyh^{-1} respectively. These values were 3.25 and 4.23 times the world average respectively. The indoor to outdoor absorbed dose rate ratio was 1.85 which was in the world range but greater than the world average by 32.1%. The mean outdoor annual effective dose rate of 0.39 mSvy^{-1} and the mean indoor annual effective dose rate of 1.46 mSvy^{-1} obtained in this study were about 5.57 and 3.56 times the world average respectively. The total annual effective dose was 1.85 mSvy^{-1}. This was about 3.85 times the world-wide average and 77.1% of the natural background radiation. The mean radiation absorbed dose rate and the annual effective dose rates in rock samples from Butare iron ore mine are as presented in Table 4.16 below.

Table 4.16: Gamma Dose Rates in waste rock samples from Butare Iron Ore Mine

Parameter	Absorbed Dose Rate/nGyh^{-1}		Annual Effective Dose Rate/mSvy^{-1}		
	D_{out}	D_{in}	E_{out}	E_{in}	Total
Mean	114.87	214.73	0.23	0.88	1.11
Standard deviation	61.62	127.74	0.12	0.52	0.65
Standard error of the Mean	17.79	36.88	0.04	0.15	0.19
Maximum error of the Mean ($t_{\alpha=0.10}$)	31.95	66.23	0.06	0.27	0.34
Maximum error of the Mean ($t_{\alpha=0.05}$)	39.15	81.16	0.08	0.33	0.41
Maximum error of the Mean ($t_{\alpha=0.01}$)	55.25	114.53	0.11	0.47	0.58

The mean outdoor and indoor absorbed dose rates in the waste rock samples from Butare iron ore mine were 114.87 $nGyh^{-1}$ and 214.73 $nGyh^{-1}$ respectively. These values were 1.95 and 2.56 times the world average. The indoor to outdoor absorbed dose rate ratio was 1.87 was in the world range but greater than the world average by 33.6%. The mean outdoor annual effective dose of 0.23 $mSvy^{-1}$ and the mean indoor annual effective dose of 0.88 $mSvy^{-1}$ obtained in this study were about 3.29 and 2.15 times the world average respectively. The total annual effective dose was 1.11 $mSvy^{-1}$. This was about 2.31 times the world average and 46.3% of the natural background radiation.

The mean gamma dose rates for the mine tailings from Mashonga, Kikagati and Butare mines are as presented in Table 4.17 and Table 4.18 below.

Table 4.17: Comparison of Mean Gamma Dose Rates in waste soil samples

Mine	Absorbed Dose Rate/$nGyh^{-1}$		Annual Effective Dose Rate/$mSvy^{-1}$		
	D_{out}	D_{in}	E_{out}	E_{in}	Total
Mashonga	181.23±34.63	338.29±67.15	0.37±0.07	1.39±0.28	1.76±0.35
Kikagati	167.16±21.85	309.92±46.29	0.34±0.04	1.27±0.19	1.61±0.23
Butare	191.62±15.58	355.20±32.27	0.39±0.03	1.46±0.013	1.85±0.16

Waste soil samples from Butare iron ore mine had the highest mean outdoor and indoor absorbed dose rates of (191.62±15.58 $nGyh^{-1}$ and 355.20±32.27 $nGyh^{-1}$) followed by (181.23±34.63 $nGyh^{-1}$ and 338.29±67.15 $nGyh^{-1}$) for Mashonga gold mine and (167.16±21.85 $nGyh^{-1}$ and 309.92±46.29 $nGyh^{-1}$) for Kikagati tin mine respectively.

A column chart comparing the mean absorbed dose rates for the waste soil samples from Mashonga, Kikagati and Butare mines is as presented in the Figure 4.7 below.

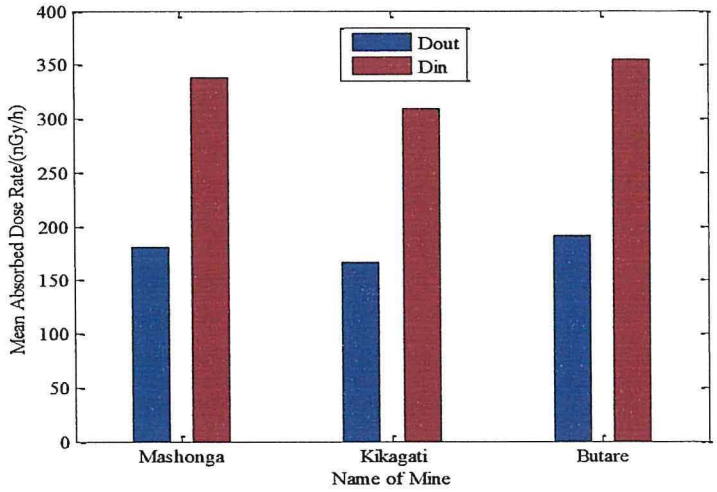

Figure 4.7: Comparison of Mean Absorbed Dose Rates the waste soil samples

As observed in Figure 4.7 above, the mean indoor absorbed dose rates were about twice the mean outdoor absorbed dose rates in the waste soil samples from Mashonga, Kikagati and Butare mines.

For the mean outdoor and indoor annual effective dose rates, Butare mine had the highest values of (0.39±0.03 $mSvy^{-1}$ and 1.46±0.01 $mSvy^{-1}$) followed by Mashonga mine with values of (0.37±0.07 $mSvy^{-1}$ and 1.39±0.28 mSv y^{-1}) and Kikagati mine with (0.34±0.04 $mSvy^{-1}$ and 1.27±0.19 $mSvy^{-1}$) respectively. The total annual effective dose rates of 1.76±0.35 $mSvy^{-1}$, 1.61±0.23 $mSvy^{-1}$ and 1.85±0.16 $mSvy^{-1}$ in waste soil tailing samples from Mashonga, Kikagati and Butare mines were above the world range and also greater than the recommended maximum permissible dose limit of 1 $mSvy^{-1}$ for a member of the public by 0.76 $mSvy^{-1}$, 0.61 $mSvy^{-1}$ and 0.85 $mSvy^{-1}$ respectively. This could be due to radon (decay product of ^{238}U (^{226}Ra)), emanating from the ground and from building materials and concentrates in poorly ventilated buildings and underground mines and is known to deliver an average dose rate of 1.2 $mSvy^{-1}$ (WHO, 2009; Turner, 2007; BEIR VII; UNSCEAR, 2008). This radon dose is comparable to the indoor annual effective dose rates obtained in this current study. The mean outdoor, indoor and the total annual effective dose equivalent rates in the waste soil samples from Mashonga, Kikagati and Butare mines are compared in the column charts in Figure 4.8 below.

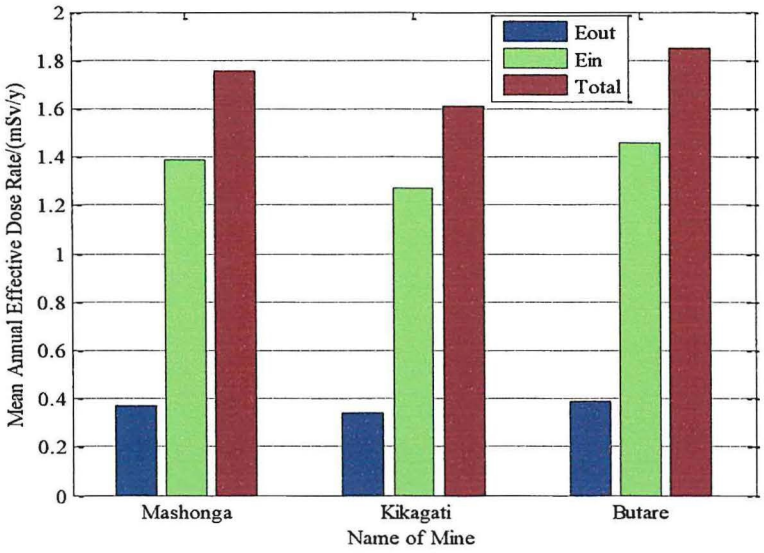

Figure 4.8: Comparison of Mean Annual Effective Dose Rates in the waste soil samples

As observed in Figure 4.8 above, the mean outdoor annual effective dose rates for the waste soil tailing samples from Mashonga, Kikagati and Butare mines were above the dose limit of 1 $mSvy^{-1}$ recommended for the public. The mean indoor annual effective dose rates were about 4 times the mean outdoor annual effective dose rates because people spend most of their time indoors than outdoors. The total annual effective dose rates were below the natural background radiation by about 30%.

Table 4.18: Comparison of Mean Gamma Dose Rates in waste rock samples

Mine	Absorbed Dose Rate/$nGyh^{-1}$		Annual Effective Dose Rate/$mSvy^{-1}$		
	D_{out}	D_{in}	E_{out}	E_{in}	Total
Mashonga	67.15±48.46	126.75±102.27	0.14±0.10	0.52±0.42	0.66±0.52
Kikagati	84.53±35.07	158.95±79.74	0.17±0.07	0.65±0.33	0.82±0.40
Butare	114.87±31.95	214.73±66.23	0.23±0.06	0.88±0.27	1.11±0.34

Butare mine had the highest mean outdoor and indoor absorbed dose rates of (114.87±31.95 $nGyh^{-1}$ and 214.73±66.23 $nGyh^{-1}$) followed by Kikagati mine with

(84.53±35.07 $nGyh^{-1}$ and 158.95±79.74 $nGyh^{-1}$) and Mashonga mine with (67.15±48.46 $nGyh^{-1}$ and 126.75±102.27 $nGyh^{-1}$) respectively for the waste rock tailing samples.

A column chart comparing the mean absorbed dose rates in the waste rock samples from Mashonga, Kikagati and Butare mines is as presented in the Figure 4.9 below.

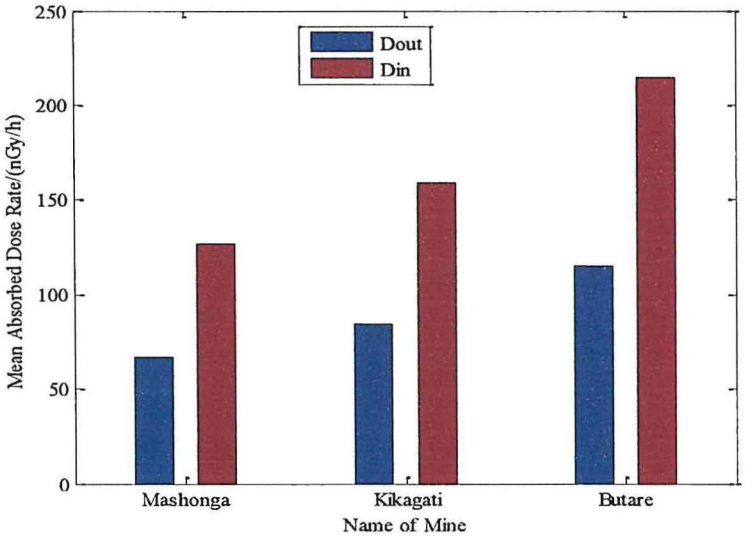

Figure 4.9: Comparison of Mean Absorbed Dose Rates in the waste rock samples

As observed in Figure 4.9 above, the mean indoor absorbed dose rates were about twice the mean outdoor dose rates.

The mean absorbed dose rates in mine tailings from tailings from Mashonga, Kikagati and Butare mines were compared using the column charts as presented in Figure 4.10 below.

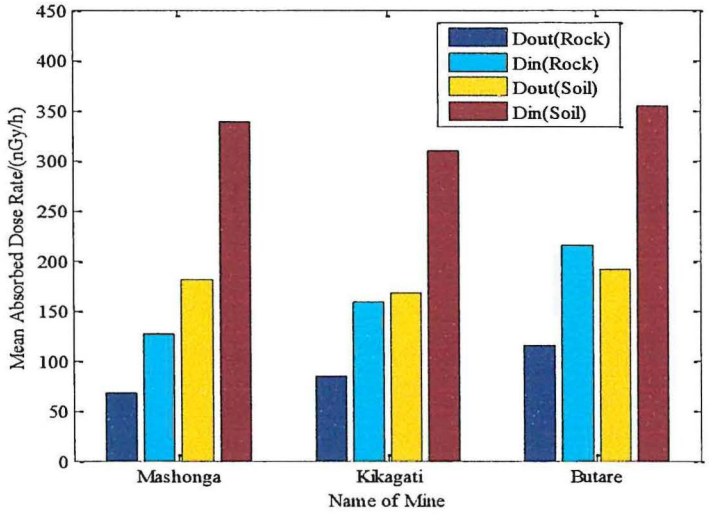

Figure 4.10: Comparison of Mean Absorbed Dose Rates in the mine tailings

The mean indoor and outdoor absorbed dose rates in the waste soil tailings samples from Mashonga, Kikagati and Butare mines were about 3, 2 and 2 times that in waste rock tailing samples respectively. The mean outdoor and indoor annual effective dose rates of (0.23±0.06 $mSvy^{-1}$ and 0.88±0.27 $mSvy^{-1}$) for waste rock samples from Butare mine were the highest, followed by (0.17±0.07 $mSvy^{-1}$ and 0.65±0.33 $mSvy^{-1}$) for Kikagati mine and (0.14±0.10 $mSvy^{-1}$ and 0.52±0.42 $mSvy^{-1}$) for Mashonga mine respectively. The total annual effective dose rates of 0.66±0.52 $mSvy^{-1}$, 0.82±0.40 $mSvy^{-1}$ and 1.11±0.34 $mSvy^{-1}$ in waste rock tailing samples from Mashonga, Kikagati and Butare mines were above the world range. These values were below the recommended dose limit of 1 mSv y^{-1} for a member of the public by 0.34 $mSvy^{-1}$ and 0.18 $mSvy^{-1}$ for Mashonga and Kikagati mines respectively but higher by 0.11 $mSvy^{-1}$ for Butare mine.

The outdoor, indoor and the total annual effective dose rates in the waste rock samples from Mashonga, Kikagati and Butare mines were compared using the column charts presented in Figure 4.11 below.

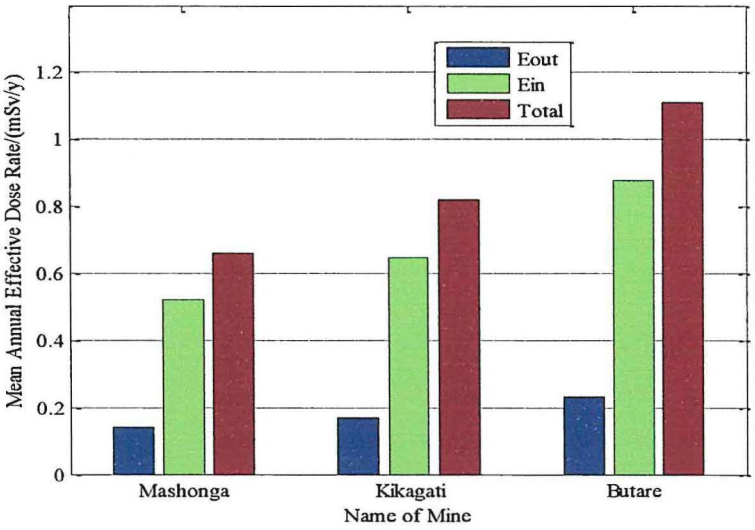

Figure 4.11: Comparison of Annual Effective Dose Rates in the waste rock samples

As observed in Figure 4.11 above, the mean outdoor, indoor and total annual effective dose rates in waste rock samples from tailings of the three sites were below the dose limit of 1 $mSvy^{-1}$ for the public for Mashonga and Kikagati mines but higher for Butare mine.

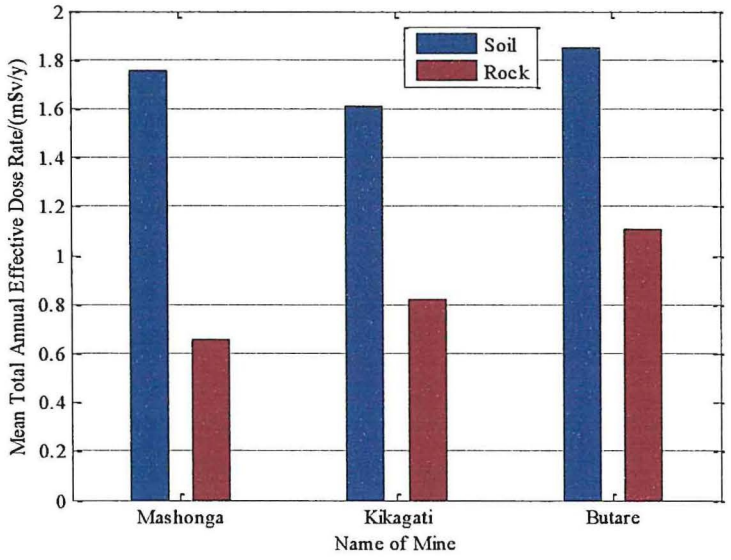

Figure 4.12: Comparison of Annual Effective Dose Rates in the mine tailing

A comparison between the total annual effective dose rates in the mine tailings from all the sites was made using column charts shown in Figure 4.12 above. The total annual effective dose rates in the waste soil tailing samples from Mashonga, Kikagati and Butare mines were above those for the waste rock tailings. The total annual effective dose rates from waste soil tailing samples from Mashonga, Kikagati and Butare mines were 74.6%, 67.1% and 77.1% of the natural background radiation of 2.4 $mSvy^{-1}$ as compared to those of the waste rock tailing samples that were 27.5%, 34.2% and 46.3% of the natural background radiation. This shows that the waste soil tailings from Mashonga, Kikagati and Butare mines contributed more than twice as much dose rate as that from waste rock tailings to the background radiation respectively.

The Table 4.19 below gives the t test values (at 90% confidence level) obtained in this study for gamma dose rates in the mine tailing.

Table 4.19: Statistical t test for Mean Gamma Dose Rates

Waste soil samples

	Dout in soil	**Effective Dose**
Mashonga	181.23	1.76
Kikagati	167.16	1.61
Df	22	22
Calculated $t_{\alpha=0.10}$	0.62	0.64
Table value $t_{\alpha=0.10}$	1.72	1.72

(a)

Waste soil samples

	Dout in soil	**Effective Dose**
Mashonga	181.23	1.76
Butare	191.62	1.85
df	22	22
Calculated $t_{\alpha=0.10}$	-0.49	-0.42
Table value $t_{\alpha=0.10}$	1.72	1.72

(b)

Waste soil samples

	Dout in soil	**Effective Dose**
Kikagati	167.16	1.61
Butare	191.62	1.85
Df	22	22
Calculated $t_{\alpha=0.10}$	-1.64	-1.51
Table value $t_{\alpha=0.10}$	1.72	1.72

(c)

Waste rock samples

	Dout in rocks	**Effective Dose**
Mashonga	67.15	0.66
Kikagati	84.53	0.82
df	22	22
Calculated $t_{\alpha=0.10}$	-0.52	-0.46
Table value $t_{\alpha=0.10}$	1.72	1.72

(d)

Waste rock samples

	Dout in rocks	**Effective Dose**
Mashonga	67.15	0.66
Butare	114.87	1.11
Df	22	22
Calculated $t_{\alpha=0.10}$	-1.48	-1.33
Table value $t_{\alpha=0.10}$	1.72	1.72

(e)

Waste rock samples

	Dout in rocks	**Effective Dose**
Kikagati	84.53	0.82
Butare	114.87	1.11
df	22	22
Calculated $t_{\alpha=0.10}$	-1.15	-1.00
Table value $t_{\alpha=0.10}$	1.72	1.72

(f)

Since the calculated values of $t_{\alpha=0.10}$ presented in Table 4.19 above are below the table values, then the gamma dose rates in the mine tailings from Mashonga gold mine, Kikagati tin mine and Butare iron ore mine were statistically not significantly different.

4.4 Radiological Hazard Indices in Mine Tailings

The radiological hazard indices which have been presented under this section are: the radium equivalent activity (Ra_{eq}), external hazard index (H_{ex}), internal hazard index (H_{in}) and the excess lifetime cancer risk (ELCR).

The Radium Equivalent Activity due to the gamma radiation from radionuclides in the mine tailings was obtained using the equation $Ra_{eq} = A_{Ra} + 1.43 \times A_{Th} + 0.077 \times A_K$ $Bqkg^{-1}$ where $A_{Ra}(A_U)$, A_{Th} and A_K are the mean specific activities of ^{238}U, ^{232}Th and ^{40}K radionuclides respectively. The results of the radium equivalent activity levels obtained in this study were compared to the maximum permissible limit of 370 Bq kg^{-1} recommended for materials used for construction purposes (UNSCEAR, 2000; Beretka and Mathew, 1985).

The External Hazard Index (H_{ex}) and Internal Hazard Index (H_{in}) were obtained using the equations

$$H_{ex} = \frac{A_{Ra}}{370} + \frac{A_{Th}}{259} + \frac{A_K}{4810} \text{ and } H_{in} = \frac{A_{Ra}}{185} + \frac{A_{Th}}{259} + \frac{A_K}{4810} \text{ respectively}$$

where $A_{Ra}(A_U)$, A_{Th} and A_K are the mean specific activities of ^{238}U, ^{232}Th and ^{40}K radionuclides respectively. The results of the external hazard index and the internal hazard index obtainded in this study were compared to the maximum permissible limit of unity (UNSCEAR, 2000; Beretka and Mathew, 1985).

The excess lifetime cancer risk (ELCR) was determined using the equation

$$ELCR = AEDE \times 50.4y \times 0.05Sv^{-1}$$

where AEDE ($mSv\ y^{-1}$) is the total annual effective dose equivalent rate. The results of the excess lifetime cancer risk obtained in this study for the soil and rock tailing samples were compared to the world average lifetime fatal cancer risk of 1.68×10^{-3} based on the total external terrestrial gamma dose rate of 0.48 $mSvy^{-1}$ (UNSEAR, 2000).

4.4.1: Radiological Hazard Indices of mine tailings from Mashonga gold mine

The mean values of the radium equivalent activity, the external hazard index, internal hazard index and excess lifetime cancer risk in waste soil samples from Mashonga gold mine are as presented in Table 4.20 below.

Table 4.20: Hazard Indices of waste soil samples from Mashonga Gold Mine

Parameter	Ra_{eq}/Bqkg^{-1}	H_{ex}	H_{in}	ELCR×10^{-3}
Mean	404.15	1.09	1.25	4.43
Standard deviation	161.99	0.44	0.53	1.68
Standard error of the Mean	46.76	0.13	0.15	0.49
Maximum error of the Mean ($t_{\alpha=0.10}$)	83.98	0.23	0.27	0.87
Maximum error of the Mean ($t_{\alpha=0.05}$)	102.92	0.28	0.33	1.07
Maximum error of the Mean ($t_{\alpha=0.01}$)	145.24	0.39	0.47	1.51

The mean radium equivalent activity of 404.15 Bqkg^{-1} obtained for waste soil samples from Mashonga gold mine was above the maximum permissible limit recommended for building materials by 9.2%. The external hazard index and the internal hazard index of 1.09 and 1.25 respectively for the waste soil samples from Mashonga gold mine were greater than unity by 9% and 25% respectively. This means that external and internal exposure to radionuclides in the waste soil tailings from Mashonga gold mine may be hazardous to the people who work or live around the mines and therefore must not be used for construction of buildings. The mean excess lifetime cancer risk of 4.43×10^{-3} for the waste soil samples from Mashonga gold mine was 2.64 times the world average.

The mean radium equivalent activity, the external hazard index, internal hazard index and excess lifetime cancer risk of waste rock samples from Mashonga gold mine are as presented in Table 4.21 below.

Table 4.21: Hazard Indices of waste rock samples from Mashonga Gold Mine

Parameter	Ra_{eq}/Bqkg^{-1}	H_{ex}	H_{in}	ELCR×10^{-3}
Mean	142.73	0.39	0.45	1.65
Standard deviation	209.00	0.56	0.63	2.52
Standard error of the Mean	60.33	0.16	0.18	0.73
Maximum error of the Mean ($t_{\alpha=0.10}$)	108.36	0.29	0.33	1.31
Maximum error of the Mean ($t_{\alpha=0.05}$)	31.28	0.08	0.09	1.60
Maximum error of the Mean ($t_{\alpha=0.01}$)	187.39	0.51	0.57	2.26

The mean radium equivalent activity of 142.73 $Bqkg^{-1}$ due to radionuclides in the waste rock tailings from Mashonga gold mine was below the maximum permissible limit for building materials by 61.4%. The mean external hazard index and internal hazard index of 0.39 and 0.45 respectively in the waste rock tailings were below unity by 61% and 55% respectively. This implies that the radiation hazard from radionuclides in the waste rock tailings from Mashonga gold mine were low. The mean excess lifetime cancer risk of 1.65×10^{-3} for the waste rock samples from Mashonga gold mine was 0.98 times the world average.

4.4.2: Radiological Hazard Indices of mine tailings from Kikagati tin mine

The mean radium equivalent activity, the external hazard index, internal hazard index and excess lifetime cancer risk of waste soil samples from Kikagati tin mine are as presented in Table 4.22 below.

Table 4.22: Hazard Indices of waste soil samples from Kikagati Tin Mine

Parameter	$Ra_{eq}/Bqkg^{-1}$	H_{ex}	H_{in}	$ELCR\times10^{-3}$
Mean	382.58	1.03	1.17	4.06
Standard deviation	100.80	0.27	0.30	1.14
Standard error of the Mean	29.10	0.08	0.09	0.33
Maximum error of the Mean ($t_{\alpha=0.10}$)	52.26	0.14	0.15	0.59
Maximum error of the Mean ($t_{\alpha=0.05}$)	64.04	0.17	0.19	0.72
Maximum error of the Mean ($t_{\alpha=0.01}$)	90.38	0.24	0.27	1.02

The mean radium equivalent activity of 382.58 $Bqkg^{-1}$ obtained for waste soil samples from Kikagati tin mine was above the maximum permissible limit by 3.4%. The mean external hazard index and the internal hazard index of 1.03 and 1.17 respectively were greater than unity by 3% and 17% respectively. This means that external and internal exposure to radionuclides in the waste soil tailings from Kikagati tin mine may be hazardous to the people who work or live around the mines. The mean excess lifetime cancer risk of 4.08×10^{-3} for the waste soil samples from Kikagati tin mine was 2.43 times the world average.

The mean radium equivalent activity, the external hazard index, internal hazard index and excess lifetime cancer risk of waste rock samples from Kikagati tin mine are as presented in Table 4.23 below.

Table 4.23: Hazard Indices of waste rock samples from Kikagati Tin Mine

Parameter	Ra_{eq}/Bqkg^{-1}	H_{ex}	H_{in}	ELCR×10^{-3}
Mean	181.47	0.49	0.56	2.08
Standard deviation	141.03	0.38	0.43	1.94
Standard error of the Mean	40.71	0.11	0.12	0.56
Maximum error of the Mean ($t_{\alpha=0.10}$)	73.12	0.20	0.22	1.00
Maximum error of the Mean ($t_{\alpha=0.05}$)	89.61	0.24	0.27	1.23
Maximum error of the Mean ($t_{\alpha=0.01}$)	126.45	0.34	0.38	1.74

The mean radium equivalent activity of 181.47 Bqkg^{-1} due to radionuclides in the waste rock tailings was below the maximum permissible limit for building materials by 51.0%. The mean external hazard index and internal hazard index of 0.49 and 0.56 respectively in the waste rock tailings from Kikagati tin mine were below unity by 51% and 44% respectively. This implies that the radionuclides in the waste rock tailings from Kikagati tin mine do not present a serious health hazard to the people who work or live around the mine. The mean excess lifetime cancer risk of 2.08×10^{-3} for the waste rock samples from Kikagati tin mine was 1.24 times the world average.

4.4.3: Radiological Hazard Indices of mine tailings from Butare iron ore mine

The mean the radium equivalent activity, the external hazard index, and internal hazard index of the waste soil samples from Butare iron ore mine are as presented in Table 4.24 below.

Table 4.24: Hazard Indices of waste soil samples from Butare Iron Ore Mine

Parameter	Ra_{eq}/Bqkg^{-1}	H_{ex}	H_{in}	ELCR×10^{-3}
Mean	439.22	1.19	1.34	4.65
Standard deviation	69.67	0.19	0.21	0.80
Standard error of the Mean	20.11	0.05	0.06	0.23
Maximum error of the Mean ($t_{\alpha=0.10}$)	36.12	0.10	0.11	0.41
Maximum error of the Mean ($t_{\alpha=0.05}$)	44.27	0.12	0.14	0.51
Maximum error of the Mean ($t_{\alpha=0.01}$)	62.47	0.17	0.19	0.72

The mean radium equivalent activity of 439.22 Bqkg^{-1} obtained for waste soil samples from Butare iron ore mine was above the maximum permissible limit for building materials by 18.7%. The external hazard index and the internal hazard index of 1.19 and 1.34 respectively were greater than unity by 19% and 34% respectively. This means that the radiation hazard from radionuclides in the waste soil tailings in Butare iron ore mine may present significant external and internal health hazards to the people who work or live around the mine. The mean excess lifetime cancer risk of 4.65×10^{-3} for the soil samples from tailings from Butare tin mine was 2.77 times the world average.

The mean radium equivalent activity, the external hazard index, internal hazard index and excess lifetime cancer risk of the waste rock samples from Butare iron ore mine are as presented in Table 4.25 below.

Table 4.25: Hazard Indices of waste rock samples from Butare Iron Ore Mine

Parameter	Ra_{eq}/Bqkg^{-1}	H_{ex}	H_{in}	ELCR×10^{-3}
Mean	418.47	0.71	0.86	2.81
Standard deviation	398.09	0.37	0.42	1.64
Standard error of the Mean	114.92	0.11	0.12	0.47
Maximum error of the Mean ($t_{\alpha=0.10}$)	206.39	0.19	0.22	0.85
Maximum error of the Mean ($t_{\alpha=0.05}$)	370.68	0.34	0.39	1.04
Maximum error of the Mean ($t_{\alpha=0.01}$)	356.94	0.33	0.37	1.47

The mean radium equivalent activity of 418.47 Bq kg^{-1} due to the radionuclides in the waste rock tailings from Butare iron ore mine was above the maximum permissible limit for building materials by 13.1%. The mean external hazard index and internal hazard

index of 0.71 and 0.86 respectively in the waste rock tailings were below unity by 29% and 14% respectively. This means that exposure to the radionuclides in the waste rock tailings from Butare iron ore mine do not present serious hazards to the people who work or live around the mine. The mean excess lifetime cancer risk of 2.81×10^{-3} in waste rock samples from Butare iron ore mine was 1.67 times the world average.

The mean radiological hazard indices in the mine tailings for Mashonga, Kikagati and Butare mines are as presented in Table 4.26 and Table 4.27 below.

Table 4.26: Comparison of Hazard Indices in waste soil samples

Mine	Ra_{eq}/Bqkg^{-1}	H_{ex}	H_{in}	ELCR$\times10^{-3}$
Mashonga	404.15±83.98	1.09±0.23	1.25±0.27	4.43±0.87
Kikagati	382.58±52.26	1.03±0.14	1.17±0.15	4.06±0.59
Butare	439.22±36.12	1.19±0.10	1.34±0.11	4.65±0.41

Waste soil tailing samples from Butare mine had the highest mean radium equivalent activity of 404.15±83.98 Bqkg^{-1} followed by Mashonga mine (404.15±83.98 Bqkg^{-1}) and Kikagati mine (382.58±52.26 Bqkg^{-1}). The mean external hazard index and internal hazard index of 1.19±0.10 and 1.34±0.11 were the highest in waste soil tailing samples from Butare mine, followed by Mashonga mine (1.09±0.23 and 1.25±0.27) and Kikagati mine (1.03±0.14 and 1.17±0.15) respectively. The mean excess lifetime cancer risk in the waste soil tailing samples was the highest in samples from Butare mine ($4.65\pm0.41\times10^{-3}$) followed by Mashonga mine ($4.43\pm0.87\times10^{-3}$) and Kikagati mine ($4.06\pm0.59\times10^{-3}$).

Table 4.27: Comparison of the Hazard Indices in waste rock samples

Mine	Ra_{eq}/Bqkg^{-1}	H_{ex}	H_{in}	ELCR$\times10^{-3}$
Mashonga	142.73±108.36	0.39±0.29	0.45±0.33	1.65±1.31
Kikagati	181.47±73.12	0.49±0.20	0.56±0.22	2.08±1.00
Butare	418.47±206.36	0.71±0.19	0.86±0.22	2.81±0.85

Waste rock tailing samples from Butare mine had the highest mean radium equivalent activity of 418.47±206.36 Bqkg^{-1} followed by Kikagati mine (181.47±73.12 Bqkg^{-1}) and

Mashonga mine (142.73±108.36 $Bqkg^{-1}$). The mean external hazard index and internal hazard index of 0.71±0.19 and 0.86±0.22 were the highest in the waste rock tailing samples from Butare mine, followed by Kikagati mine (0.49±0.20 and 0.56±0.22) and Mashonga mine (0.39±0.29 and 0.45±0.33) respectively. The mean excess lifetime cancer risk in waste rock tailing samples was the highest in samples from Butare mine ($2.81\pm0.85\times10^{-3}$) followed by Kikagati mine ($2.08\pm1.00\times10^{-3}$) and Mashonga mine ($1.65\pm1.31\times10^{-3}$).

The mean radium equivalent activities in the mine tailing samples from Mashonga, Kikagati and Butare mines were compared using the column charts as shown in Figure 4.13 below.

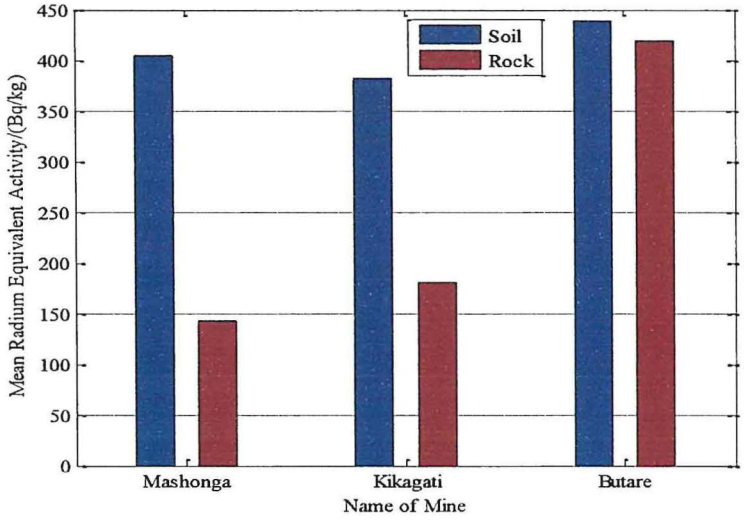

Figure 4.13: Comparison of Mean Radium Equivalent Activities of mine tailings

As observed in Figure 4.13 above, the mean radium equivalent activities for waste soil samples from all the three sites and waste rock tailing samples from Butare were higher than the maximum permissible limit of 370 $Bqkg^{-1}$ recommended for building materials, required to keep the dose equivalent for the public to below 1 $mSvy^{-1}$. The mean radium equivalent activities in waste soil tailing samples from Mashonga, Kikagati and Butare mines were above the maximum permissible limit for building materials by 9.2%, 3.5% and 18.6% respectively. This implies that the soil tailings from Mashonga, Kikagati and Butare may not be suitable for use as building materials. The mean radium equivalent

activities for waste rock samples from Mashonga and Kikagati mines were 61.4% and 51.0% below the maximum permissible limit for building materials while that for waste rock samples from Butare mine was above the maximum permissible limit by 13.1%.

The mean external hazard index in the mine tailing samples from Mashonga, Kikagati and Butare mines were compared using the column charts as shown in Figure 4.14 below.

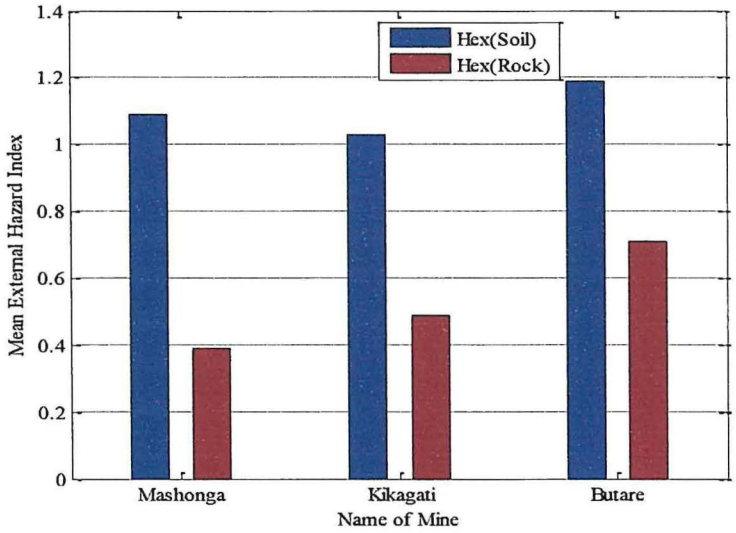

Figure 4.14: Comparison of Mean External Hazard Indices in the mine tailings

As observed in Figure 4.14 above, the external hazard index in the waste soil samples from the three sites were above unity while the external hazard index in waste rock samples were below unity. The external hazard indices in the waste soil samples from tailings from Mashonga, Kikagati and Butare mine were above unity by 9%, 3% and 19% while external hazard indices in waste rock samples were below unity by 61%, 51% and 29% respectively. This shows that the external gamma radiation hazard is more significant in waste soil tailings than in waste rock tailings when used as construction building materials. This implies that waste soil tailings should not be used in bulk as construction building materials.

The mean internal hazard index in the mine tailing samples from Mashonga, Kikagati and Butare mines were compared using the column charts as shown in Figure 4.15 below.

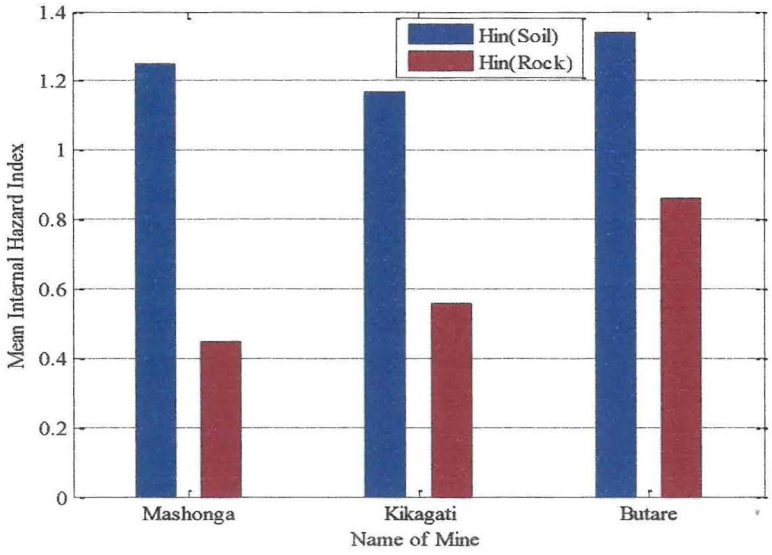

Figure 4.15: Comparison of Mean Internal Hazard Indices in mine tailings

As observed in Figure 4.15 above, the mean internal hazard indices in the waste soil tailing samples from all the three sites were above unity while the mean internal hazard indices in waste rock samples from all the three sites were below unity. The mean internal hazard indices in waste soil samples from tailings from Mashonga, Kikagati and Butare mines were greater than unity by 25%, 17% and 34% respectively. For the rock samples, the mean internal hazard indices were below unity by 55%, 44% and 14% for Mashonga, Kikagati and Butare mines respectively. This implies that the gamma radiation hazard from internally deposited radionuclides from the waste soil tailings in all the three mines may cause serious health hazards to the workers and to the public around those mines.

The mean excess lifetime cancer risks in the mine tailing samples from Mashonga, Kikagati and Butare mines were compared using the column charts as shown in Figure 4.16 below.

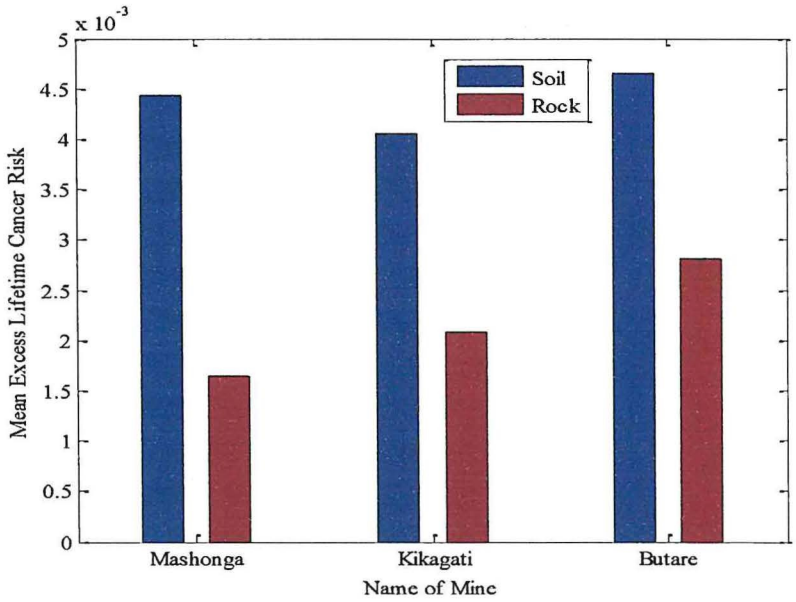

Figure 4.16: Comparison of Mean Excess Lifetime Cancer Risks in mine tailings

As observed in Figure 4.16 above, the mean excess lifetime cancer risk levels in the waste soil tailings from Mashonga, Kikagati and Butare mines were above the levels in waste rock tailings. The mean excess lifetime cancer risk levels in the soil tailing samples from Mashonga, Kikagati and Butare mines were 2.7, 2.0 and 1.7 times that in waste rock tailings from the same sites respectively. The probability of cancer induction due to gamma radiation exposure was greatest in the waste soil tailings and lowest in the waste rock tailings. At least 4 per 1000 people and at least 2 per 1000 people might develop fatal cancer due to the gamma radiation exposure from the waste soil and rock tailings from Mashonga, Kikagati and Butare mines respectively.

The Table 4.28 below gives the t test values (at 90% confidence level) obtained in this study for the radiological hazard indices the mine tailing.

Table 4.28: Statistical t test for Hazard Indices in mine

Waste soil samples

	Ra_{eq}	H_{in}	ELCR
Mashonga	404.15	1.25	4.43
Kikagati	382.58	1.17	4.06
Df	22	22	22
Calculated $t_{\alpha=0.10}$	0.39	0.47	0.63
Table value $t_{\alpha=0.10}$	1.72	1.72	1.72

(a)

Waste soil samples

	Ra_{eq}	H_{in}	ELCR
Mashonga	404.15	1.25	4.43
Butare	439.22	1.34	4.65
df	22	22	22
Calculated $t_{\alpha=0.10}$	-0.69	-0.56	-0.41
Table value $t_{\alpha=0.10}$	1.72	1.72	1.72

(b)

Waste soil samples

	Ra_{eq}	H_{in}	ELCR
Kikagati	382.58	1.17	4.06
Butare	439.22	1.34	4.65
Df	22	22	22
Calculated $t_{\alpha=0.10}$	-1.60	-1.65	-1.47
Table value $t_{\alpha=0.10}$	1.72	1.72	1.72

(c)

Waste rock samples

	Ra_{eq}	H_{in}	ELCR
Mashonga	142.73	0.45	1.65
Kikagati	181.47	0.56	2.08
df	22	22	22
Calculated $t_{\alpha=0.10}$	-0.53	-0.49	-0.47
Table value $t_{\alpha=0.10}$	1.72	1.72	1.72

(d)

Waste rock samples

	Ra_{eq}	H_{in}	ELCR
Mashonga	142.73	0.45	1.65
Butare	418.47	0.86	2.81
Df	22	22	22
Calculated $t_{\alpha=0.10}$	-2.12	-1.90	-1.34
Table value $t_{\alpha=0.10}$	1.72	1.72	1.72

(e)

Waste rock samples

	Ra_{eq}	H_{in}	ELCR
Kikagati	181.47	0.56	2.08
Butare	418.47	0.86	2.81
df	22	22	22
Calculated $t_{\alpha=0.10}$	-1.94	-1.79	-1.00
Table value $t_{\alpha=0.10}$	1.72	1.72	1.72

(f)

Since the calculated $t_{\alpha=0.10}$ value for the mean excess lifetime cancer risk in the waste soil and rock samples are below the table values, then levels in those sites were not statistically significantly different. The levels of the mean radium equivalent activity and internal hazard index in the waste soil and rock samples from Mashonga, Kikagati and Butare mines were statistically significantly different as observed only in (e) and (f) above.

CHAPTER FIVE: DISCUSSION, CONCLUSIONS AND RECOMMENDATIONS

5.1 Introduction

This chapter has discussed the results presented in Chapter Four. The findings have also been compared with similar studies done in Uganda and world over. Possible conclusions and recommendations have been drawn.

5.2 Discussion of Results of the Study

This section has discussed the results of the gamma activity levels and gamma dose rates (absorbed dose rates and annual effective dose rates). The results of radiological hazard indices (radium equivalent activity, external hazard index and internal hazard index and excess lifetime cancer risk) in waste soil and rock samples from Mashonga gold mine, Kikagati tin mine and Butare iron ore mine have been discussed in this section.

5.2.1 Gamma Activity levels in Mine Tailings

The specific activity levels of ^{238}U, ^{232}Th and ^{40}K in the waste soil and rock samples varied from one mine to another. This may be due to differences in the geology, topography and geographical conditions of the mining areas studied (UNSCEAR, 2000).

The mean specific activity levels of ^{238}U in waste soil samples for Mashonga, Kikagati and Butare mine at 90% confidence level were 58.75±15.87 $Bqkg^{-1}$ (37.70 – 147.02 $Bqkg^{-1}$), 49.72±5.65 $Bqkg^{-1}$ (35.47 – 69.59 $Bqkg^{-1}$) and 57.62±5.06 $Bqkg^{-1}$ (44.25 – 72.59 $Bqkg^{-1}$). For waste rock samples, the mean specific activity levels of ^{238}U for Mashonga, Kikagati and Butare mine at 90% confidence level were 23.30±13.56 Bq kg^{-1} (3.20 – 99.82 $Bqkg^{-1}$), 24.87±9.30 $Bqkg^{-1}$ (2.87 – 51.22 $Bqkg^{-1}$) and 58.59±9.94 $Bqkg^{-1}$ (25.46 – 90.26 $Bqkg^{-1}$). According to Baxter (1993), the mean specific activity of ^{238}U in sands and gravels varies from 20 – 90 Bq kg^{-1} and has a mean value of 48 $Bqkg^{-1}$ in igneous rocks and 24 $Bqkg^{-1}$ in sedimentary sandstone. The values obtained in waste soil samples for ^{238}U lie within range of sands according to Baxter since soils contain a substantial amount of sand. The values for waste rock samples are close to those of Baxter for igneous and sedimentary rocks. The low specific activity levels of ^{238}U in waste rock samples from Mashonga and Kikagati could be due to the fact that highly weathered granite, quartz, mica and potassium feldspar rocks release ^{238}U into the soil. Therefore the

concentration of ^{238}U is increased in slightly weathered soils (Dickson and Scott, 1997). According to a study by Lemeriga (1998), the mean specific activity of ^{238}U in the soil samples from places in Mukono, Mbale and Hoima was 23.97 $Bqkg^{-1}$ and varied from 7 – 55 $Bqkg^{-1}$. The mean specific activity levels of ^{238}U obtained this study appear to lie in the range of Lemeriga.

The mean specific activity levels of ^{232}Th in the waste soil samples for Mashonga, Kikagati and Butare mine at 90% confidence level were 193.46±35.60 $Bqkg^{-1}$ (133.12 – 376.73 $Bqkg^{-1}$), 211.69±31.19 $Bqkg^{-1}$ (119.33 – 306.79 $Bqkg^{-1}$) and 244.43±18.98 $Bqkg^{-1}$ (185.30 – 297.75 $Bqkg^{-1}$). For waste rock samples, the mean specific activity of ^{232}Th for Mashonga, Kikagati and Butare mine at 90% confidence level were 48.66±39.08 $Bqkg^{-1}$ (3.20 – 270.23 $Bqkg^{-1}$), 69.03±35.60 $Bqkg^{-1}$ (1.86 – 183.83 $Bqkg^{-1}$) and 129.74±35.03 $Bqkg^{-1}$ (24.53 – 221.24 $Bqkg^{-1}$). According to UNSCEAR, (2000), ^{232}Th is concentrated in monazite sands and is released from the rocks into the soil during weathering. This is the reason why the activity level of ^{232}Th is lower in the waste rock tailings than in the waste soil tailings studied. According to Baxter, (1993), the mean specific activity of ^{232}Th in sands and gravels varies from 20 – 200 $Bqkg^{-1}$. The studied samples had their mean specific activities in this range. A study of soil samples from places in Mukono, Mbale and Hoima by Lemeriga, (1998) revealed that the specific activity of ^{232}Th varied from 111 – 286 $Bqkg^{-1}$ and had a mean value of 173.88 $Bqkg^{-1}$. The mean specific activities of ^{232}Th in waste soil samples, this current study obtained appear to be in the range of Lemeriga. According to the Mining Journal Uganda, (2012), the Karagwe-Ankolean system is mainly composed of pegmatite, granites, sandstone, quartz and mica rocks which are hosts of gold, iron ore, tin and other minerals. The fact that the mean specific activity of ^{232}Th in granite rocks is 80 Bq kg^{-1} (Baxter, 1993), the sampled waste rocks might have been of granite origin.

The mean specific activity level of ^{40}K in waste soil samples for Mashonga, Kikagati and Butare mine at 90% confidence level were 892.90±167.35 $Bqkg^{-1}$ (565.92 – 1658.51 $Bqkg^{-1}$), 391.53±84.83 $Bqkg^{-1}$ (141.01 – 629.23 $Bqkg^{-1}$) and 416.43±84.17 $Bqkg^{-1}$ (266.07 – 836.74 $Bqkg^{-1}$). For waste rock samples, the mean specific activities of ^{40}K for Mashonga, Kikagati and Butare mine at 90% confidence level were 647.23±585.04 $Bqkg^{-1}$ (7.20 – 3781.30 $Bqkg^{-1}$), 751.66±400.18 $Bqkg^{-1}$ (2.24 – 1991.63 $Bqkg^{-1}$) and 226.43±231.83 $Bqkg^{-1}$ (5.58 – 1379.02 $Bqkg^{-1}$). According to UNSCEAR (2000), ^{40}K is

more concentrated in potassium feldspar and micas as well as in granite rocks and its activity level is enhanced in the clay soil due to weathering of the rocks (Dickson and Scott, 1997). The activity levels of ^{40}K in the waste soil samples were high due to presence of weathered potassium feldspar, zircon, quartz-mica and granite rocks in the waste soil tailings of Mashonga gold mine. The low values of ^{40}K in the waste soil samples from Kikagati and Butare mines could be due to erosion and leaching (Hermann et. al., 2010) when it rains as these two sites are hilly (over 1200 m above sea level). Over cropping may also result in reduction in the activity of ^{40}K since crops continuously remove potassium from the soil when it is released from weathered rocks (Hermann, et. al., 2010). According to Baxter, (1993), the mean specific activity of ^{40}K in igneous rocks is 800 $Bqkg^{-1}$. This shows that the studied rock tailing samples from Mashonga and Kikagati were composed of igneous rocks of granite composition. Therefore differences in geology and topography of the areas studies caused the differences in the specific activity of ^{40}K in the waste soil tailings.

According to the United Nations Scientific Committee on Effects of Atomic Radiation (UNSCEAR, 2000), the ranges of specific activities of ^{238}U, ^{232}Th, ^{40}K in soil and rocks are 16 – 110 $Bqkg^{-1}$, 11 – 64 $Bqkg^{-1}$ and 140 – 850 $Bqkg^{-1}$ with the world population weighted average values of 33 $Bqkg^{-1}$, 45 $Bqkg^{-1}$ and 420 $Bqkg^{-1}$ respectively. The mean specific activities of ^{238}U and ^{40}K obtained in this study for the waste soil and rock samples from Mashonga, Kikagati and Butare mines appeared to be in their respective world ranges. For Kikagati, the mean specific activity of ^{40}K was 0.93 times the world average for waste soil samples and 1.79 times the world average for the waste rock tailing samples. For Mashonga gold mine, the mean specific activities of ^{40}K in the waste soil and rock samples were 2.13 and 1.54 times the world average respectively. For waste soil and rock samples from Butare, the mean specific activities of ^{40}K were 0.99 and 0.54 times the world average respectively. The mean specific activities of ^{232}Th in the waste soil tailings for all the sites were about five times the world average. For waste rock samples, the mean specific activity of ^{232}Th for Mashonga was 1.08 times the world average. The mean specific activity of ^{232}Th in waste rock samples from Kikagati and Butare mines were 1.53 and 2.88 times the world average.

5.2.2 Gamma dose rates in mine tailings

The mean outdoor and indoor absorbed dose rates in air for the waste soil samples of Mashonga, Kikagati and Butare mine at 90% confidence level were (181.23±34.63 $nGyh^{-1}$ and 338.29±67.15 $nGyh^{-1}$), (167.16±21.85 $nGyh^{-1}$ and 309.92±46.29 $nGyh^{-1}$) and (191.62±15.58 $nGyh^{-1}$ and 355.20±32.27 $nGyh^{-1}$) respectively. For the waste rock samples from Mashonga, Kikagati and Butare, the mean outdoor and indoor absorbed dose rates at 90% confidence level were 67.15±48.46 $nGyh^{-1}$ and 126.75±102.27 $nGyh^{-1}$), (84.53±35.07 $nGyh^{-1}$ and 158.95±79.74 $nGyh^{-1}$) and (114.87±31.95 $nGyh^{-1}$ and 214.73±66.23 $nGyh^{-1}$) respectively. The ratio of the indoor to outdoor mean absorbed dose dose rates was 1.9. This ratio was higher than the world average (UNSCEAR, 2000) by 35.7% but was in the range of the world average. The main contributor to the absorbed dose rates in the waste soil tailings was ^{232}Th at 64%. In the waste rocks, ^{232}Th and ^{40}K were the main contributors to the absorbed dose rates at 44% and 40% respectively. The world population weighted outdoor and indoor absorbed dose rates are 59 $nGyh^{-1}$ and 84 $nGyh^{-1}$ (UNSCEAR, 2000) respectively. The mean outdoor and indoor absorbed dose rates in the waste soil tailings for Mashonga, Kikagati and Butare mines were about 3 and 4 times the world averages respectively. For waste rock samples, the mean outdoor and indoor absorbed dose rates for Mashonga, Kikagati and Butare mines were (13.8%, 43.3% and 94.7%) and (50.9%, 89.0% and 156.0%) higher than the world averages respectively. Higher concentrations of ^{238}U, ^{232}Th and ^{40}K in the waste soil and cosmic rays at higher altitudes may have greatly contributed to these levels since the studied areas were hilly.

A comparison of the mean outdoor absorbed dose rates in the studied mines in Southwestern Uganda with those reported from similar studies around the world was done. Isinkaye, (2013) obtained mean absorbed dose rates of 110.78±32.92 $nGyh^{-1}$ and 108.55±17.38 $nGyh^{-1}$ for soil and sediment samples from Ijero mine and 61.18±12.58 $nGyh^{-1}$ and 79.39±26.14 $nGyh^{-1}$ for soil and sediment samples from Ilesa mine in Southwestern Nigeria. These values are 1.9 times the world average for soil and sediment samples from Ijero mine while for Ilesa mine, the mean absorbed dose rates were 1.05 and 1.37 times the world average given by UNSCEAR, (2008) report. Faanu, (2011) obtained a dose rate of 27.55±15.10 $nGyh^{-1}$ for the tailing samples from Tarkwa gold mine in Ghana. This was about 0.47 times the world average and 0.15, 0.16 and 0.14 times the value obtained in this current study for Mashonga, Kikagati and Butare mines

respectively. Usikalu et al., (2011) studied natural radioactivity in the tailing samples from two mining sites (Jos tin mine in Northen Nigeria) obtained 1828.66 $nGyh^{-1}$ for site one and 252.08 $nGyh^{-1}$ for site two. The value for site one is about 10 times the values obtained in this current study for Mashonga, Kikagati and Butare mines respectively.

The mean outdoor and indoor annual effective dose rates for the waste soil tailing samples from Mashonga, Kikagati and Butare mines at 90% confidence level were (0.37±0.07 $mSvy^{-1}$ and 1.39±0.28 $mSvy^{-1}$) , (0.34±0.04 $mSvy^{-1}$ and 1.27±0.19 $mSvy^{-1}$) and (0.39±0.03 $mSvy^{-1}$ and 1.46±0.01 $mSvy^{-1}$) respectively. The total annual effective dose rates for Mashonga, Kikagati and Butare mines were 1.76±0.35 $mSvy^{-1}$, 1.61±0.23 $mSvy^{-1}$ and 1.85±0.16 $mSvy^{-1}$ respectively for the waste soil tailing samples. The total annual effective dose rates in the waste soil tailing samples from Mashonga, Kikagati and Butare mines were 73%, 67% and 77% of the natural background radiation and were above the maximum permissible dose limit of 1 mSv y^{-1} recommended for a member of the public (UNSCEAR, 2000; ICRP, 2007) by 76%, 61% and 85% respectively. The high mean indoor and total annual effective dose rates in the waste soil tailing samples could be attributed to higher concentrations of radon inside dwellings and underground mines which according to UNSCEAR, BEIR VII and IAEA (BEIR VII; IAEA-TECHDOC-1363, 2003; UNSCEAR, 2000) generate an average dose rate of 1.2 mSv y^{-1}. The outdoor external gamma radiation may also penetrate the walls of houses and buildings made of soil since they are inefficient in screening it out (UNSCEAR, 2000; EC, 1999). This therefore may increase the indoor effective dose rates. For the waste rock tailing samples, the mean outdoor and indoor annual effective dose rates for Mashonga, Kikagati and Butare mines were (0.14±0.10 $mSvy^{-1}$ and 0.52±0.42 $mSvy^{-1}$), (0.17±0.07 $mSvy^{-1}$ and0.65±0.33 $mSvy^{-1}$) and (0.23±0.06 $mSvy^{-1}$ and 0.88±0.27 $mSvy^{-1}$) respectively. The total annual effective dose rates in waste rock tailings samples from Mashonga, Kikagati and Butare mines were 0.66±0.52 $mSvy^{-1}$, 0.82±0.40 $mSvy^{-1}$ and 1.11±0.34 $mSvy^{-1}$ respectively. The total annual effective dose rates in the waste rock tailing samples from Mashonga, Kikagati and Butare mines were 28%, 34% and 46% of the natural background radiation and were below the maximum permissible dose limit of 1 mSv y^{-1} recommended for a member of the public (UNSCEAR, 2000; ICRP, 2007) by 34%, 18% for Mashonga and Kikagati mines and above by 11% for Butare mine. Higher activity levels of ^{232}Th and ^{40}K were responsible for the higher values of the total annual effective

dose rates in the waste soil and rock tailings. Prolonged exposure to low doses of gamma radiation may result in cancer induction (UNSCEAR, 2000). As the total annual effective dose rates in the waste soil tailings were higher than the maximum permissible dose limit of 1 $mSvy^{-1}$ for the public, it is necessary to provide safety measures in order to prevent harmful effects of radiation exposure such as lung cancer. Since the total annual effective dose rates measured in Mashonga, Kikagati and Butare mines were below the natural background radiation, then the working environment of the mines is still radiologically safe.

The health hazards associated with exposure to gamma emitting radionuclides in the mine tailings were assessed through calculation of radium equivalent activity, external hazard index, internal hazard index and the excess lifetime cancer risk, which are discussed in the following section.

5.2.3 Radiological hazard indices in mine tailings

The mean radium equivalent activities for waste soil samples for Mashonga, Kikagati and Butare mines at 90% confidence level were 404.15±83.98 $Bqkg^{-1}$, 382.58±52.26 $Bqkg^{-1}$ and 439.22±36.12 $Bqkg^{-1}$ respectively. For the waste rock samples for Mashonga, Kikagati and Butare mines, the mean radium equivalent activities at 90% confidence level were 142.73±108.36 $Bqkg^{-1}$, 181.47±73.12 $Bqkg^{-1}$ and 418.47±206.39 $Bqkg^{-1}$ respectively. The maximum limit of radium equivalent activity recommended for building materials is 370 $Bqkg^{-1}$(UNSCEAR, 2000). The mean radium equivalent activities for the waste soil samples from Mashonga, Kikagati and Butare mines were above the maximum permissible limit by 9.2%, 3.5% and 18.6% respectively. The mean radium equivalent activities of the waste rock samples from Mashonga and Kikagati mines were below the maximum limit by 61.4% and 50.9%. The mean radium equivalent activity for the waste rock samples from Butare mine was above the maximum permissible limit by 13.1%. On the basis of radiation protection using radium equivalent activity, the waste soil tailings from the studied sites may be regarded as not safe for use as building materials because they exceed the maximum permissible limit of 370 $Bqkg^{-1}$ recommended for materials for public use. Materials containing ^{238}U, ^{232}Th and ^{40}K are regarded as safe if their radium equivalent activity is below 370 $Bqkg^{-1}$ and corresponds to a dose rate of less than 1 $mSvy^{-1}$ set for the public (UNSCEAR, 2000).

The mean external hazard indices of waste soil samples for Mashonga, Kikagati and Butare mines at 90% confidence level were 1.09±0.28, 1.03±0.17 and 1.19±0.12. The mean external hazard indices of waste rock samples for Mashonga, Kikagati and Butare mines at 90% confidence level were 0.39±0.36, 0.49±0.24 and 0.71±0.23 respectively. The maximum limit of external hazard index and internal hazard index is unity. It is meant to keep the dose rate from radiation exposure to below the maximum permissible dose limit of 1 mSv y^{-1} for the public and ensures that the radiation hazards are kept as low as possible (UNSCEAR, 2000 and Beretka and Mathew, 1985). The mean external hazard index was above unity by 9%, 3% and 19% for the waste soil samples from Mashonga, Kikagati and Butare mines respectively. The mean external hazard index levels in the waste rock samples from Mashonga, Kikagati and Butare mines were below unity by 61%, 51% and 29% respectively. This suggests that external exposure to radionuclides in the waste soil tailings may pose radiological hazards to the workers and the members of the public while waste rock tailings are safe.

The mean internal hazard indices of the waste soil tailings for Mashonga, Kikagati and Butare mines at 90% confidence level were 1.25±0.33, 1.17±0.19 and 1.34±0.14 while that in the waste rock tailings were 0.45±0.40, 0.56±0.27 and 0.86±0.26 respectively. The mean internal hazard indices in the waste soil samples from Mashonga, Kikagati and Butare mines were above unity by 25%, 17% and 34% while those of the waste rock samples were below unity by 55%, 44% and 14% respectively. This suggests that exposure to radionuclides in the waste rock tailings may not pose serious radiological hazards to the workers and the members of the public and hence waste rock tailings on this basis are safe. Thus internally deposited radionuclides from the waste soil tailings from Mashonga, Kikagati and Butare mines may deposit significant gamma radiation doses which may be detrimental to the health of the exposed population.

The excess lifetime cancer risk is the probability of developing cancer from exposure to low levels of gamma radiation from radionuclides in the waste soil and rocks. The mean excess lifetime cancer risk levels for the waste soil samples from Mashonga, Kikagati and Butare mines at 90% confidence level were $4.43\pm0.87\times10^{-3}$, $4.06\pm0.59\times10^{-3}$ and $4.65\pm0.41\times10^{-3}$ respectively. This indicates that at least 4 in every 1000 people exposed to the radionuclides in the waste soil tailings of these mines may develop fatal cancer in later stages of their lives. The mean excess lifetime cancer risk in the waste soil samples

from Mashonga, Kikagati and Butare mines were 2.6, 2.4 and 2.8 times the world average respectively. For the waste rock samples from Mashonga, Kikagati and Butare mines, the mean excess lifetime cancer risk at 90% confidence level were $1.65\pm1.31\times10^{-3}$, $2.08\pm1.00\times10^{-3}$ and $2.81\pm0.85\times10^{-3}$ which were about 1.0, 1.2 and 1.7 times the world average respectively. This indicates that at least 2 in every 1000 people (Mashonga and Kikagati) and at least 3 in every 1000 people (Butare) exposed to the radionuclides in the waste rock tailings of these mines may develop fatal cancer in later stages of their lives. The lower excess lifetime cancer risk levels in the waste rock tailings are indicative of lower gamma dose rates mainly due to lower activity levels of ^{238}U, ^{232}Th and ^{40}K in waste rock tailings.

5.3 Conclusions

The gamma ray spectrometric analysis for ^{238}U, ^{232}Th and ^{40}K in mine tailings from Southwestern Uganda was done for the three mines of Mashonga (gold mine), Kikagati (tin mine) and Butare (iron ore mine). The mean specific activities at 90% confidence level for ^{238}U, ^{232}Th and ^{40}K in the waste soil samples for Mashonga were 58.75 ± 15.87 $Bqkg^{-1}$, 193.46 ± 35.60 $Bqkg^{-1}$ and 892.90 ± 167.35 $Bqkg^{-1}$, for Kikagati were 49.72 ± 5.65 $Bqkg^{-1}$, 211.69 ± 31.19 $Bqkg^{-1}$ and 391.53 ± 84.83 $Bqkg^{-1}$, and for Butare were 57.62 ± 5.06 $Bqkg^{-1}$, 244.43 ± 18.98 $Bqkg^{-1}$ and 416.43 ± 84.17 $Bqkg^{-1}$. The activity levels of ^{238}U and ^{232}Th in waste soil tailings in the three mines are comparable except for ^{40}K which is higher in Mashonga than in Kikagati and Butare mines which are comparable.

For the waste rock samples, the mean specific activities at 90% confidence level for ^{238}U, ^{232}Th and ^{40}K for Mashonga were 23.30 ± 13.56 $Bqkg^{-1}$, 48.66 ± 39.08 $Bqkg^{-1}$ and 647.23 ± 585.04 $Bqkg^{-1}$, for Kikagati were 24.87 ± 9.30 $Bqkg^{-1}$, 69.03 ± 35.60 $Bqkg^{-1}$ and 751.66 ± 400.18 $Bqkg^{-1}$ and for Butare were 58.59 ± 9.94 $Bqkg^{-1}$, 129.74 ± 35.03 $Bqkg^{-1}$, and 226.43 ± 231.83 $Bqkg^{-1}$. The activity levels of ^{238}U, ^{232}Th and ^{40}K in waste rock tailings in Butare mine do not compare with those of Mashonga and Kikagati mines. However, the activity level of ^{40}K in waste rock tailings in Kikagati mine is more enhanced but comparable with that of Mashonga mine.

The mean outdoor and indoor absorbed dose rates in the waste soil samples from Mashonga, Kikagati and Butare mines at 90% confidence level were (181.23 ± 34.63 $nGyh^{-1}$ and 338.29 ± 67.15 $nGyh^{-1}$), (167.16 ± 21.85 $nGyh^{-1}$ and 309.92 ± 46.29 $nGyh^{-1}$) and

(191.62±15.58 $nGyh^{-1}$ and 355.20±32.27 $nGyh^{-1}$) respectively. The outdoor and indoor absorbed dose rates in the waste soil tailings in the three mines are comparable. Although the outdoor and indoor absorbed dose rates in waste soil tailings in the three mines are three and four times the world averages, they are still in the range of the world average (UNSCEAR, 2000).

The mean outdoor and indoor absorbed dose rates in the waste rock samples from Mashonga, Kikagati and Butare mines at 90% confidence level were (67.15±48.46 $nGyh^{-1}$ and 126.75±102.27 $nGyh^{-1}$), (84.53±35.07 $nGyh^{-1}$ and 158.95±79.74 $nGyh^{-1}$) and (114.87±31.95 $nGyh^{-1}$ and 214.73±66.23$nGyh^{-1}$). The outdoor and indoor absorbed dose rates in the waste rock tailings in the three mines are not comparable and above the world averages, but still in the range of world averages (UNSCEAR, 2000).

The mean total annual effective dose rates for waste soil tailings for Mashonga, Kikagati and Butare mines at 90% confidence level were 1.76±0.35 $mSvy^{-1}$, 1.61±0.23 $mSvy^{-1}$ and 1.85±0.16 $mSvy^{-1}$. The total annual effective dose rates for waste soil tailings in the three mines are significantly higher than the maximum permissible dose limit for the members of the public of 1 $mSvy^{-1}$ (UNSCEAR, 2000; ICRP, 2007). All the three mines have enhanced background radiation levels due to natural radionuclides in the waste soil tailings.

The mean total annual effective dose rates for waste rock tailings for Mashonga, Kikagati and Butare mines at 90% confidence level were 0.66±0.52 $mSvy^{-1}$, 0.82±0.40 $mSvy^{-1}$ and 1.11±0.34 $mSvy^{-1}$ which are comparable to the maximum permissible dose limit of 1 $mSvy^{-1}$ for the members of the public except for rock tailings in Butare mine. This shows that the background radiation of Butare mine is slightly more enhanced as compared to that of Kikagati mine or Mashonga mine due to the natural radionuclides in the waste rock tailings.

The mean radium equivalent activities for waste soil tailings of Mashonga, Kikagati and Butare mines at 90% confidence level were 404.15±83.98 $Bqkg^{-1}$, 382.58±52.26 $Bqkg^{-1}$ and 439.22±36.12 Bq kg^{-1}. The radium equivalent activities of waste soil tailings of the three mines are greater than the maximum permissible limit of 370 $Bqkg^{-1}$ for building materials (UNSCEAR, 2000; Beretka and Mathew, 1985). This means that the gamma radiation hazard is very high in the three mines due to presence of larger concentrations

of ^{238}U, ^{232}Th and ^{40}K in the waste soil tailings and therefore must not be used as building materials.

The mean radium equivalent activities for waste rock tailings of Mashonga, Kikagati and Butare mines at 90% confidence level were 142.73±108.36 $Bqkg^{-1}$ and 181.47±73.12 $Bqkg^{-1}$ and 418.47±206.39 $Bqkg^{-1}$. The radium equivalent activities of waste rock tailings of the Mashonga and Kikagati mines are comparable below the maximum permissible limit of 370 Bq kg^{-1} for building materials. However, the radium equivalent activity of waste rock tailings of Butare mine is not comparable with that of Mashonga or Kikagati mine as it is above the maximum permissible limit of 370 $Bqkg^{-1}$ for building materials. Therefore the waste rock tailings of Butare mine must not be used as building materials.

The mean external hazard indices of waste soil tailings for Mashonga, Kikagati and Butare mines at 90% confidence level were 1.09±0.23, 1.03±0.14 and 1.19±0.10 and the mean internal hazard indices were 1.25±0.33, 1.17±0.19 and 1.34±0.14. These values are comparable and above the maximum permissible limit of unity recommended for the members of the public. This means that the external and internal gamma irradiation exposure hazards are significantly higher in the three mines most especially Butare and Mashonga mines.

The mean external hazard indices of waste rock tailings for Mashonga, Kikagati and Butare mines at 90% confidence level were 0.39±0.29, 0.49±0.20 and 0.71±0.19 and internal hazard indices were 0.45±0.40, 0.56±0.27 and 0.86±0.26. These values are comparable and below the maximum permissible limit of unity. Thus waste rock tailings of Mashonga and Kikagati are safe radiologically and therefore can be used as construction building materials.

The mean excess lifetime cancer risk levels of Mashonga, Kikagati and Butare mines for the waste soil tailings at 90% confidence level were $4.43\pm0.87\times10^{-3}$, $4.06\pm0.59\times10^{-3}$ and $4.65\pm0.41\times10^{-3}$ and $1.65\pm1.31\times10^{-3}$, $2.08\pm1.00\times10^{-3}$ and $2.81\pm0.85\times10^{-3}$ for the waste rock tailings. The excess lifetime cancer risks for the waste soil tailings of the three mines are comparable but those for waste rock tailings are not comparable. Butare mine has the greatest excess lifetime cancer risks as compared to Mashonga and Kikagati indicating a greater chance of developing the cancer after gamma irradiation.

5.4 Recommendations

1. The Ministry of Energy and Mineral Development must enact policies to ensure that radioactive wastes in mines are properly disposed off and the Atomic Energy Council must enforce Radiation Safety Guidelines in all the mines and the Ministry of Health must carry out an epidemiological study in this study area.

2. Waste soil tailings in Mashonga, Kikagati and Butare mines as well as waste rock tailings in Butare mine are radiologically not safe and must not be used as building materials.

3. A similar study should be carried out to measure the gamma ray activity levels of radionuclides in mine tailings and the background radiation in Southwestern Uganda.

REFERENCES

ARPANSA, (2002). Australian Radiation Protection and Nuclear Safety Agency. *Recommendations for limiting exposure to ionizing radiation (1995)* (Guidance note [NOHSC:3022(1995)]) *and National standard for limiting occupational exposure to ionizing radiation* [NOHSC:1013(1995)] Radiation Protection Series Publication No. 1. ISBN 0-642-79403-0 and ISSN 1445-9760.

Avwiri, G. O., Ajibode, M. O., and Agbalagba, E. O. (2013). *Evaluation of Radiation Hazard Indices in an Oil Mineral Lease (Oil Block) in Dealta State, Nigeria.* Nigeria Atomic Energy Commission, Abuja, Nigeria. International Journal of Engineering and Applied Sciences. ISSN 2305-8269.

Baguma, Z. (2009). *Status of Radioacive Elements in Uganda.* Department of Geological Survey and Mines. Technical Meeting on Uranium from Unconventional Resources, Vienna Austria.

Beretka, J., and Mathew P. J. (1985). *Natural radioactivity of Australian Building Materials, Industrial Wastes and By-products*. Health Physics. 48: 87-95.

Cember, H., and Thomas, E. J. (2009). *Introduction to Health Physics*. Fourth edition. Department of Environment and Radiological Health sciences Colorado State University. Fort Collins Colorado.

David, S., Nick K., and Kelley B. (2006). *Gamma Spectroscopy Formal Report*. University of Michigan Nuclear Engineering & Radiological Sciences.

Department of Geological Survey and Mines, Uganda. (2012). *Geology and mineral Occurrences*. Mining Journal Special Publication-Uganda. Ministry of Energy and Mineral development. Entebbe, Uganda. December 2012.

Dickson, B. L., and Scott K. M. (1997). *Interpretation of aerial gamma-ray surveys; adding the geochemical factors*. AGSO Journal Of Australia Geology and Geophysics, 17(2), 187 – 200. Commonwealth of Australia.

Dirk, W. (2011). *An Introduction to Gamma rays, Detectors, and Spectrometers*. Exotic Beams Summer School 2011, MSU.

Eisenbud, M., and Gusell T. (1997). *Environmental radioactivity from natural, industrial, and military sources*. Academic press, Inc.

European Commission (EC). (1999). *Radiological Protection Principles concerning the Natural Radioactivity of Building Materials*. Radiation protection 112 with Annexes I and II. Contract No 96-ET-003, STUK (Finland).

Faanu, A., Darko E. O., and Ephraim J. H. (2011). *Determination of Natural Radioactivity and Hazard in Soil, Rock, waste and tailing samples in a mining area in Ghana.* West African Journal of Applied Ecology Volume 19.

Federation for Sustainable Environment (FSE). (2006). *Written Submissions on West Rand District Municipality*. Integrated management Plan. NPO Number: 062986-NPO, Registration Number: 2006/217972/23.

Fergal, N. (2009). *International workshop on Radiation Safety and the Mine Worker*. Radiation Safety Institute of Canada.

Fleur, S., Wilde-Ramsing J., and Esther D. (2011). *Uranium from Africa, Mitigation of Uranium mining impacts on society and environment by Industry and Governments*. WISE and SOMO, Amsterdam. ISBN: 978-90-71284-82-3.

GRS. (2013). *Advanced Physics Laboratory*. Department of physics, University of Florida.

Guagliardi, I., Buttafuoco, G., Apollaro C., et. al. (2013). *Using Gamma Ray Spectroscopy and Geostatistics for Assessing Geochemical Behaviour of Radio-active Elements in Lese Catchment* (Southern Italy). International Journal of Environmental Research 7 (3) page 645 – 658, ISSN: 1735-6865.

Health Protection Agency (HPA). (2011). *Risks of Solid Cancers following Radiation Exposure: Estimates for the UK population*. Report of the Independent Advisory Group on Ionising Radiation. Page 18. ISBN: 978-0-85951-705-8.
http://en.wikipedia.org/wingiki/Min: Accessed on 7th August 2014.

International Atomic Energy Agency (IAEA). (2003). Guidelines for radioelement mapping using gamma ray spectrometry data. International Atomic Energy Agency. Vienna Austria. IAEA-TECDOC-1363, ISBN 92-0-108303-3.

International Atomic Energy Agency (IAEA). (2004). International Atomic Energy Agency. *Radiation, People, and the Environment*. Division of radiation and Waste safety, Austria.

International Atomic Energy Agency (IAEA). (2005). *Naturally Occurring Radioactive Materials (iv)*. Proceedings of an International Conference held in Szczyrk. IAEA-TECDOC-1472, Poland.

International Atomic Energy Agency (IAEA). (2006). International Atomic Energy Agency. *Assessing the need for radiation protection measures in work involving minerals and raw materials.* Safety reports series No 49. Vienna Austria.

International Atomic Energy Agency (IAEA). (2007). *Update of X Ray and Gamma Ray Decay Data Standards for Detector Calibration and Other Applications*. Volume 1, STI/PUB/1287, Vienna Austria, ISBN 92-0-113606-4.

International Atomic Energy Agency (IAEA). (2008). *Assessment of levels and health effects of airborne particulate matter in mining, mineral refining and metal working industries*. Tech Doc-1576, Vienna, Austria.

International Atomic Energy Agency (IAEA). (2009). *Basic Safety Standards for protecting the People and the Environment*. International Basic Safety Standards for protection against Ionizing Radiation and for the Safety of Radiation Sources. Safety Series No 115. Vienna Austria, May 2009.

International Atomic Energy Agency (IAEA). (2010). *Radiation Protection and the Management of Radioactive Waste in the Oil and Gas Industry*. Training Course Series 40, Vienna Austria.

International Atomic Energy Agency (IAEA). (2011). *Safety Standards for protecting people and the environment*. Radiation Protection and Safety of

Radiation Sources: International Basic Safety Standards, INTERIM EDITION STI/PUB/1531, ISBN 978–92–0–120910–8. Vienna Austria.

International Atomic Energy Agency (IAEA). (2014). *Remediation of Land Contaminated by Radioactive Material Residues*. Summary of An International Conference organized by the International Atomic Energy Agency and Hosted by the Government of Kazakhstan and held in Astana, May 2009. ISBN 978-92-0-142310-8.

International Commission on Radiological Protection (ICRP). (1991). Recommendations of the International Commission of Radiological Protection. ICRP Publication 60, 1990. Pergamon Press, Oxford.

Isinkaye, M. O. (2013). *Natural radioactivity levels and the radiological health implications of tailing enriched soil and sediment samples around two mining sites (around an abandoned gold mining site located at Itagunmodi village in Ilesa and tin, tantalite and kaolin mining sites in Ijero-Ekiti) both in Southwest Nigeria.* Radiation protection and Environment. Vol 36 Issue 3 DOI: 10.4103/0972-0464.137477.

Jiri, H., Jaroslav, V., and Jiri, T. (2008). *Natural Radioactivity in Building Materials-Czech Experience and European Legislation*. Proceedings of the American Association of Radon Scientists and technologists 2008 International Symposium, Las Vegas NV. National Radiation Protection Institute, Bartoskova 28, 140 00 Praha.

Joseph, E., and Nasiru, R. (2013). *Geommetry Correction in Efficiency of NaI (Tl) Detector*. Pelagia Research Library. Advances in Applied Science Research, 2013, 4(1): 400-406. ISSN: 0976-8610.

Keith, F.E., Richard, W.L., Christopher, B.N., Jerome, S.P., and Allan, C.B.R. (1999). *Cancer Risk Coefficients for Environmental Exposure to Radionuclides.* United States Environmental Protection Agency (US EPA). Federal Guidance Report Number 13. EPA 402-R-99-001. September 1999.

Knoll, G. F. (1999). *Radiation Detection and Measurements*. Third Edition, New

York: John Wiley and Sons, Inc. ISBN: 0-471-07338-5.

Lederer, C.M., and Shirley, V.S. (1978). *Table of isotopes*. 7th Ed., John Wiley and Sons, Inc., New York.

Lemeriga, Y. (1998). Msc. Dissertation titled: *Low level counting of Cs, K, U, and Th in selected Ugandan foods and their corresponding soils of growth*. Makerere University.

Ludger, H., Ulrich S., et. al. (2010). *The Potential of Gamma ray Spectrometry for Soil Mapping*. World Congress of Soil Science, Soil Solutions for a Changing World, Brisbane, Australia. Published on DVD.

Mangset, W. E., and Sheyin A. T. (2009). *Measurement of Radionuclides in Processed Mine Tailings in Jos, Plateau State*. Bajopas Volume 2 Number 2 December, 2009. Bayero Journal of Pure and Applied Sciences, 2(2): 56 – 60.

Martin, A., Mead, S., and Wade, B. O. (1997). *Materials containing radionuclides in enhanced concentrations*. European Union Report on Environment, Nuclear and Civil protection. ISBN 92-828-0191-8.

Michalis, T., and Haralabos, T. (2002). *Gamma ray measurements of naturally occurring radioactive samples from Cyprus characteristic geological rocks*. Department of Physics, University of Cyprus, Nicosia, Cyprus, UCY-PHY-02/02.

Micheal, C. H. (2014). Fact Sheet on Radiation and Radiation Therapy. Cancer Association of South Africa. March 2014.

Mishra, U. C., Lalit, B. Y., Shukla, V.K., Ramachandran, T.V. (1981). *Standardized low-level measurement methods for environmental studies*. Environmental migration of long lived radionuclides, IAEA Publication Vienna, Australia.

Nagudi, B. (2011). *Status of Geological Resources in Uganda*. For the Embassy of the Republic of Korea in Uganda. December, 2011.

National Academy of Sciences (NAS), Biological Effects of Ionizing Radiation (BEIR). (2006). *Health risks from exposure to low levels of ionizing radiation*: BEIR VII, Phase 2 / Committee to Assess Health Risks from Exposure to Low Levels of Ionizing Radiation, Board on Radiation Effects, Research Division on Earth and Life Studies, National Research Council of the National Academies. ISBN: 0-309-53040-7.

National Council on Radiation Protection and Measurements (NCRP). (1985). *Handbook on radioactivity measurements procedures*. Report No. 58. 7910 Woodmont Avenue/Bethesda, MD. 20814 No. 13 (6601J), 402-R-99-001.

Parks, J. E. (2009). *The Compton Effect--Compton Scattering and Gamma Ray Spectroscopy*. Department of Physics and Astronomy, University of Tennessee.

Podgorsak, E. B. (2005). *Radiation Physics for Medical Physicists*. McGill University Health Centre. Department of Medical Physics, Montr'eal, Canada. Springer Berlin Heidelberg New York. ISSN 1618-7210, ISBN-10 3-540-25041-7

Roger, H.C. (2011). *Changes in the Underlying Science and Protection Policy and their Impact on European and UK Domestic Regulation*. International Commission on Radiological Protection (ICRP). Evolution of ICRP Recommendations 1977, 1990, and 2007. OECD 2011, NEA No 6920 ISBN 978-92-64-99153-8.

Shleien, B., and Terpilak, M.S. (1987). *The Health Physics and Radiological Health Handbook*. 7th Printing, Nucleon Lectern Associates, Inc., Olney, MD.

Tsoulfanidis, N. (1983). *Measurement and Detection of radiation*. Hemisphere Publishing Corporation, USA.

Turner, J. E. (2007). *Atoms, Radiation and Radiation Protection*. WILEY-VCH Verlag GmbH & Co. KGaA, Weinheim, 3rd Edition. ISBN 978-3-527-40606-7.

Uganda Bureau of Statistics (UBOS). (2002). *2002 Uganda Population and Housing Census, Population Size and Distribution*. Analytical report. Kampala, Uganda. October 2006.

Uganda Bureau of Statistics (UBOS). (2012). *Uganda Demographic and Health Survey* 2011, Page 3, Kampala-Uganda.

Uganda Bureau of Statistics (UBOS). (2013). *The National Labour force and Child Activities Survey, 2011/2012*. National Labour force Survey Report page 44 – 48, Kampala-Uganda.

United Nations Scientific Committee on Effects of Atomic Radiation (UNSCEAR). (1988). *Sources, Effects and Risks of ionizing Radiation*, Report to the General Assembly with Annexes, New York. ISBN 92-1-142143-8.

United Nations Scientific Committee on Effects of Atomic Radiation (UNSCEAR). (2000). United Nations Scientific Committee on Effects of Atomic Radiation. *A report to the general assembly.* Radiological protection bulletin with annexes A and B.

United Nations Scientific Committee on Effects of Atomic Radiation (UNSCEAR). (2008). United Nations Scientific Committee on the Effects of Atomic Radiation. *Sources and Effects of Ionizing Radiation.* A Report to the General Assembly with Scientific Annexes. ISBN 978-92-1-142274-0, Vol 1.

United States Environmental Protection Agency (US EPA). (2012). *Radiological Laboratory Sample Analysis Guide for Incident Response –Radionuclides in Soil.* Office of Radiation and Indoor Air, National Air and Radiation Environmental Laboratory. EPA 402-R-12-006.

Usikalu, M.R., Anoka, O.C., and Balogun, F.A. (2011). *Radioactivity Measurements of the Jos Tin Mine Tailing in Northern Nigeria*. Scholars Research Library. National Institute of Radiation Protection and Research, University of Ibadan, Ibadan. Archives of Physics Research, 2011, 2 (2):80-86. ISSN 0976-0970.

World Health Organisation (WHO). (2009). *HandBook on Indoor Radon.* A Public Health Perspective. Department of Public Health and Environment. WHO, Geneva. ISBN: 978-92-4-1547673.

www.camberra.com. Accessed on 26th February 2014.

www.epa.gov/radiation/radionuclides/thorium.html. Accessed on: 23rd April 2014.

www.epa.gov/radiation/understand/gamma.html. Accessed on: 28th December 2014.

www.epa.gov/rpdweb00/radionuclides/uranium.html. Accessed on: 23rd April 2014.

www.gammadata.net. Accessed on 14th January 2016.

www.greatmining.com/iorore.html. Accessed on: 26th April 2014.

www.kip.uni- heidelberg.de/~coulon/Lectures/Detectors/Free-PDFs/Lecture4.pdf, Accessed on: 28th December 2014.

www.ortec-online.com. Accessed on 26th July 2014.

www.physics.isu.edu. Accessed on: 27th December 2014.

Wymer, D. G. (2002). *Radiological hazards in mining industry*. Occupational Health: Impact Prevention and Aftermath Strategies Annual Conference. Mine Ventilation Society of South Africa, Pretoria; 2002.

Xinwei, L. (2005). *Radiological Analysis of cement and its products collected from Shaanxi, China*. Health Physics. 84-86.

Zaini, H., Ahmad S., Noor, H. M., and Seh Datul, R. (2008). *Surface Radiation Dose and Radionuclide Measurement in an Ex-Tin Mining Area, Kg Gajah in Kinta valley Perak, Malaysia*. The Malaysian Journal of Analytical Sciences, Vol 12, No 2 (2008): 419 – 431.

APPENDICES

APPENDIX A

BASIC DATA FOR MINE TAILINGS

BASIC DATA FOR WASTE SOIL SAMPLES FROM MASHONGA GOLD MINE

Sample Name	Mass /kg	Average Energy /keV	Standard deviation /keV	FWHM /keV	Radionuclide	Rate /s^{-1}
BTS1	0.5740	208.70	9.94	20.41	^{232}Th (Pb-212)	0.9635
		262.89	8.68	23.35	^{238}U (Pb-214)	0.1745
		314.62	12.66	29.75	^{238}U (Pb-214)	0.5928
		541.66	23.51	55.24	^{232}Th (Tl-208)	0.7701
		1321.91	41.77	98.15	^{40}K	0.8465
BTS2	0.5045	207.92	10.06	23.63	^{232}Th (Pb-212)	1.0994
		261.28	9.40	22.08	^{238}U (Pb-214)	0.1701
		314.85	13.08	30.75	^{238}U (Pb-214)	0.5686
		544.88	24.99	58.72	^{232}Th (Tl-208)	0.7329
		1320.21	35.36	83.09	^{40}K	1.4482
BTS3	0.6720	207.72	9.96	23.41	^{232}Th (Pb-212)	1.0245
		259.77	8.62	20.25	^{238}U (Pb-214)	0.1975
		314.99	12.12	28.49	^{238}U (Pb-214)	0.5462
		543.31	22.73	53.40	^{232}Th (Tl-208)	0.7333
		1319.31	37.13	87.25	^{40}K	0.9137
BTS4	0.4590	209.21	8.78	20.63	^{232}Th (Pb-212)	1.1372
		262.64	8.97	21.08	^{238}U (Pb-214)	0.2634
		316.03	10.93	25.69	^{238}U (Pb-214)	0.6917
		545.84	21.96	51.61	^{232}Th (Tl-208)	0.8788
		1319.29	41.96	98.61	^{40}K	1.0147
BTS5	0.6670	209.30	9.23	21.70	^{232}Th (Pb-212)	2.3240
		261.45	8.60	20.20	^{238}U (Pb-214)	0.8319
		314.92	11.12	26.13	^{238}U (Pb-214)	1.8889
		550.17	21.54	50.61	^{232}Th (Tl-208)	2.1519
		1318.48	40.46	95.07	^{40}K	2.5886
BTS6	0.4130	208.69	9.35	21.97	^{232}Th (Pb-212)	1.0117
		261.63	9.06	21.30	^{238}U (Pb-214)	0.2610
		315.77	12.14	28.52	^{238}U (Pb-214)	0.6254
		543.01	25.92	60.91	^{232}Th (Tl-208)	0.8794
		1316.35	42.58	100.06	^{40}K	1.0342
BTS7	0.5565	208.99	10.42	24.48	^{232}Th (Pb-212)	1.0347
		263.49	10.46	24.59	^{238}U (Pb-214)	0.2674
		315.75	12.13	28.50	^{238}U (Pb-214)	0.5728
		543.22	21.90	51.45	^{232}Th (Tl-208)	0.6646
		1319.66	41.61	97.79	^{40}K	1.0599
BTS8	0.6360	208.37	9.92	23.32	^{232}Th (Pb-212)	0.9550
		261.68	8.49	19.95	^{238}U (Pb-214)	0.1971
		314.23	21.81	51.24	^{238}U (Pb-214)	0.5742
		536.97	36.84	86.58	^{232}Th (Tl-208)	0.8553
		1320.74	37.51	88.15	^{40}K	0.8709
BTS9	0.5850	208.34	9.40	22.09	^{232}Th (Pb-212)	0.9040
		261.27	9.21	21.64	^{238}U (Pb-214)	0.1954
		318.06	19.35	45.47	^{238}U (Pb-214)	0.4664
		535.01	37.06	87.10	^{232}Th (Tl-208)	0.8225
		1319.19	42.56	100.02	^{40}K	0.7747
BTS10	0.6280	207.79	10.31	24.22	^{232}Th (Pb-212)	1.1312
		261.13	9.24	21.71	^{238}U (Pb-214)	0.1633
		317.08	22.46	52.78	^{238}U (Pb-214)	0.5035
		544.71	24.93	58.59	^{232}Th (Tl-208)	0.7317
		1319.97	35.78	84.07	^{40}K	1.4624
BTS11	0.5085	207.55	10.62	24.97	^{232}Th (Pb-212)	1.1762
		260.20	8.03	18.87	^{238}U (Pb-214)	0.1750
		312.56	14.84	34.88	^{238}U (Pb-214)	0.5265

		530.49	35.01	82.26	^{232}Th (Tl-208)	0.9328
		1319.61	43.88	103.13	^{40}K	1.0955
BTS12	0.5440	209.28	9.64	22.64	^{232}Th (Pb-212)	0.8908
		258.79	10.70	25.14	^{238}U (Pb-214)	0.2349
		317.51	17.32	40.70	^{238}U (Pb-214)	0.3988
		543.67	26.54	62.36	^{232}Th (Tl-208)	0.6993
		1318.78	37.69	88.56	^{40}K	0.9198

BASIC DATA FOR ROCK SAMPLES FROM MASHONGA GOLD MINE

Sample Name	Mass /kg	Average Energy /keV	Standard deviation/keV	FWHM/keV	Radionuclide	Rate /s^{-1}
BTR1	0.3825	203.90	9.47	22.25	^{232}Th (Pb-212)	0.1934
		264.59	12.14	28.52	^{238}U (Pb-214)	0.0725
		314.27	5.58	13.11	^{238}U (Pb-214)	0.0451
		551.09	6.86	16.12	^{232}Th (Tl-208)	0.0422
		1313.38	27.18	63.87	^{40}K	0.7113
BTR2	0.4330	202.14	8.47	19.90	^{232}Th (Pb-212)	0.1704
		265.87	7.43	17.47	^{238}U (Pb-214)	0.0214
		313.27	1.88	4.41	^{238}U (Pb-214)	0.0145
		538.07	5.15	12.10	^{232}Th (Tl-208)	0.0297
		1315.51	5.17	12.15	^{40}K	0.0179
BTR3	0.4690	207.60	10.43	24.51	^{232}Th (Pb-212)	0.4826
		259.05	7.43	17.46	^{238}U (Pb-214)	0.1005
		313.36	10.95	25.73	^{238}U (Pb-214)	0.3155
		536.37	6.37	14.97	^{232}Th (Tl-208)	0.0601
		1319.12	23.23	54.59	^{40}K	0.4401
BTR4	0.4020	207.20	8.82	20.72	^{232}Th (Pb-212)	1.1858
		258.24	9.87	23.20	^{238}U (Pb-214)	0.3313
		312.64	11.57	27.19	^{238}U (Pb-214)	0.7845
		543.11	21.73	51.07	^{232}Th (Tl-208)	0.9002
		1317.22	25.60	60.16	^{40}K	1.7530
BTR5	0.2190	212.53	2.62	6.15	^{232}Th (Pb-212)	0.0107
		269.97	4.07	9.56	^{238}U (Pb-214)	0.0148
		310.36	2.47	5.81	^{238}U (Pb-214)	0.0085
		544.25	3.35	7.88	^{232}Th (Tl-208)	0.0122
		1331.27	5.64	13.25	^{40}K	0.0095
BTR6	0.4695	203.38	11.40	26.78	^{232}Th (Pb-212)	0.5095
		261.04	8.69	20.43	^{238}U (Pb-214)	0.1465
		315.27	12.50	29.37	^{238}U (Pb-214)	0.3307
		547.19	18.85	44.31	^{232}Th (Tl-208)	0.3770
		1316.43	32.07	75.36	^{40}K	4.1543
BTR7	0.1855	2.5.909	10.61	24.93	^{232}Th (Pb-212)	0.2178
		269.03	6.36	14.93	^{238}U (Pb-214)	0.0457
		315.98	7.24	17.01	^{238}U (Pb-214)	0.0619
		545.43	9.51	22.34	^{232}Th (Tl-208)	0.0737
		1315.57	7.08	16.63	^{40}K	0.0307
BTR8	0.2855	201.41	10.36	24.34	^{232}Th (Pb-212)	0.1370
		262.87	11.43	26.86	^{238}U (Pb-214)	0.0757
		317.22	4.66	10.95	^{238}U (Pb-214)	0.0232
		556.22	2.96	6.96	^{232}Th (Tl-208)	0.0115
		1323.42	15.50	36.43	^{40}K	0.0327
BTR9	0.2250	206.61	10.79	25.34	^{232}Th (Pb-212)	0.3202
		261.31	8.45	19.86	^{238}U (Pb-214)	0.0537
		322.02	9.96	23.41	^{238}U (Pb-214)	0.0791
		547.27	8.47	19.90	^{232}Th (Tl-208)	0.0743
		1314.46	24.87	58.45	^{40}K	0.3554
BTR10	0.2370	205.07	22.06	51.84	^{232}Th (Pb-212)	0.0403
		282.14	9.02	21.19	^{238}U (Pb-214)	0.0648
		326.25	3.10	7.29	^{238}U (Pb-214)	0.0166
		546.84	9.82	23.09	^{232}Th (Tl-208)	0.0277
		1307.92	21.95	51.58	^{40}K	0.0426
BTR11	0.2245	207.18	5.26	12.36	^{232}Th (Pb-212)	0.0150
		269.15	13.03	30.61	^{238}U (Pb-214)	0.0616

		327.63	3.38	7.94	^{238}U (Pb-214)	0.0155
		542.45	1.88	4.41	^{232}Th (Tl-208)	0.0060
		1317.08	2.95	6.93	^{40}K	0.0058
BTR12	0.2085	206.36	0.00	0.00	^{232}Th (Pb-212)	0.0030
		276.61	7.16	16.82	^{238}U (Pb-214)	0.0280
		327.41	2.71	6.36	^{238}U (Pb-214)	0.0113
		537.95	3.72	8.74	^{232}Th (Tl-208)	0.0062
		1322.95	1.81	4.24	^{40}K	0.0035

BASIC DATA FOR WASTE SOIL SAMPLES FROM KIKAGATI TIN MINE

Sample Name	Mass /kg	Average Energy /keV	Standard deviation /keV	FWHM /keV	Radionuclide	Rate /s^{-1}
ITS1	0.6580	208.77	9.55	22.45	^{232}Th (Pb-212)	2.5033
		259.58	9.77	22.95	^{238}U (Pb-214)	0.1928
		311.79	16.06	37.73	^{238}U (Pb-214)	0.7010
		541.95	22.92	53.86	^{232}Th (Tl-208)	1.1449
		1324.08	32.54	76.46	^{40}K	0.5371
ITS2	0.5060	208.35	9.83	23.10	^{232}Th (Pb-212)	1.9274
		258.29	7.90	18.55	^{238}U (Pb-214)	0.1391
		314.24	16.53	38.84	^{238}U (Pb-214)	0.5676
		544.37	23.78	55.89	^{232}Th (Tl-208)	0.9204
		1324.07	52.10	122.43	^{40}K	0.7450
ITS3	0.5335	208.22	9.89	23.23	^{232}Th (Pb-212)	2.4907
		257.45	7.93	18.62	^{238}U (Pb-214)	0.1854
		309.02	12.62	29.66	^{238}U (Pb-214)	0.7072
		538.52	20.69	48.61	^{232}Th (Tl-208)	1.0699
		1321.79	32.02	75.24	^{40}K	0.6255
ITS4	0.4750	207.61	10.41	24.47	^{232}Th (Pb-212)	2.6780
		257.02	9.97	23.43	^{238}U (Pb-214)	0.1939
		309.42	15.52	36.47	^{238}U (Pb-214)	0.7463
		540.34	20.90	49.11	^{232}Th (Tl-208)	0.9798
		1319.43	32.11	75.46	^{40}K	0.6256
ITS5	0.5840	208.16	9.69	22.77	^{232}Th (Pb-212)	1.7039
		259.56	7.92	18.62	^{238}U (Pb-214)	0.1781
		312.38	17.33	40.71	^{238}U (Pb-214)	0.6658
		540.30	22.17	52.09	^{232}Th (Tl-208)	0.8266
		1322.29	35.48	83.37	^{40}K	0.3397
ITS6	0.6575	207.36	9.92	23.32	^{232}Th (Pb-212)	1.8838
		259.79	8.13	19.10	^{238}U (Pb-214)	0.1320
		312.36	13.87	32.59	^{238}U (Pb-214)	0.5325
		541.40	22.49	52.86	^{232}Th (Tl-208)	0.9622
		1326.68	21.68	50.96	^{40}K	0.2169
ITS7	0.5310	208.98	9.06	21.29	^{232}Th (Pb-212)	2.3489
		260.70	7.83	18.39	^{238}U (Pb-214)	0.2001
		309.73	10.88	25.56	^{238}U (Pb-214)	0.7487
		542.44	23.41	55.01	^{232}Th (Tl-208)	1.2551
		1317.54	44.45	104.46	^{40}K	0.4438
ITS8	0.6790	208.37	9.92	23.32	^{232}Th (Pb-212)	0.9550
		261.53	8.55	20.09	^{238}U (Pb-214)	0.2007
		314.38	21.94	51.57	^{238}U (Pb-214)	0.5668
		547.51	25.43	59.77	^{232}Th (Tl-208)	0.6597
		1320.60	37.39	87.86	^{40}K	0.8667
ITS9	0.6180	207.95	9.18	21.57	^{232}Th (Pb-212)	1.5320
		260.49	9.48	22.28	^{238}U (Pb-214)	0.2678

		313.39	11.72	27.55	^{238}U (Pb-214)	0.7432
		542.53	22.00	51.70	^{232}Th (Tl-208)	0.9935
		1321.43	59.82	140.57	^{40}K	0.7673
ITS10	0.7010	209.24	9.93	23.32	^{232}Th (Pb-212)	1.3603
		263.04	8.49	19.95	^{238}U (Pb-214)	0.2088
		313.97	12.67	29.78	^{238}U (Pb-214)	0.6463
		543.20	22.61	53.14	^{232}Th (Tl-208)	0.8305
		1324.56	37.49	88.10	^{40}K	0.6234
ITS11	0.7210	208.24	9.13	21.45	^{232}Th (Pb-212)	2.0365
		259.45	8.92	20.97	^{238}U (Pb-214)	0.2121
		310.44	14.54	34.16	^{238}U (Pb-214)	0.6117
		540.32	20.03	47.07	^{232}Th (Tl-208)	0.8986
		1324.05	34.41	80.86	^{40}K	0.4209
ITS12	0.7320	208.00	9.97	23.42	^{232}Th (Pb-212)	1.9640
		259.93	8.16	19.18	^{238}U (Pb-214)	0.1698
		310.33	12.53	29.45	^{238}U (Pb-214)	0.7094
		540.48	20.57	48.35	^{232}Th (Tl-208)	0.8942
		1321.65	34.67	81.47	^{40}K	0.3496

BASIC DATA FOR ROCK SAMPLES FROM KIKAGATI TIN MINE

Sample Name	Mass/kg	Average Energy /keV	Standard deviation /keV	FWHM /keV	Radionuclide	Rate /s^{-1}
ITR1	0.4385	208.57	10.59	24.88	^{232}Th (Pb-212)	0.4598
		259.57	11.69	27.48	^{238}U (Pb-214)	0.1712
		317.92	15.08	35.43	^{238}U (Pb-214)	0.3098
		541.15	25.15	59.09	^{232}Th (Tl-208)	0.4000
		1315.94	31.10	73.08	^{40}K	1.9740
ITR2	0.3840	207.24	9.76	22.92	^{232}Th (Pb-212)	1.0807
		261.19	8.01	18.81	^{238}U (Pb-214)	0.0925
		311.33	15.25	35.83	^{238}U (Pb-214)	0.3294
		539.19	22.22	52.21	^{232}Th (Tl-208)	0.5335
		1320.81	33.97	79.82	^{40}K	0.4695
ITR3	0.4090	203.54	9.11	21.40	^{232}Th (Pb-212)	0.1413
		279.72	11.17	26.24	^{238}U (Pb-214)	0.0775
		321.28	9.10	21.38	^{238}U (Pb-214)	0.0450
		538.45	4.19	9.85	^{232}Th (Tl-208)	0.0259
		1355.68	4.13	9.71	^{40}K	0.0061
ITR4	0.5030	207.62	9.59	22.53	^{232}Th (Pb-212)	0.4720
		257.98	8.31	19.53	^{238}U (Pb-214)	0.2051
		316.32	12.73	29.91	^{238}U (Pb-214)	0.5134
		543.95	22.69	53.33	^{232}Th (Tl-208)	0.5407
		1320.59	31.67	74.43	^{40}K	0.7022
ITR5	0.6185	207.10	9.66	22.70	^{232}Th (Pb-212)	1.4317
		258.83	9.41	22.12	^{238}U (Pb-214)	0.1094
		308.90	12.21	28.70	^{238}U (Pb-214)	0.4944
		535.79	20.95	49.23	^{232}Th (Tl-208)	0.6308
		1319.00	32.96	77.45	^{40}K	1.1357
ITR6	0.6135	203.73	10.63	24.99	^{232}Th (Pb-212)	0.2230
		273.11	6.06	14.25	^{238}U (Pb-214)	0.0321
		329.07	13.87	32.60	^{238}U (Pb-214)	0.0723
		547.30	8.65	20.32	^{232}Th (Tl-208)	0.0525
		1315.25	26.75	62.87	^{40}K	0.3912
ITR7	0.4670	209.23	6.15	14.45	^{232}Th (Pb-212)	0.0882
		274.46	7.29	17.13	^{238}U (Pb-214)	0.0357
		319.65	6.63	15.58	^{238}U (Pb-214)	0.0382
		539.19	4.36	10.25	^{232}Th (Tl-208)	0.0250
		1327.87	21.09	49.57	^{40}K	0.0721
ITR8	0.5735	201.15	9.68	22.75	^{232}Th (Pb-212)	0.0439
		275.76	6.66	15.66	^{238}U (Pb-214)	0.0342
		314.41	1.53	3.60	^{238}U (Pb-214)	0.0060

		535.43	2.41	5.67	^{232}Th (Tl-208)	0.0035
		1359.73	3.05	7.17	^{40}K	0.0030
ITR9	0.5015	204.64	12.51	29.40	^{232}Th (Pb-212)	0.4409
		263.04	13.45	31.61	^{238}U (Pb-214)	0.1452
		317.48	13.74	32.29	^{238}U (Pb-214)	0.2368
		544.18	10.59	24.89	^{232}Th (Tl-208)	0.1206
		1315.18	33.66	79.11	^{40}K	2.3372
ITR10	0.4715	206.37	10.04	23.60	^{232}Th (Pb-212)	0.7698
		258.83	11.79	27.71	^{238}U (Pb-214)	0.1625
		316.18	15.68	36.86	^{238}U (Pb-214)	0.3916
		533.15	18.22	42.81	^{232}Th (Tl-208)	0.3106
		1317.15	31.22	73.36	^{40}K	1.3127
ITR11	0.4990	206.87	12.85	30.20	^{232}Th (Pb-212)	0.2246
		254.92	10.94	25.71	^{238}U (Pb-214)	0.1038
		321.96	8.44	19.83	^{238}U (Pb-214)	0.0522
		548.12	11.51	27.04	^{232}Th (Tl-208)	0.0703
		1315.29	28.32	66.54	^{40}K	0.7427
ITR12	0.4770	206.75	10.51	24.70	^{232}Th (Pb-212)	0.9042
		258.28	8.77	20.62	^{238}U (Pb-214)	0.0725
		311.28	13.28	31.22	^{238}U (Pb-214)	0.2704
		536.70	15.07	35.42	^{232}Th (Tl-208)	0.2725
		1318.34	32.34	76.01	^{40}K	1.1470

BASIC DATA FOR SOIL SAMPLES FROM BUTARE IRON ORE MINE

Sample Name	Mass /kg	Average Energy /keV	Standard deviation /keV	FWHM /keV	Radionuclide	Rate /s^{-1}
KTS1	0.4985	209.57	9.54	22.41	^{232}Th (Pb-212)	1.7987
		257.34	10.79	25.36	^{238}U (Pb-214)	0.1574
		313.62	11.89	27.95	^{238}U (Pb-214)	0.6057
		540.92	20.78	48.82	^{232}Th (Tl-208)	0.8424
		1318.63	27.16	63.83	^{40}K	0.4653
KTS2	0.5510	208.35	9.17	21.55	^{232}Th (Pb-212)	2.0826
		261.32	10.23	24.04	^{238}U (Pb-214)	0.2071
		312.52	12.41	29.17	^{238}U (Pb-214)	0.8198
		541.19	21.03	49.41	^{232}Th (Tl-208)	1.0691
		1320.07	28.19	66.24	^{40}K	0.4893
KTS3	0.4390	208.52	9.68	22.75	^{232}Th (Pb-212)	1.7430
		260.57	8.44	19.82	^{238}U (Pb-214)	0.1682
		313.44	11.85	27.85	^{238}U (Pb-214)	0.5970
		539.60	21.25	49.95	^{232}Th (Tl-208)	0.8844
		1317.50	28.90	67.92	^{40}K	0.4082
KTS4	0.5880	208.61	9.77	22.97	^{232}Th (Pb-212)	2.3965
		260.48	8.82	20.72	^{238}U (Pb-214)	0.2509
		310.86	12.74	29.94	^{238}U (Pb-214)	0.8507
		541.49	21.43	50.36	^{232}Th (Tl-208)	1.1275
		1321.74	32.62	76.67	^{40}K	1.1513
KTS5	0.4730	208.85	8.78	20.63	^{232}Th (Pb-212)	1.7556
		261.24	8.98	21.09	^{238}U (Pb-214)	0.1144
		312.76	11.83	27.81	^{238}U (Pb-214)	0.6792
		540.69	21.48	50.47	^{232}Th (Tl-208)	1.0007
		1321.08	31.12	73.13	^{40}K	0.5528
KTS6	0.5390	207.81	10.15	23.84	^{232}Th (Pb-212)	2.4202
		259.48	8.19	19.25	^{238}U (Pb-214)	0.2101
		310.34	11.98	28.16	^{238}U (Pb-214)	0.8184
		539.60	20.53	48.24	^{232}Th (Tl-208)	1.1259
		1318.05	27.60	64.87	^{40}K	0.5287
KTS7	0.4675	207.62	9.49	22.30	^{232}Th (Pb-212)	1.3106
		259.72	8.73	20.52	^{238}U (Pb-214)	0.1186
		312.29	12.17	28.60	^{238}U (Pb-214)	0.4705
		541.61	21.79	51.21	^{232}Th (Tl-208)	0.6572

		1319.59	34.89	81.99	^{40}K	0.4502
KTS8	0.4940	207.84	9.65	22.68	^{232}Th (Pb-212)	1.4887
		257.59	7.32	17.20	^{238}U (Pb-214)	0.1258
		312.98	12.13	28.51	^{238}U (Pb-214)	0.4998
		539.27	22.55	52.98	^{232}Th (Tl-208)	0.7573
		1318.92	26.49	62.25	^{40}K	0.3859
KTS9	0.6360	207.79	8.80	20.68	^{232}Th (Pb-212)	1.7780
		262.65	7.20	16.91	^{238}U (Pb-214)	0.0827
		310.95	13.48	31.67	^{238}U (Pb-214)	0.7416
		538.37	20.96	49.26	^{232}Th (Tl-208)	0.9272
		1319.11	26.55	62.39	^{40}K	0.3960
KTS10	0.4910	207.84	8.38	19.70	^{232}Th (Pb-212)	2.0798
		258.90	7.24	17.01	^{238}U (Pb-214)	0.1408
		311.10	11.45	26.91	^{238}U (Pb-214)	0.7844
		536.98	21.09	49.57	^{232}Th (Tl-208)	1.1311
		1318.68	23.48	55.19	^{40}K	0.3390
KTS11	0.5050	207.51	9.20	21.62	^{232}Th (Pb-212)	1.6749
		260.11	8.15	19.15	^{238}U (Pb-214)	0.1188
		307.96	13.47	31.64	^{238}U (Pb-214)	0.5818
		536.82	22.15	52.05	^{232}Th (Tl-208)	0.8648
		1313.11	27.79	65.30	^{40}K	0.3736
KTS12	0.4605	207.56	8.93	20.97	^{232}Th (Pb-212)	1.8937
		261.04	9.10	21.39	^{238}U (Pb-214)	0.2090
		309.81	11.82	27.77	^{238}U (Pb-214)	0.7382
		538.90	20.54	48.27	^{232}Th (Tl-208)	0.9903
		1320.84	33.86	79.57	^{40}K	0.4778

BASIC DATA FOR ROCK SAMPLES FROM BUTARE IRON ORE MINE

Sample Name	Mass /kg	Average Energy /keV	Standard deviation /keV	FWHM /keV	Radionuclide	Rate /s^{-1}
KTR1	0.3410	207.95	11.33	26.63	^{232}Th (Pb-212)	0.2024
		262.55	11.66	27.39	^{238}U (Pb-214)	0.1522
		316.79	13.59	31.93	^{238}U (Pb-214)	0.2251
		544.73	18.74	44.05	^{232}Th (Tl-208)	0.1894
		1316.76	9.96	23.40	^{40}K	0.0297
KTR2	0.2760	205.42	9.59	22.54	^{232}Th (Pb-212)	0.5299
		259.23	12.47	29.31	^{238}U (Pb-214)	0.1804
		315.12	12.58	29.56	^{238}U (Pb-214)	0.3419
		541.44	22.01	51.71	^{232}Th (Tl-208)	0.4375
		1316.11	32.05	75.33	^{40}K	0.8906
KTR3	0.2570	206.57	11.27	26.48	^{232}Th (Pb-212)	0.3212
		258.35	10.63	24.98	^{238}U (Pb-214)	0.2392
		316.23	12.70	29.84	^{238}U (Pb-214)	0.3932
		542.04	22.54	52.97	^{232}Th (Tl-208)	0.4361
		1322.75	22.29	52.38	^{40}K	0.0915
KTR4	0.2170	201.47	7.71	18.13	^{232}Th (Pb-212)	0.0701
		260.63	10.49	24.65	^{238}U (Pb-214)	0.1176
		313.68	11.26	26.45	^{238}U (Pb-214)	0.1625
		556.50	14.93	35.09	^{232}Th (Tl-208)	0.1257
		1354.10	7.32	17.19	^{40}K	0.0153
KTR5	0.2390	207.63	11.99	28.16	^{232}Th (Pb-212)	0.1848
		263.84	10.16	23.89	^{238}U (Pb-214)	0.1370
		317.88	13.58	31.92	^{238}U (Pb-214)	0.1919
		542.89	14.23	33.43	^{232}Th (Tl-208)	0.0862
		1320.56	4.27	10.03	^{40}K	0.0103
KTR6	0.3740	207.43	10.69	25.12	^{232}Th (Pb-212)	0.2594
		258.84	10.37	24.36	^{238}U (Pb-214)	0.2054
		317.19	14.84	34.88	^{238}U (Pb-214)	0.4269
		544.05	22.99	54.03	^{232}Th (Tl-208)	0.3794
		1324.55	16.94	39.82	^{40}K	0.0380
KTR7	0.2855	208.56	6.60	15.52	^{232}Th (Pb-212)	0.0850
		253.21	4.05	9.52	^{238}U (Pb-214)	0.0487

		314.31	9.87	23.19	^{238}U (Pb-214)	0.1564
		544.76	9.98	23.46	^{232}Th (Tl-208)	0.0566
		1302.17	5.17	12.14	^{40}K	0.0064
KTR8	0.2800	208.79	6.10	14.32	^{232}Th (Pb-212)	0.1226
		259.51	11.14	26.17	^{238}U (Pb-214)	0.1563
		318.39	8.82	20.72	^{238}U (Pb-214)	0.1437
		551.62	17.91	42.08	^{232}Th (Tl-208)	0.2354
		1311.19	4.50	10.57	^{40}K	0.0037
KTR9	0.2290	205.42	10.35	24.32	^{232}Th (Pb-212)	0.5965
		258.47	7.78	18.27	^{238}U (Pb-214)	0.1177
		314.20	11.67	27.42	^{238}U (Pb-214)	0.3048
		546.12	18.92	44.46	^{232}Th (Tl-208)	0.3676
		1322.36	31.34	73.66	^{40}K	0.1948
KTR10	0.2515	207.03	8.87	20.85	^{232}Th (Pb-212)	0.5396
		259.23	8.49	19.96	^{238}U (Pb-214)	0.1427
		313.81	14.24	33.47	^{238}U (Pb-214)	0.4636
		546.63	18.97	44.58	^{232}Th (Tl-208)	0.3988
		1319.69	4.24	9.96	^{40}K	0.0193
KTR11	0.3060	204.02	10.70	25.15	^{232}Th (Pb-212)	0.5200
		260.42	7.95	18.68	^{238}U (Pb-214)	0.1365
		541.45	21.99	51.68	^{238}U (Pb-214)	0.3908
		315.51	13.13	30.86	^{232}Th (Tl-208)	0.4138
		1313.39	27.76	65.25	^{40}K	0.3039
KTR12	0.2255	204.93	9.88	23.22	^{232}Th (Pb-212)	0.4600
		258.91	9.04	21.25	^{238}U (Pb-214)	0.1092
		314.58	12.85	30.20	^{238}U (Pb-214)	0.2956
		539.91	22.94	53.91	^{232}Th (Tl-208)	0.4275
		1316.29	17.31	40.67	^{40}K	0.1165

Specific Activity levels in soil samples from Kikagati tin mine

Sample Name	Mass/kg (± 0.0001)	Specific Activity /Bqkg^{-1}		
		^{238}U	^{232}Th	^{40}K
ITS1	0.6580	47.88 ± 0.66	234.85 ± 2.14	348.83 ± 6.14
ITS2	0.5060	48.98 ± 0.75	242.74 ± 2.47	629.23 ± 9.34
ITS3	0.5335	58.85 ± 0.81	275.34 ± 2.55	501.04 ± 9.34
ITS4	0.4750	69.59 ± 0.80	296.96 ± 2.37	562.87 ± 7.87
ITS5	0.5840	50.87 ± 0.72	188.13 ± 2.04	248.57 ± 5.49
ITS6	0.6575	35.47 ± 0.56	192.02 ± 1.96	141.01 ± 3.91
ITS7	0.5310	62.90 ± 0.84	306.79 ± 2.77	357.14 ± 6.92
ITS8	0.6790	40.30 ± 0.59	119.33 ± 1.55	545.51 ± 7.53
ITS9	0.6180	58.37 ± 0.75	199.94 ± 2.10	530.63 ± 7.81
ITS10	0.7010	40.66 ± 0.56	149.22 ± 1.67	380.03 ± 6.12
ITS11	0.7210	40.69 ± 0.58	169.85 ± 0.61	249.46 ± 5.33
ITS12	0.7320	42.09 ± 0.06	165.08 ± 1.65	204.08 ± 4.31
Mean ± C.D		**49.72 ± 5.65**	**211.69 ± 31.19**	**391.53 ± 84.83**

Specific Activity levels in rock samples from Kikagati tin mine

Sample Name	Mass/kg (±0.0001)	Specific Activity /Bqkg^{-1}		
		^{238}U	^{232}Th	^{40}K
ITR1	0.4385	40.03 ± 0.75	107.55 ± 1.87	1923.82 ± 17.67
ITR2	0.3840	38.76 ± 0.77	183.83 ± 2.50	522.55 ± 9.84
ITR3	0.4090	11.66 ± 0.43	11.95 ± 0.54	6.41 ± 1.05
ITR4	0.5030	51.22 ± 0.77	121.87 ± 1.86	596.5 ± 9.03
ITR5	0.6185	34.11 ± 0.57	139.04 ± 1.69	784.69 ± 9.50
ITR6	0.6135	6.14 ± 0.25	14.45 ± 0.50	272.53 ± 5.62
ITR7	0.4670	5.95 ± 0.28	8.41 ± 0.45	65.97 ± 3.15
ITR8	0.5735	2.87 ± 0.18	1.86 ± 0.15	2.24 ± 0.51
ITR9	0.5015	27.95 ± 0.57	38.26 ± 0.91	1991.± 16.42
ITR10	0.4715	42.23 ± 0.74	92.07 ± 1.56	1189.8 ± 13.40
ITR11	0.4990	12.27 ± 0.39	21.35 ± 0.69	636.05 ± 9.26
ITR12	0.4770	25.31 ± 0.56	87.75 ± 1.46	1027.62 ± 12.33
Mean ± C.D		**24.87 ± 9.30**	**69.03 ± 35.60**	**751.66 ± 400.18**

C.D represents 90% confidence deviation

Specific Activity levels in soil samples from Butare iron ore mine

Sample Name	Mass/kg (±0.0001)	Specific Activity /Bqkg^{-1}		
		^{238}U	^{232}Th	^{40}K
KTS1	0.4985	53.82 ± 0.79	226.67 ± 2.40	398.91 ± 7.50
KTS2	0.5510	65.46 ± 0.84	254.27 ± 2.46	379.53 ± 7.00
KTS3	0.4390	61.50 ± 0.90	264.76 ± 2.78	397.41 ± 7.94
KTS4	0.5880	66.23 ± 0.82	256.89 ± 2.37	836.74 ± 10.05
KTS5	0.4730	58.07 ± 0.84	270.51 ± 2.74	499.41 ± 8.60
KTS6	0.5390	67.06 ± 0.86	280.66 ± 2.59	419.20 ± 7.44
KTS7	0.4675	44.25 ± 0.75	185.30 ± 2.28	411.54 ± 7.92
KTS8	0.4940	44.47 ± 0.72	201.34 ± 2.27	333.80 ± 6.81
KTS9	0.6360	44.35 ± 0.63	190.32 ± 1.98	266.07 ± 5.45
KTS10	0.4910	65.35 ± 0.88	297.75 ± 2.84	295.05 ± 6.54
KTS11	0.5050	48.32 ± 0.75	224.09 ± 2.42	316.14 ± 6.68
KTS12	0.4605	72.59 ± 0.97	280.56 ± 2.83	443.39 ± 8.28
Mean ± C.D		**57.62 ± 5.06**	**244.43 ± 18.98**	**416.43 ± 84.17**

C.D represents 90% confidence deviation

Specific Activity levels in rock samples from Butare iron ore mine

Sample Name	Mass/kg (±0.0001)	Specific Activity /Bqkg^{-1}		
		^{238}U	^{232}Th	^{40}K
KTR1	0.3410	40.84 ± 0.80	64.74 ± 1.53	37.19 ± 2.58
KTR2	0.2760	68.87 ± 1.15	188.53 ± 2.90	1379.00 ± 17.58
KTR3	0.2570	90.26 ± 1.30	188.58 ± 2.93	152.19 ± 3.25
KTR4	0.2170	47.83 ± 1.17	62.68 ± 2.10	30.17 ± 3.15
KTR5	0.2390	50.95 ± 1.15	48.43 ± 1.62	18.45 ± 2.34
KTR6	0.3740	61.21 ± 0.93	111.86 ± 1.98	43.47 ± 2.68
KTR7	0.2855	25.46 ± 0.69	24.53 ± 1.03	9.62 ± 1.47
KTR8	0.2800	40.67 ± 0.96	90.45 ± 2.23	5.58 ± 1.19
KTR9	0.2290	66.05 ± 1.32	201.76 ± 3.46	363.48 ± 10.63
KTR10	0.2515	85.38 ± 1.38	192.27 ± 3.18	32.88 ± 2.96
KTR11	0.3060	61.39 ± 1.10	161.85 ± 2.73	424.37 ± 9.91
KTR12	0.2255	64.12 ± 1.31	221.24 ± 3.75	220.77 ± 8.33
Mean ± C.D		**58.59 ± 9.94**	**129.74 ± 35.03**	**226.43 ± 231.83**

ABSORBED DOSE RATES IN MINE TAILINGS FOR DIFFERENT SITES

Absorbed Dose Rates in the soil tailing samples collected from Mashonga Gold Mine

Sample Name	Specific Activity /Bqkg^{-1}			D_{out} /nGyh^{-1}	D_{in} /nGyh^{-1}	D_{in}/D_{out}
	^{238}U	^{232}Th	^{40}K			
BTS1	47.25	160.44	630.24	145.02	270.38	1.86
BTS2	51.79	179.67	1226.70	183.60	343.42	1.87
BTS3	39.49	133.12	581.03	122.88	229.24	1.87
BTS4	74.45	230.30	944.74	212.89	397.40	1.87
BTS5	147.02	376.73	1658.51	364.63	682.35	1.87
BTS6	77.14	251.12	1070.14	231.94	432.81	1.87
BTS7	54.58	148.82	813.92	149.04	279.03	1.87
BTS8	43.17	157.85	585.17	139.69	260.17	1.86
BTS9	40.67	164.63	565.92	141.82	263.78	1.86
BTS10	37.70	144.98	995.16	146.48	273.78	1.87
BTS11	49.03	219.66	920.70	193.72	360.40	1.86
BTS12	42.66	154.21	722.58	142.98	266.69	1.87
Mean	**58.75**	**193.46**	**892.90**	**181.23**	**338.29**	**1.87**

Absorbed Dose Rates in the rock tailing samples collected from Mashonga Gold Mine

Sample Name	Specific Activity /(Bqkg^{-1})			D_{out} /nGyh^{-1}	D_{in} /nGyh^{-1}	D_{in}/D_{out}
	^{238}U	^{232}Th	^{40}K			
BTR1	11.92	19.25	794.75	50.28	95.72	1.90
BTR2	3.20	13.27	17.66	10.23	18.95	1.85
BTR3	31.46	29.61	400.97	49.14	93.60	1.90
BTR4	99.82	270.23	1863.54	287.05	538.17	1.87
BTR5	4.15	6.30	18.61	6.50	12.24	1.88
BTR6	36.64	97.36	3781.30	233.41	443.31	1.90
BTR7	21.51	58.66	70.76	48.32	89.98	1.86
BTR8	13.90	11.86	48.95	15.63	29.75	1.90
BTR9	21.79	56.11	675.11	72.11	135.78	1.88
BTR10	13.87	14.37	76.87	18.29	34.72	1.90
BTR11	13.88	3.74	11.09	9.14	17.77	1.95
BTR12	7.47	3.20	7.20	5.68	10.97	1.93
Mean	**23.30**	**48.66**	**647.23**	**67.15**	**126.75**	**1.89**

Absorbed Dose Rates in the soil tailing samples collected from Kikagati Tin Mine

Sample Name	Specific Activity /Bqkg^{-1}			D_{out} /nGyh^{-1}	D_{in} /nGyh^{-1}	D_{in}/D_{out}
	^{238}U	^{232}Th	^{40}K			
ITS1	47.88	234.85	348.83	178.52	330.29	1.85
ITS2	48.98	242.74	629.23	195.49	362.42	1.85
ITS3	58.85	275.34	501.04	214.39	397.11	1.85
ITS4	69.59	296.96	562.87	234.99	435.71	1.85
ITS5	50.87	188.13	248.57	147.49	273.62	1.86
ITS6	35.47	192.02	141.01	138.24	255.13	1.85
ITS7	62.90	306.79	357.14	229.25	423.91	1.85
ITS8	40.30	119.33	545.51	113.44	211.98	1.87
ITS9	58.37	199.94	530.63	169.86	316.09	1.86
ITS10	40.66	149.22	380.03	124.76	231.95	1.86
ITS11	40.69	169.85	249.46	131.79	244.23	1.85
ITS12	42.09	165.08	204.08	127.66	236.64	1.85
Mean	**49.72**	**211.69**	**391.53**	**167.16**	**309.92**	**1.85**

Absorbed Dose Rates in the rock tailing samples collected from Kikagati Tin Mine

Sample Name	Specific Activity /Bq kg^{-1}			D_{out} /nGy h^{-1}	D_{in} /nGy h^{-1}	D_{in}/D_{out}
	^{238}U	^{232}Th	^{40}K			
ITR1	40.03	107.55	1923.82	163.68	309.04	1.89
ITR2	38.76	183.83	522.55	150.73	279.68	1.86
ITR3	11.66	11.95	6.41	12.87	24.38	1.89
ITR4	51.22	121.87	596.58	122.15	228.91	1.87
ITR5	34.11	139.04	784.69	132.46	247.10	1.87
ITR6	6.14	14.45	272.53	22.93	43.34	1.89
ITR7	5.95	8.41	65.97	10.58	20.01	1.89
ITR8	2.87	1.86	2.24	2.54	4.87	1.91
ITR9	27.95	38.26	1991.63	119.08	227.14	1.91
ITR10	42.23	92.07	1189.83	124.74	235.31	1.89
ITR11	12.27	21.35	636.05	45.09	85.66	1.90
ITR12	25.31	87.75	1027.62	107.55	202.02	1.88
Mean	**24.87**	**69.03**	**751.66**	**84.53**	**158.95**	**1.88**

Absorbed Dose Rates in the soil tailing samples collected from Butare Iron Ore Mine

Sample Name	Specific Activity /Bqkg^{-1}			D_{out} /nGyh^{-1}	D_{in} /nGyh^{-1}	D_{in}/D_{out}
	^{238}U	^{232}Th	^{40}K			
KTS1	53.82	226.67	398.91	178.41	330.76	1.85
KTS2	65.46	254.27	379.53	199.65	370.28	1.85
KTS3	61.50	264.76	397.41	204.90	379.61	1.85
KTS4	66.23	256.89	836.74	220.65	410.45	1.86
KTS5	58.07	270.51	499.41	211.04	390.93	1.85
KTS6	67.06	280.66	419.20	217.98	403.96	1.85
KTS7	44.25	185.30	411.54	149.53	277.47	1.86
KTS8	44.47	201.34	333.80	156.07	289.09	1.85
KTS9	44.35	190.32	266.07	146.54	271.43	1.85
KTS10	65.35	297.75	295.05	222.34	411.26	1.85
KTS11	48.32	224.09	316.14	170.86	316.25	1.85
KTS12	72.59	280.56	443.39	221.49	410.87	1.86
Mean	**57.62**	**244.43**	**416.43**	**191.62**	**355.20**	**1.85**

Absorbed Dose Rates in the rock tailing samples collected from Butare Iron Ore Mine

Sample Name	Specific Activity /Bqkg^{-1}			D_{out} /nGyh^{-1}	D_{in} /nGyh^{-1}	D_{in}/D_{out}
	^{238}U	^{232}Th	^{40}K			
KTR1	40.84	64.74	37.19	59.52	111.76	1.88
KTR2	68.87	188.53	1379.02	203.19	381.06	1.88
KTR3	90.26	188.58	152.19	161.95	302.65	1.87
KTR4	47.83	62.68	30.17	61.21	115.36	1.88
KTR5	50.95	48.43	18.45	53.56	101.62	1.90
KTR6	61.21	111.86	43.47	97.66	182.84	1.87
KTR7	25.46	24.53	9.62	26.98	51.18	1.90
KTR8	40.67	90.45	5.58	73.65	137.35	1.86
KTR9	66.05	201.76	363.48	167.54	311.79	1.86
KTR10	85.38	192.27	32.88	156.95	292.68	1.86
KTR11	61.39	161.85	424.37	143.82	268.46	1.87
KTR12	64.12	221.24	220.77	172.46	320.02	1.86
Mean	**58.59**	**129.74**	**226.43**	**114.87**	**214.73**	**1.87**